COPYRIGHT STATEMENT

Trace Metal and Speciation Analysis using Ion-Exchange and Energy Dispersive X-ray Fluorescence Spectrometry

by

ELENA MENÉNDEZ-ALONSO

A thesis submitted to the University of Plymouth

in partial fulfilment for the degree of

DOCTOR OF PHILOSOPHY

Department of Environmental Sciences

University of Plymouth

Plymouth

U.K.

September 2000

ABSTRACT

TRACE METAL AND SPECIATION ANALYSIS USING ION-EXCHANGE AND ENERGY DISPERSIVE X-RAY FLUORESCENCE SPECTROMETRY

Elena Menéndez-Alonso

Studies have been carried out on specific ion-exchange (Dowex 50W-X8 and Dowex 1-X8) and chelation (Chelex-100) resins, in order to determine their physical and chemical characteristics, to understand and explain their limits of function and to optimise their use as substrates in trace metal and speciation measurement by EDXRF.

Structural information was obtained by scanning electron microscopy and x-ray microanalysis showing a homogeneous distribution of functional groups and retained ions on both sectioned and whole resins. Particle size experiments performed on Dowex 50W-X8 (38 - 840 μm) showed that this parameter has no effect on the relationship between intensity of fluorescence and concentration or mass of resin. Inter-element effects were not observed in the analysis of multielemental specimens prepared on ion-exchange / chelation media by EDXRF. This indicates that the proposed method has a significant advantage when compared with other methodologies. A theoretical 'model', based on the formation of thin films on the surface of the resin beads, has been proposed in order to link and explain the effects observed in these experiments.

The use of a batch retention system has shown distinct advantages over using columns in terms of linearity, accuracy, precision, rapidity and simplicity. Parameters such as pH and ionic strength of the solution, concentration of competing ions and volume of the sample have been proven to be critical. The maximum retention capacity has been determined as 3.2, 1.1 and 0.67 mEq g^{-1} for Dowex 50W-X8, Dowex 1-X8 and Chelex-100 respectively. The optimum mass of resin for XRF analysis was found to be 0.5 g, for all resins tested. The linear range covered 4 to 5 orders of magnitude.

These findings show the potential of the investigated media to overcome instrumental and sample limitations. Based on the physico-chemical information found, methodologies for three different applications of the resins to EDXRF determinations have been developed and their analytical possibilities explored.

The multi-elemental determination of metals in sewage sludge digests was achieved by retaining the metals on Dowex 50W-X8 at pH 2 and Chelex-100 at pH 4. Chelex-100 allows quantitative recoveries for Cu and Zn. A wider range of elements was determined on Dowex 50W-X8, although with poorer recoveries (60 - 90%). The limits of detection were 10 - 21 μg when Dowex 50W-X8 was used and 8 - 49 μg for Chelex-100. The method was validated by the analysis of a certified material.

The determination of Kβ/Kα intensity ratios for Cr and Mn species and its potential as a tool for direct elemental speciation has also been studied. A difference in Kβ/Kα between the oxidation states of the analytes was only observed during the analysis of solutions of the metal species by EDXRF at the 98 % level of confidence.

Finally, the speciation and preconcentration of Cr(III) and Cr(VI) in waters has been performed by retention on Dowex 50W-X8 and Dowex 1-X8 followed by EDXRF determination. Efficient recoveries and preconcentration factors of up to 500 were achieved, leading to limits of detection of 30 μg L^{-1} for Cr(VI) and 40 μg L^{-1} for Cr(III). This method is simple, fast and inexpensive, allowing quantitative recoveries in the speciation of chromium in waste waters.

AUTHOR'S DECLARATION

At no time, during the registration for the degree of Doctor of Philosophy, has the author been registered for any other U.K. University award.

This study was financed with the aid of a studentship from the University of Plymouth and has been conducted in the Department of Environmental Sciences of the University of Plymouth.

Signed ……..

Elena Menéndez-Alonso
September 2000

LIST OF CONTENTS

LIST OF TABLES

LIST OF FIGURES

LIST OF PLATES

ACKNOWLEDGEMENTS

Having completed this PhD Thesis, I would like to thank those people that believed I could do it and helped me to achieve it. First of all, I would like to acknowledge my supervisors' work and gratefully thank Dr Mike Foulkes for giving me the opportunity to take on the project, for encouraging and guiding me through it and for putting up with my 'Spanish temperament'. Thank you also to Prof. Steve Hill for his helpful advice and a special thank you to Dr Jim Crighton of BP Chemicals, for always being ready to give his expert support to these investigations and making the Philips PV9500 XRF Spectrometer available. Financial support from the University of Plymouth is also much appreciated.

I am very grateful to the technical staff of the Department of Environmental Sciences, especially to Ian Doidge, Andy Arnold, Andy Tonkin, Dr Roger Evens and Rob Harvey for their continuous assistance throughout the project. Many thanks to Dr Ken Vines, Roger Bowers and Peter Davies of the Department of Geological Sciences for their technical assistance regarding the use of the Link Analytical XR300 XRF spectrometer. Much appreciated is the work by Dr Roy Moate and Peter Bond in the Electron Microscopy Unit. I would also like to thank Paul Russell and Mike Hocking of the Department of Biological Sciences for their assistance with the ultramicrotome.

I gratefully acknowledge all the members of the Department of Environmental Sciences, for their support and suggestions. Thank you in particular to everyone who has worked in labs 103, 104 and 607, for sharing the experience of the 'daily fight' with scientific research and for always being ready to make an escape to the pub, when everything got just too much.

Also, thanks to my friends in Plymouth and far away (Ana Soldado, Covi, Mabel, María, Cris Sariego, Kathryn, Ana Marcos, Belén, Cris Rivas, Fi, Neil, Rebeca and Warren), for all the different ways in which they have helped me through. A very special thank you to Andy Fisher, not only for being such a good friend, but also for his invaluable assistance in the lab and proof-reading this thesis.

Finally, to my family, especially to Mum and Dad, for starting it all (in more than one sense!) and for always being there with continuous support and encouragement; to my brother Luis, for keeping the musical therapy going and to Jason for being, also in more senses than one, 'the beginning of the end'.

Esta Tésis se la dedico a mis abuelos, Maruja Menéndez Fernández y José Alonso Celemín, q.e.p.d.

También al resto de mi familia y, en especial, a mis padres, con todo mi cariño y agradecimiento por el apoyo que siempre me han dado.

1. INTRODUCTION

Chapter 1. Introduction

1.1 Energy Dispersive X-ray Fluorescence Spectrometry in Trace Metal Analysis

Energy dispersive x-ray fluorescence spectrometry (EDXRF) is a powerful and well established technique for elemental analysis whose capabilities for obtaining qualitative and semiquantitative information are beyond any doubt. When quantitative information is required, the technique certainly offers advantages: it is non-destructive, allows the analysis of liquids and solids of different composition, many elements can be measured simultaneously and in just a few seconds per sample. In addition, the price of an average EDXRF spectrometer is low enough to have allowed this instrument to become an essential part of the modern routine control laboratory. Unfortunately, the technique also possesses a number of serious limitations such as its lack of sensitivity, in particular for elements with low atomic number. More important is the effect of the matrix; a direct consequence of x-ray emission being generated at depth and, therefore, interacting with the whole of the sample. This means that any difference in the physical or chemical composition of the samples and the standards will lead to a loss of linearity of the calibration graph and hence, inaccuracy in the analysis.

All these limitations are deeply rooted in the same characteristics that make the technique such an important tool in the analytical laboratory. This is the reason why before going any further into the issues surrounding the determination of trace

metals it would be necessary to take an insight into some of the fundamental principles of XRF.

1.2 PRINCIPLES OF X-RAY FLUORESCENCE SPECTROMETRY

1.2.1 X-radiation and x-ray spectrometry.

X-rays and their absorption properties were first described by Roentgen in 1896[1]. They can be defined as that small fraction of the electromagnetic spectrum with wavelengths in the region of 0.1-100 Å (1Å = 10^{-10} m)[2]. Wavelengths of x-rays are therefore between 10^2 and 10^4 times shorter than those of visible radiation. This is a consequence of the electronic transitions that cause x-ray emission involving the inner shells of the atom. These electrons deep inside of the atom are strongly bound to the nucleus and require a highly energetic source of bombarding radiation for them to be removed or excited to 'vacant' outer shells.

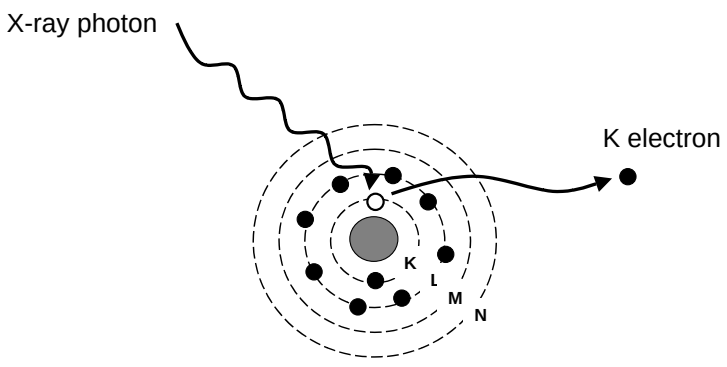

Figure 1.1 Ionisation of the K shell by an x-ray photon

When the atoms in a sample are bombarded with sufficiently energetic x-ray photons, the energy of these photons is transferred to the atoms causing the ejection of electrons from their energy levels (Figure 1.1).

This ionised state of the atom is energetically unstable and, in order to recover equilibrium, a series of electronic transitions from outer to inner shells occurs. In this process, the electron loses energy, equivalent to the difference between the binding energies of the two shells, which is dissipated in the form of an x-ray photon. Because the different energy levels are unique and dependant on the atomic number of the element, the energy of the x-ray photon is characteristic of the atom in which it was produced. When this photon escapes the atom, its energy can be detected and used for analytical purposes. This is known as *characteristic radiation*[3].

1.2.2 The interaction of x-rays with matter

When x-rays pass through matter, a reduction in intensity occurs. This attenuation process leads to emission of secondary x-radiation by the material. Mainly, two processes rule the interaction between the x-ray beam and the matter. The x-rays may be *photoelectrically* absorbed by matter. This process may cause i) fluorescent emission of x-rays characteristic of the absorbing medium, therefore, with energies that are independent of the primary radiation source ($E_{fluorescence} < E_{primary\ radiation}$) and ii) emission of photoelectrons such as *Auger* electrons. The x-rays may also suffer *scattering* after collision with electrons. This scattering can be i) *coherent*, if there is no loss of energy for the incident x-ray photon ($E_{coh\ scattering} =$

$E_{primary\ radiation}$) or ii) *incoherent*, when there is a small loss of energy ($E_{incoh\ scattering} < E_{primary\ radiation}$)[2].

1.2.2.1 Photoelectric absorption of x-radiation

The ability of x-rays to penetrate and even pass through matter is one of their best known properties. However, part of this radiation will be absorbed by the material. The decrease in intensity (attenuation) of the incident x-ray beam will be directly proportional to the thickness of the absorbing matter.

Considering an almost 'infinitely' thin layer of pure, single element material of thickness dx and a monochromatic beam of x-radiation of intensity I_0, the incremental loss of intensity, dI will be:

$$dI = - \mu I\, dx \qquad (1\text{-}1)$$

where μ is a proportionality constant, known as the *linear absorption coefficient*. This constant combines effects of the photoelectric and scattering processes. If τ represents the photoelectric absorption and σ the total scatter, then $\mu = \tau + \sigma$. In most cases, the scattering effect is small compared with the absorption effect and, for practical purposes, it is possible to say that $\mu \approx \tau$.

Equation 1-1 can also be expressed as:

$$\frac{dI}{I} = -\mu \cdot dx \qquad (1\text{-}2)$$

Thus, if we integrate equation 1-2 for a finite thickness, x:

$$\left[\ln I\right]_{I_o}^{I_l} = \left[-\mu x\right]_0^x \qquad (1\text{-}3)$$

which can be shown in its more general form:

$$\ln I_l - \ln I_o = -\mu x \qquad (1\text{-}4)$$

and rearranged to give:

$$I_l = I_o \cdot e^{-\mu x} \qquad (1\text{-}5)$$

This expression is of a type known as the *Beer-Lambert Law* and shows the attenuation of an x-ray beam when it passes through a material layer of thickness x.

The linear absorption coefficient, μ, is proportional to the density of a material and, therefore, depends upon the chemical and physical arrangement of the constituent atoms. A more convenient expression of the equation can be shown as:

$$I = I_o \cdot e^{-\mu_o \cdot \rho \cdot x} \qquad (1\text{-}6) \qquad \text{where: } \mu_o = \frac{\mu}{\rho}$$

Here, μ_o is designated the *mass absorption coefficient* if ρ is the density of the material. For a given wavelength and absorbing material, μ_o ($cm^2\ g^{-1}$) is constant and is independent of the chemical and physical form of the matter. The mass absorption coefficient of a mixture of elements is related to all component elements according to the expression:

$$\mu_{mix} = \sum_i \mu_i W_i \qquad (1\text{-}7)$$

where μ_i is the mass absorption coefficient of the pure element and W_i is the weight fraction of the element.

The mass absorption coefficient, as stated, depends on the wavelength and, hence, the energy of the incident radiation and on the atomic number of the absorbing element. When μ is plotted against the energy of radiation for any absorber, a general decrease in the value of μ is observed as the energy increases. However, the variation is not continuous and shows abrupt discontinuities called *absorption edges* for certain values of energy (Figure 1.2).

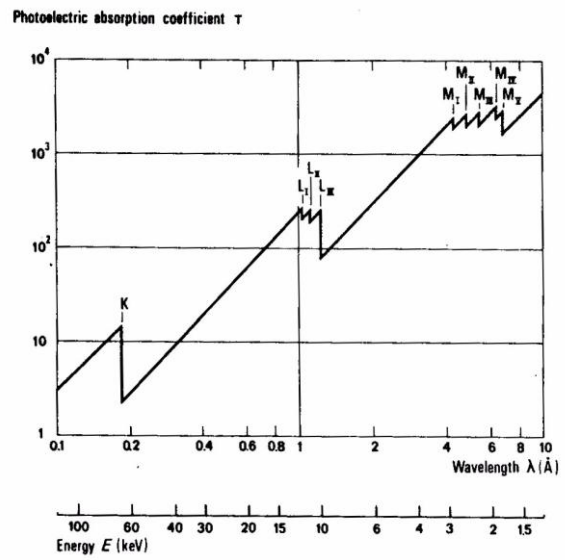

Figure 1.2 **Photoelectric absorption coefficient for W as a function of wavelength and energy**[3]

There is an absorption edge for each spectral series and subseries (K, L_I, L_{II}, L_{III}, M_I, M_{II}, etc.). The energy of the absorption edge is the equivalent of the *critical excitation potential* of each particular spectral series, that is the energy required to eject an electron from its atomic orbital. In Figure 1.2 the energy from the primary radiation increases from right to left and eventually reaches the binding energy of the electrons for each level. Thus an abrupt increase in mass absorption coefficient occurs as the electron leaves a particular orbital and the overall pattern reflects the electronic structure of the shells and subshells of an atom in terms of their energy.

The incident radiation with energies just higher than the absorption edge (shorter λ) will be absorbed and achieve ionisation. Those with energies just lower (longer λ) cannot affect ionisation at that energy level and will either pass through the absorbent material or become involved in alternative energetic processes.

The excess of absorbed x-ray energy above the electron binding energy (E_o) is used as kinetic energy by the free electrons (called photoelectrons) according to *Einstein's equation*:

$$h\nu = E_o + 1/2\ mv^2 \qquad (1\text{-}8)$$

where m is the mass of the electron, v is its velocity, h is *Plank's constant* and ν is the frequency of the x-radiation.

The intensity of any subsequent fluorescent x-ray lines resulting from the above process will therefore depend on a series of probabilities, the first of these being the chance that an incident photon is used to ionise the atom and not absorbed by the matter.

1.2.2.2 Fluorescence yield and Auger effect

As discussed earlier, when a photon interacts with a bound electron and the energy of the photon is greater than the binding energy of the electron, the photon can transfer all its energy to the electron which will be ejected from its shell as represented in Figure 1.1. This electron is known as a *photoelectron*. The vacancy in the K shell now represents an unstable situation. An electron from an outer shell with lower binding energy, for example the L shell, will be transferred into the K shell, emitting the difference in binding energy as a K x-ray secondary or fluorescent photon [Figure 1.3(a)]. However, this is not the only possibility. A competing process exists in which the energy of the x-ray photon is absorbed within the same atom causing ionisation in an outer shell on its way out [Figure 1.3(b)]. The emission of electrons from outer shells in which the atom acquires a state of double ionisation is known as the *Auger effect* [3,4].

Based on these two possibilities, the probability that a characteristic x-ray will be emitted after a vacancy has been created is known as *fluorescence yield* (ω).

$$\omega = n_f / n \qquad (1\text{-}9)$$

where: n= number of primary photons inducing ionisation

n_f = number of fluorescent secondary photons

$n - n_f$ = number of Auger electrons

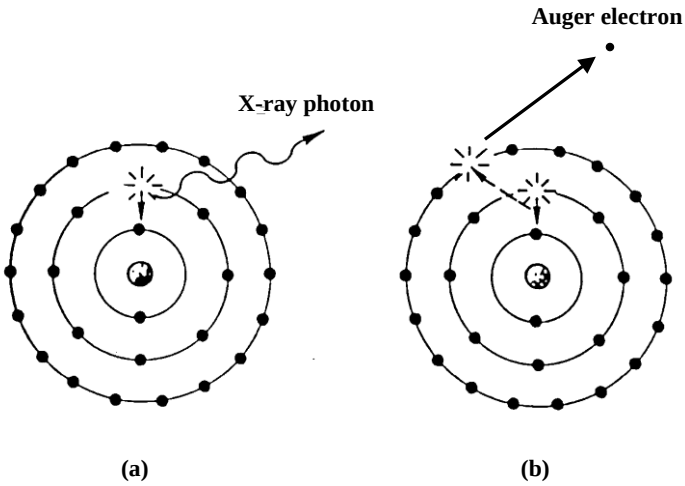

Figure 1.3 Emission of fluorescent radiation (a) and Auger effect (b)[4]

The value of the fluorescence yield is always between 0 and 1 and is a second factor determining the intensity of the fluorescence lines. It is known from experimental data and theoretical calculations that ω increases with the atomic number (Auger effect is greater at low atomic numbers) and that it depends on the spectral series considered (ω_K » ω_L » ω_M) [3,4].

1.2.2.3 Scattering of x-rays

As stated previously, scattering of the incident radiation can also occur when a x-ray photon interacts with an atom of the sample. The scattered radiation (σ) is mathematically described as:

$$\sigma = Z\, f^2 + (1 - f^2) \qquad (1\text{-}10)$$

where f is the *atomic scattering factor* (ratio of the amplitude of the wave scattered by an atom, to the wave scattered by a free electron), and Z is the *atomic number*.

Coherent scattering or the *Rayleigh effect* occurs as a consequence of a collision between an x-ray photon and an atom where the photon is scattered without any loss of energy (i.e., no change of wavelength). This effect is mathematically represented by the first term of equation 1-10. When scattering originates from a single atom, the photon can be re-emitted in any direction. Coherent scattering is always present in the x-ray fluorescence spectrum and is the main cause of background signals.

Incoherent scattering or the *Compton effect* (second term of equation 1-10) occurs when the x-ray photon loses part of its energy in the collision. The electron involved in the scattering process will gain some of the energy of the photon, as the *total momentum* is to be maintained. The wavelength of the scattered photon will increase according to the expression:

$$\Delta\lambda = 0.0243\,(1 - \cos\phi) \qquad (1\text{-}11)$$

where ϕ is the angle of scatter and λ is the wavelength measured in Å. This type of scatter tends to displace the continuum background to the low energy regions. Broad peaks, corresponding to the characteristic primary wavelengths of the anode material of the x-ray tube, can also be found in that area of the spectrum[5].

It should be noted, from equation 1-10, that scatter is atomic number-dependent. Incoherent scatter will become more manifest for those samples with a higher proportion of light elements, whereas coherent scatter mainly occurs in samples heavy elements. Ultimately, scatter will condition the limit of detection in the analysis by XRF spectrometry[5].

1.2.2.4 Emission of characteristic or secondary radiation

The situation encountered in an x-ray fluorescence spectrometer can be summarised by Figure 1.4.

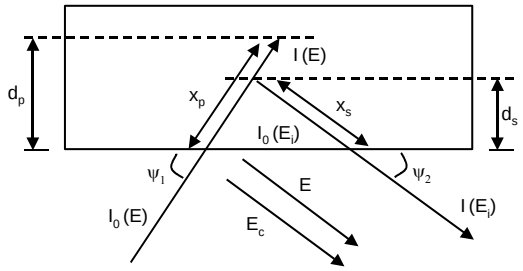

Figure 1.4 Primary beam interaction with a specimen, i, in the x-ray spectrometer

The diagram illustrates a beam of primary radiation of energy E (although in practice the incident beam used in energy dispersive systems would be polyenergetic) which collides with the specimen i at an angle ψ_1, dependent on the geometry of the spectrometer. A portion of the beam, I (E), travels a distance x_p into the specimen, reaching a depth d_p which depends on the mass absorption coefficient of i for radiation of energy E and on the density of the specimen, ρ_i. If the energy of

incident radiation is greater than the critical excitation potential of i, there will be an emission of characteristic fluorescent x-radiation [2,5].

If the secondary fluorescent beam, with an initial intensity I_0 (E_i), originates from a depth d_s, only a fraction of this radiation, I (E_i), emerges at the surface and can be measured. This fraction will be dependent on the angle ψ_2, determined by the position of the detector with respect to the sample, on the mass absorption coefficient of i for E_i and on ρ_i [2,5].

There is a point at which increasing d_s gives no significant increase in the intensity of the characteristic radiation. The less energetic fluorescent radiation will be absorbed, undetected, before it reaches the surface of sample. This distance is called *critical penetration depth*[6] and can be defined as the depth at which 99% of the intensity of the fluorescent x-rays would be absorbed by the matrix before they reached the surface of the sample. This concept is very important in quantitative analysis by XRF.

1.2.3 Factors affecting quantitative analysis by x-ray fluorescence spectrometry: interelement or 'matrix' effects

1.2.3.1 General considerations

The use of x-ray fluorescence as a tool for quantitative analysis is based on the assumption that the intensity of fluorescence of the analyte ($I_{E(A)}$) in the sample and its concentration (C_A) are directly proportional,

$$C_A = k_A \cdot I_{E(A)} \qquad (1\text{-}12)$$

where k_A is a proportionality constant that can be determined from a series of standards of known composition. The intensity of fluorescence given by the standards is measured and plotted against their known concentrations to produce a *calibration curve* (Figure 1.5) of equation[7]:

$$I_{E(A)} = b \cdot C_A + a \qquad (1\text{-}13)$$

which is commonly rearranged as:

$$C_A = d + e \cdot I_{E(A)} \qquad (1\text{-}14)$$

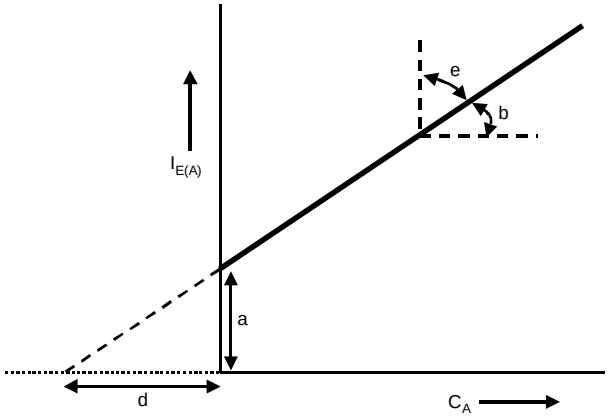

Figure 1.5 **Parameters used in the definition of the calibration curve for x-ray spectrometry**

In the presence of interelement effects caused by any other matrix element j, the calibration curve takes this form where the symbol "+" indicates negative absorption and "–" refers to self-absorption[8]:

$$C_A = [d + e \cdot I_{E(A)}] \cdot [1 \pm \Sigma(C_j \cdot \alpha_j)] \qquad (1\text{-}15)$$

where C_j is the concentration of the matrix element and the term $\Sigma(C_j \cdot \alpha_j)$ represents the *total specimen absorption* with α_j being defined as:

$$\alpha_j = \mu_j(E) + Y \cdot \mu_j(E_A) \qquad (1\text{-}16)$$

$\mu_j(E)$ is the mass absorption coefficient of j for a primary beam of energy E, $\mu_j(E_A)$ is the mass absorption coefficient of j for a secondary radiation of energy E_A and Y is a geometrical constant equal to $\sin \psi_1 / \sin \psi_2$ [2,8]. When $\sin \psi_1 = \sin \psi_2$, Y = 1, which is the case in many EDXRF spectrometers ($\psi_1 = \psi_2 = 45^o$).

In fact, as a consequence of x-radiation being generated at a certain depth inside the specimen, the applicability of the calibration curve may be questionable unless samples and standards are nearly identical in chemical and physical characteristics[8]. This is explained in more detail in the following sections.

1.2.3.2 Primary and secondary absorption effect

The intensity of the fluorescent radiation that can be measured by an x-ray spectrometer will be reduced not only by absorption of the primary incident beam by the matter, but also by attenuation of the actual fluorescent radiation which is known as *secondary absorption*.

The absorption of the secondary radiation is greater than that of the more energetic primary beam. For this reason, the most efficient primary radiation will have energy just in excess of the absorption edge of the element of interest. When using higher energies, the excitation efficiency is low due to some of the fluorescent radiation being produced so deeply inside the specimen that it cannot emerge at the surface to be detected. This phenomenon is connected to the critical penetration thickness of the specimen as described in section 1.2.2.4.

1.2.3.3 Enhancement and third element effects

These effects are due to excitation of the analyte by radiation other than that of the primary source. Although x-ray fluorescence is mainly achieved by excitation with an x-ray tube these other effects add to the intensities obtained for the analyte and must be considered when looking at causes of error in XRF spectrometry.

Enhancement effects occur when an element B (enhancing element), other than the analyte, is excited by the primary radiation and produces characteristic x-radiation which, in turn, is able to excite the analyte, A. For this to happen, the energy of the characteristic radiation of element B must be in excess of the absorption edge energy of element A [Figure 1.6(a)] [2,5]. Several elements in the sample can act as enhancing elements of the same analyte.

Third element effects occur when an element C in the sample is excited by the primary radiation and its characteristic secondary radiation is able to excite an enhancing element B which, in turn, produces excitation of the analyte A [Figure

1.6(b)]. The condition for a third element effect is $E_C > E_{EDGE\ B}$ and $E_B > E_{EDGE\ A}$. As seen in the figure, element C can also enhance the signal from A directly [2,5].

(a) (b)

Figure 1.6 Enhancement (a) and third element (b) effects

1.2.3.4 Influence of absorption and enhancement effects in the calibration graph

Inevitably, interaction occurs between the sample and the primary radiation and also between the sample and the fluorescent radiation. As a result, the intensity of fluorescence produced by the same concentration of analyte will be dependent on the matrix. Only if the specimen was infinitely thin would these effects be insignificant. Considering a simplified case of equation 1-15, the intensity of fluorescence I_A of an element A in a matrix composed of a single element B will be:

$$I_A = K\frac{C_A}{C_A \cdot \alpha_A + C_B \cdot \alpha_B} \qquad (1\text{-}17)$$

where K is a constant that depends on the geometry of the instrument and the characteristics of element A; C_A and C_B are the concentrations of the elements A and B in the matrix expressed in weight fraction such that, $C_M = C_A + C_B = 1$.

For a pure element, $C_B = 0$ and the intensity of fluorescence will be:

$$I'_A = K\frac{C_A}{C_A \cdot \alpha_A} \qquad (1\text{-}18)$$

and defining $R = \alpha_B / \alpha_A$, the relative intensity can be written as:

$$\frac{I_A}{I'_A} = \frac{C_A}{R + C_A(1-R)} \qquad (1\text{-}19)$$

When R =1, $I_A / I'_A = C_A$ and a linear calibration curve is obtained. When $R \neq 1$, the calibration curve is only linear over small intervals. If $\alpha_A < \alpha_B$, the matrix absorbs part of the radiation and the intensity of fluorescence measured decreases (*negative absorption*). If $\alpha_A > \alpha_B$, the analyte itself absorbs part of the emitted radiation and the intensity of fluorescence measured increases (*positive absorption*). The deviation from linearity will be greater when the difference in mass absorption coefficient between the analyte and the matrix increases (Figure 1.7). In the presence of enhancement effects, the calibration curves do not fit exactly the shape of a hyperbolic function, but looks more like curve F in Figure 1.7 [6,7].

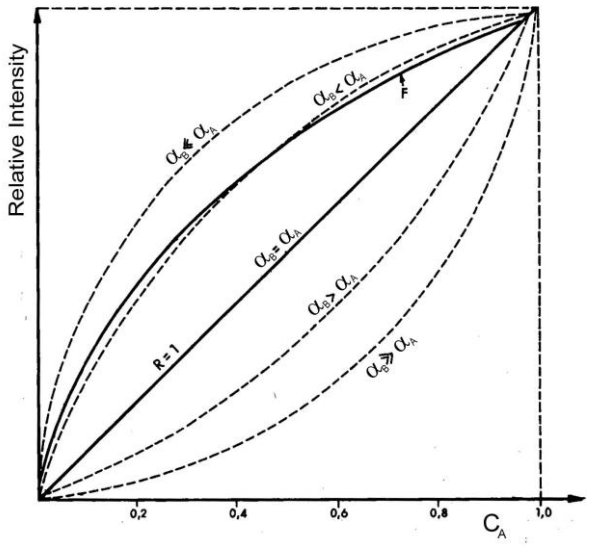

Figure 1.7 **Intensity of fluorescence emitted by an element as a function of the mass absorption coefficients of the matrix**[7]

1.2.4 Factors affecting quantitative analysis of solid samples by x-ray fluorescence spectrometry: particle size effects

Since x-radiation is only able to penetrate and emerge from a certain depth in the specimen, it is reasonable to expect a relationship between the intensity of fluorescence and the particle size of the sample.

In general, the intensity of fluorescence emitted by an element increases as the particle size of the sample decreases, up to a point at which no further increase of the signal is observed. When the particle size is large, the intensity can also be constant, but is usually lower than that obtained for fine particle samples[4,6,9].

Figure 1.8 shows the typical variation of the intensity of fluorescence with the particle size. The zone of maximum variation in the curve is known as the *transition zone*. The magnitude of the transition zone varies significantly from one material to another but, in general, the most common range of particle sizes falls within its limits[6].

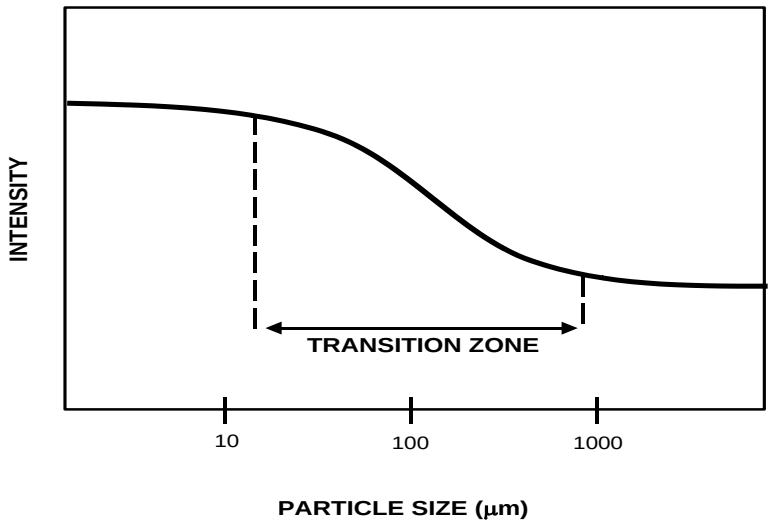

Figure 1.8 Typical effect of the particle size on the intensity of x-ray fluorescence

The effect of the particle size in the intensity of fluorescence is illustrated in Figure 1.9. The sample, a series of spherical particles, is excited by primary radiation. The angle of incidence with the apparent sample surface is Ψ_1. A part of the incident radiation does not penetrate all areas of the particles (yellow areas). Fluorescent radiation is emitted from the blue area of the spheres. However, only a part of this fluorescent radiation (green areas) is transmitted across the particles, arising at an angle Ψ_2 with the surface of the sample, thus allowing detection. The remaining radiation will be absorbed by the matter. A smaller particle size will mean

more effective transmission areas per surface unit. Maximum emission will occur when the dimensions of the particles are compatible with the geometry and with the absorption characteristics of the system[6].

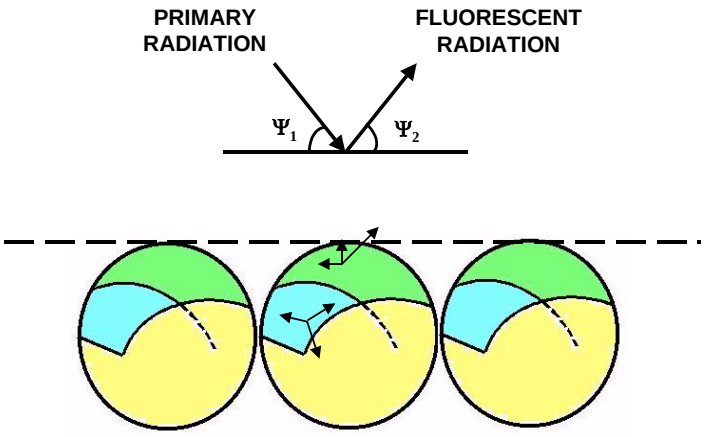

Figure 1.9 **Representation of the effect of the particle size on the intensity of the fluorescence radiation**

In order to estimate the effect of the particle size quantitatively, some authors[10,11] have attempted to calculate the thickness of the particle that absorbs radiation. The common practice is to use the concept of *infinite thickness,* i.e., the thickness of sample that absorbs the fluorescent radiation entirely, as a reference point. This concept is equivalent to that of *critical penetration depth* introduced in section 1.2.2.4. Thus, when the particle size is smaller than the infinite thickness, the intensity of fluorescence increases as the particle size decreases. The effect of the particle size rapidly diminishes once the infinite thickness is reached[6,12]. The intensity of fluorescence is independent of the particle size for particle sizes larger

than the critical penetration depth of the sample. For very small particle sizes, the effects are also negligible (as seen in Figure 1.8).

Small particle sizes are normally achieved by grinding the samples. This procedure can prove difficult for certain materials, especially when sub-micron particles are required. As an added inconvenience, the different components of the material may not necessarily grind uniformly, leading to heterogeneity of the specimen which is another source of error in the analysis.

1.3 Overcoming Analytical Limitations of XRF

From the time when the first commercial spectrometers were produced, more than forty years ago, the need to develop ways to overcome the main limitations of the technique has been apparent. Recently the range of methods used to resolve problems in XRF analysis has broadened considerably in the commercial field, although many have been available for a number of years. A list of the more common methods employed in XRF is shown in Table 1.1.

The method or combination of methods to be used will be dependent upon the characteristics of the sample and the elements to be analysed. However, none of these can be considered of universal application and careful assessment of the consequences of applying these methods is necessary prior to the analysis. For example, fusing the sample to produce a glass bead will eliminate the particle size and interelement effects but, at the same time, will cause immediate dilution of the

sample and subsequent loss of sensitivity. Similarly, grinding the sample to a very fine particle size, prior to the production of a pressed powder pellet, will reduce microabsorption effects, but the production of sub-micron particles, required for the analysis of the light elements is not achievable with standard equipment.

Table 1.1 **Methods used to overcome the main analytical limitations of XRF**

Sample modification	• Fusion
	• Pressed powders
	• Thin-film methods
Compensation methods	• Internal standard
	• Standard additions
	• Scattered radiation
Mathematical correction models	• Fundamental parameters
	• Influence coefficients
Preconcentration techniques	• Coprecipitation
	• Collection on filters, membranes, resins, absorbers, etc.

The use of thin films has been introduced in a considerable number of XRF applications. The production of a thin layer of material avoids the analyte emission at depth and the absorption of fluorescent radiation by the sample, eliminating the matrix effects. However, the method is subject to practical limitations: it is difficult to prepare sufficiently thin films or homogeneous films of reproducible thickness. Also, the sensitivity is low for the lighter elements.

Compensation methods such as the use of internal standards and standard additions are well suited to the determination of one or two elements per sample but become tedious or impractical when multielemental analysis is required.

One commonly practised technique is the use of mathematical models for the correction of the measured intensities or concentrations. The most popular are those based on the *Fundamental Parameters* method or those that use *influence coefficients*. In many cases, these procedures require previous knowledge of the sample composition, which is precisely the purpose of the analysis. This paradoxical situation is addressed by the use of iteration techniques with some success. This latter approach also requires powerful computing facilities.

Another possibility is the use of preconcentration techniques in order to obtain lower limits of detection. Many of these methods are based on coprecipitation and are, therefore, tedious and prone to spectral / matrix interferences. Other sample preparation possibilities are evaporation, extraction and electrodeposition, all with their own advantages and drawbacks[13]. Filters and membranes can be used as supports for the precipitate formed by coprecipitation but may also be employed on their own if they have absorbing or adsorbing properties. The use of ion-exchange resins, together with other types of solid retention media, is the basis of this research and will be discussed in more detail in the following section.

1.4 SOLID RETENTION MEDIA FOR X-RAY ANALYSIS

Solid retention media and, in particular, ion exchangers are at the core of analytical separation science. They have been combined both off and on-line with the majority of determination techniques available in the modern laboratory. Their potential for providing lower limits of detection and matrix removal are well known. In addition, their use for x-ray analysis may extend beyond the obvious objective of achieving preconcentration and offers a series of potentially interesting advantages:

- It is possible to prepare as many standards as necessary, either multielemental, or pure elemental standards, depending on the requirements of the analysis.

- The analytes remain on the surface of a solid support with high degree of homogeneity.

- Standards with the same composition as the sample are not always available but, by separating the analytes of interest from their original matrix and retaining them on the surface of, for example, an ion-exchanger, it is possible to 'create' an identical and preferable light matrix for standards and samples and, thereby, eliminate many of the composition-dependent errors.

- The linear range is extended as the absorption and enhancement effects are decreased. Background effects are usually reduced.

- Using solid media under different conditions makes it possible to target different analytes of interest and hence perform speciation.

The use of ion-exchange membranes as a preconcentration aid for x-ray spectrometry was first introduced by Grubb and Zemany in 1955[14] but, it was nearly a decade later, when other researchers started to take an interest in this idea, as an alternative to unsatisfactory traditional methods of sample preparation for trace metal analysis. The reasons for this interest were mainly related to the potential of ion-exchange media as a light and uniform matrix over which the analytes could be evenly distributed.

Initially, the ion-exchangers were used in three different presentations as membranes[14-16], resins[17-24] and resin loaded filter papers (made of 50:50 cellulose support and resin)[25-30]. The loaded paper approach was believed to offer the ideal sample presentation for x-ray spectrometry, being a thin target, easy to handle and with no need for further treatment prior to the analysis. Thus, exhaustive studies were carried away to establish their chemical and physical characteristics and, especially, their limitations[17, 25, 29]. Soon after, the first reports on applications were produced, not only in the analysis of metals, but also in the determination of anions in a variety of samples, for example, waters[15, 16, 24, 28], urine[23], alloys[25], metals[26, 27], steels[18] and rocks[20, 22]. This wide spread of applications seems to be a clear indication of how eager the research community was to test the possibilities of ion-exchangers in x-ray spectrometry to the limit and find solutions to multiple sample preparation problems. A review by Law and Campbell[31] in 1973 discusses in detail, including many applications, the work done to that date using resin loaded filter papers.

However, by 1975 it was clear that the use of ion-exchangers had some disadvantages, whether they were employed as loose resins or more elegant filters. At first, cation and anion exchangers of different strength were used[14, 15, 17, 18, 25-30],

but it soon became obvious that these functional groups were not selective enough and, in the presence of high concentrations of competing ions, the analytes would remain in solution. This drawback was accentuated when using filters, because of their lower capacity. Other problems associated with filters are unequal distribution of the analytes and long equilibration times.

In an attempt to improve the selectivity of the retention, research was focused on the use of chelating resins[16, 19-24]. In 1973, Leyden[22] reviewed the work published in this area to that date, which mainly involved Chelex-100 although there had also been some attempts to synthesise even more selective chelating resins[22, 24].

It is important to note that much of the work involving chelating resins was performed using a batch method. From 1975, researchers seem to focus less on a particular type of sample presentation and more on overcoming the chemistry-related problems encountered so far. Thus, Leyden and Luttrell[32] started a new trend in the use of solid media for x-ray analysis of trace metals by immobilising amines and their dithiocarbamates on silica gel. The same authors also explored a similar approach by attaching chelating groups to glass beads[33]. This was applied with success to the preconcentration and determination of certain anions by XRF[34].

Following a similar route, Van Grieken and co-workers investigated the use of activated carbon as a sample support for x-ray analysis, either on its own[35] or after chelation of the metals with oxine[36,37]. The method was successfully used to determine metals and metal species (selenium and selenite) in waters[35].

Another substrate employed for preconcentration, prior to its use in x-ray analysis, Zn-diethydithiocarbamate [$Zn(DDTC)_2$], offers a very simple procedure that has been applied to the determination of metals in water[38].

Alongside the introduction of new retention media, research continued using the already established filter papers[39-43] and resins[44,45] with workers concentrating on introducing modifications to the actual substrate or to the chemistry of the method that would improve selectivity, applicability, reduce analysis time, etc.

Kingston and Pella[46] employed conventional cation exchange resin-loaded filters but, by first using Chelex-100 to separate the analytes from the matrix (seawater and urine), they ensured that the capacity of the filters was not exceeded.

In 1979, Smits *et al.*[47] published a very interesting study in which they compared the most promising methods for preconcentration of trace metals from a wide range of waters prior to determination by XRF. Later, in 1982, Van Grieken[48] exhaustively reviewed all the work published to that date in the same field, although the methods developed had continued to be applied not only to the analysis of waters, but also urine[41, 46], plants[40, 42], rocks[45], etc.

Up to the present time, research has concentrated on developing improved, often more sophisticated and sometimes more complex methods in the application of solid retention media to x-ray analysis. Some authors have continued to explore the synthesis of more selective ion exchangers by attaching chelating agents to cellulose[49], textile materials[50] and commercially available resins[51]. An interesting variation of this last approach is the work by Ducosfonfrede *et al.* in which the anion exchanger Dowex 1-X8 is loaded with MnO_2 in order to increase the specific area of

exchange[52]. The use of adsorbers such as activated charcoal, on its own or combined with coprecipitation has also continued to be investigated and Peräniemi and co-workers have succeeded in applying it to the determination of P[53] and Cr species[54] in waste waters. A different choice of adsorber, activated alumina, has been proved to make an excellent aid for the rapid and simple determination of trace metals in liquid hazardous waste by EDXRF, with a total analysis time of 15 minutes for more than 20 elements[55]. Overall, however, recent methods are characterised by their diversity and complexity, which makes them more difficult to compare and classify or even identify in the literature. It also seems apparent that no single method is the solution to all the problems encountered in the analysis and researchers are more willing to design their own procedure from first principles instead of adapting already published methodologies.

A summary of published methods and applications of solid retention media to x-ray analysis can be found in Table 1.2.

Table 1.2 **The use of solid retention media as sample support for XRF spectrometry.**

Retention Media	Samples	Analytes	Procedure details	Analytical characteristics	Ref.
C-60 cation exchange sheet resin	Standards	Fe, Ti, V, U, Hg, Tl, etc. (up to 28 cations)	Standards prepared in 1 mL of 0.1% HNO_3 Equilibration time: 3 h Curved crystal x-ray milliprobe analysis	Best LOD: 0.01 μg Capacity : 1.6 mEq g^{-1} (dry) Recovery > 95% for 16 cations	17
A-60-2 anion exchange sheet resin	Standards	Br, Se, As, Mn, Cr, etc. (up to 15 anions)	Equilibration time: 3 h Curved crystal x-ray milliprobe analysis	Capacity : 2 mEq g^{-1} (dry) Recovery > 95% for most anions	17
SA-2 and *WA-2* cation exchange resin (*Amberlite IR-120*) loaded papers	Standards and alloys	Ni, Co, Cr, Mn, Fe, etc.	pH: 2 No. of filtrations: 7 Equilibration time: 18 s (per filtration) WDXRF determination	LOD = 0.05 – 5 μg Counting time: 10 min Sample volume: 40 mL Capacity: 0.20 mEq $disk^{-1}$ (SA-2)	25
SB-2 and *WB-2* anion exchange resin (*Amberlite IRA-400*) loaded papers	Standards	Br, I, S, V, Cr, Mn, etc.	Filters converted from Cl^- to OH^- form pH: 3.5 No. of filtrations: 7 Equilibration time: 18 s (per filtration) WDXRF determination	LOD = 0.04 – 1 μg Counting time: 10 min Sample volume: 40 mL Capacity: 0.15 mEq $disk^{-1}$ (SB-2)	25

Retention Media	Samples	Analytes	Procedure details	Analytical characteristics	Ref.
SA-2 cation exchange resin (*Amberlite IR-120*) loaded papers	Tungsten and tungsten oxide	Cu, Ni, Zn, Pb, Co	Trace metals extracted into a solution of dithizone in $CHCl_3$ from alkaline tartrate solution Dithizone oxidised with benzoyl peroxide and metals back-extracted into dilute HCl pH: 2 No. of filtrations: 7 Equilibration time: 18 s (per filtration) WDXRF determination	LOD = 0.05 – 0.4 μg Limit of determination = 0.3 –1 ppm RSD ~ 7% Counting time: 10 min Sample volume: 40 mL	26
SA-2 cation exchange resin (*Amberlite IR-120*) loaded papers	Molybdenum	Co, Cu, Fe, Pb, Mn, Ni, Zn	Sample (10 g) digestion with conc. H_3PO_4, conc. HNO_3 and 30% H_2O_2 Column separation from matrix with *Dowex 50W*, 100-200 mesh Elution with 6M HCl pH 2 No. of filtrations: 7 WDXRF determination	LOD = 0.3 – 3.8 μg RSD = 10% Counting time: 10 min Sample volume: 40 mL Capacity: 0.20 mEq $disk^{-1}$ (SA-2)	27
SB-2 anion exchange resin (*Amberlite IRA-400*) loaded papers	Water	Br	pH: 4 No. of filtrations: 3 Flow rate: 50 mL / 130 seconds Estimated preconcentration factor: × 200 WDXRF determination	LOD = 0.05 ppm RSD = 5% Linear range: 0.1 – 10 ppm Counting time: 100 s Sample volume: 50 mL Recovery ~ 100%	28

Retention Media	Samples	Analytes	Procedure details	Analytical characteristics	Ref.
Chelex-100 chelating resin, 100-200 mesh	Standards	Ba	Resin mass: 0.75 g (dried at 80 ^{o}C) pH: 11-12 Resin pelletised with paraffin Internal standard: La WDXRF determination	RSD < 5% Counting time: 10 - 100 s depending on concentration	21
Bio-Rad 1-X10 anion exchange resin, 50 – 100 mesh	Carbon steels	La, Ce, Pr	Sample (2 g) digested with HNO_3 and H_2O_2 WDXRF determination	LOD = 0.002 – 0.004% RSD = 6 – 20% Linear range: 0.002 – 0.05% Counting time: 0.4 min	18
SA-2 cation exchange resin (*Amberlite IR-120*) loaded papers	Standards	Sc, Y, Ce, Pr, Nd, Sm, Eu, Gd, Tb, Dy, Ho, Er, Tm, Yb, Lu	pH: 1.5 No. of filtrations: 6 Flow rate: 1.5 min / 10 mL WDXRF determination	LOD = 0.001- 0.04 μg RSD = 1.5% at the 10 μg level Counting time: 100 s Sample volume: 25 mL Capacity: 0.03 mEq Recoveries: Y (85%), Sc (75%), others > 98%	29
Chelex-100 chelating resin	Standards	Total Cr, Cr^{III}	For total Cr analysis, Cr^{VI} is reduced with sodium bisulfite pH: 6.4 – 6.6 Equilibration time: 30 min The resin was pelletised WDXRF determination	RSD = 3% at the 0.1 μmol level Counting times adjusted to RSD < 1% Sample volume: 15 mL Quantitative recoveries	29

Retention Media	Samples	Analytes	Procedure details	Analytical characteristics	Ref.
Chelex-100 chelating resin, 100-200 mesh	Rocks	Co, Ni	Samples dissolved in HF and HNO_3 and run through Dowex 50W-X8 (0.5 g) column to eliminate Fe interference Resin mass: 200 mg (later pelletised) pH: 9 Equilibration time: 3 h WDXRF determination	RSD = 0.1 – 8% Sample volume: 100 mL Recoveries: 95 – 140%	20, 22
Chelex-100 chelating resin, 100-200 mesh	Rocks	Bi	Samples (1 – 20 g) dissolved in HF and HNO_3 Fe interference eliminated by reduction with ascorbic acid Resin mass: 180 mg (later pelletised) pH: 2 Equilibration time: 24 h WDXRF determination	RSD = 4 – 20% Recoveries: 10 – 125%	20, 22
NMRR chelating ion-exchange resin, 100-200 mesh	Rocks	Au	Samples (5 – 20 g) dissolved in aqua regia Resin mass: 150 mg (later pelletised) pH: 0.5 - 1 Equilibration time: 24 h WDXRF determination	LOD < 0.01μmol RSD = 6 – 25% Recoveries: 73 - 100%	20, 22

Retention Media	Samples	Analytes	Procedure details	Analytical characteristics	Ref.
SA-2 cation exchange resin (*Amberlite IR-120*) loaded papers	Standards	Ca, Ba, Pb, U	pH: 2 No. of filtrations: 7 Equilibration time: 5 min Non-dispersive XRF analysis	LOD < 0.2 ppm Counting times adjusted for RSD < 1% Sample volume: 40 mL Capacity: 0.2 mEq g^{-1} (dry)	30
MC-3142 ion exchange membrane	Waters, milk	Pb, Cd, Hg	6 × 20 mm membranes equilibrated with sample Equilibration time: several days PIXE analysis	LOD ~ 0.1 ppb Pb Sample volume: 1 L	15
Chelex-100 chelating resin, 100-200 mesh	Urine	Cu, Zn, Pb	Resin mass: 0.1 g (dry) pH: 7 Equilibration time: 1.5 h Internal standard: Y EDXRF determination	LOD ~ 50 ppb Counting times: 10 – 40 min depending on concentration	23
TEPA chelating resin	Sea water	Cu, Zn, Ni	Resin (0.150 g) used in columns pH: 6 / 8.2 Equilibration time: 48 h Columns emptied and resins pelletised WDXRF determination	LOD = 0.1 – 0.3 µg L^{-1} RSD = 5 - 10% Counting time: 100 s Sample volume: 4 L Recovery > 92%	24
Amines and their dithiocarbamates immobilised on silica gel	Standards	Cu, Zn, Ni, Fe, Cd, Cr, Co, etc.	Study of the characteristics of the exchangers including: Capacity, metal uptake with time, pH dependence, distribution coefficients WDXRF determination	Capacity: 0.5 – 1.0 mmol g^{-1} silylated silica gel	32

Retention Media	Samples	Analytes	Procedure details	Analytical characteristics	Ref.
Chelex-100 filter membranes	Water	K, Ca, Mn, Co, Ni, Cu, Zn, Pb, Sr	Two membranes are used for optimum recovery pH: 7 - 8 No. of filtrations: 1 Filtration rate < 10 mL min^{-1} EDXRF determination	LOD = 1 – 20 ppb RSD = 10 - 15% Counting time: 2000 s Sample volume: 200 mL Capacity: 0.07 mEq	16
8-hydroxyquinoline adsorbed onto activated carbon (AC)	Tap waters	Mn, Fe, Co, Ni, Zn, Pb	50 – 150 mg AC and 30 ppm oxine pH: 8 Equilibration time: 1 h (shaking) EDXRF determination	RSD = 5 – 10% Sample volume: 1 L Capacity: 0.5 mM MOx_2 g^{-1} Recoveries: 70 – 100%	37
Activated carbon	Water	Total Se and selenite	Total Se determined after refluxing with thiourea and adsorbing onto AC Se^{IV} reduced with L-ascorbic acid and determined as elemental Se Mass of activated carbon: 100 mg Equilibration time: 15 min EDXRF determination	LOD = 50 – 60 ng L^{-1} RSD ~ 10% (at 0.5 – 1μg Se L^{-1}) Counting time: 3000 s Sample volume: 1 L Recovery ~ 85%	35
SA-2 cation exchange resin (*Amberlite IR-120*) loaded papers	Sea water, urine, coal and urban particles	Ni, Mn, Fe, Zn, Cu, Pb, Ti	Coal and urban particulate digested prior to loading the filters pH: 2 No. of filtrations: 7 EDXRF determination	LOD < 0.2 μg cm^{-2} RSD = 2.1 – 23.5% Counting time: 5000 s Capacity: 0.25 mEq	46

Retention Media	Samples	Analytes	Procedure details	Analytical characteristics	Ref.
Zn-diethyldithiocarbamate	Water	Ni, Co, Mn, Cu, Pb, Cd	Sample thickness: 0.5 mm pH: 3 – 4 WDXRF determination	LOD = 2 – 3 μg L^{-1} RSD = 3 - 16% Sample volume: 100 – 500 mL Recovery > 90%	38
Chelating 2,2'-diaminodiethylamine (DEN) on cellulose filters	Drinking and river water	Cr, Mn, Ni, Cu, Zn, Pb, U	pH: natural (> 5 – 6) Filtration rate < 1 mL min^{-1} cm^{-2} EDXRF determination	LOD ~ 0.5 μg L^{-1} RSD ~ 10% Counting time: 3000 s Sample volume: 100 mL Capacity: 3 μEq cm^{-2} filter Recovery > 90%	39
Anion exchange filter paper	Plant material	Mo, W, Nb, Ta	Sample (1 g) digested with HNO_3, H_2O_2 and HF WDXRF determination	LOD = 0.3 – 0.6 μg g^{-1} RSD = 3 - 8% Recovery > 95%	40
Expapier F-2 chelating filter paper	Urine	Mn, Ni, Cu, Zn	Urine decomposed with HNO_3 and H_2O_2 Filter thickness: 0.27 mm pH: 6.5 Internal standards: Cr and Ga EDXRF determination	LOD (μg L^{-1}): Cr (3), Mn (2), Fe (30), Co (2), Ni (0.2), Cu (3), Zn (1) RSD ~ 10% Linear range (μg L^{-1}): 0 – 60 for Cr, Mn, Ni, Cu and 0 – 600 for Zn Counting time: 2000 s Sample volume: 40 mL	41

Retention Media	Samples	Analytes	Procedure details	Analytical characteristics	Ref.
SB-2 anion exchange filter paper	Plant material	Ag, Bi, Cd, Hg, Tl	WDXRF determination	LOD = 0.2 – 0.6 μg g^{-1} RSD = 6 - 30% Counting time: 100 s Recovery > 95% for V < 50 mL	42
SA-2 cation exchange filter paper	Plant material	Pb	WDXRF determination	LOD = 0.2 μg g^{-1} RSD = 7 - 25% Counting time: 100 s Recovery > 95% for V < 100 mL	42
Expapier F-1, F-2 and *F-3* chelating filter paper	Fresh waters	Na, Si, S, Cl, K, Ca, Fe, Cu, Zn, Br, Sr	F-1 is used to collect common cations, F-2 for heavy metals and F-3 for common anions Filtering procedures: 200 mL (pH 2 - 5) through F1 750 mL (pH 6.5 – 7.0) through F2 300 mL (neutral pH) through F3 Flow rate: 10 – 20 mL min^{-1} EDXRF determination	LOD = 3.3 – 43 μg RSD = 8 – 26% Linear range: 0 – 100 μg Counting time: 1000 s Capacity: F-1 – 6.0 mg Na^{+} / sheet F-2 – 10.0 mg Cu^{2+} / sheet F-3 – 10.2 mg Cl^{-} / sheet	43
OSTSORBOXIN chelating ion exchanger (oxine bound to pearly cellulose)	Drinking water	Cr, Fe, Cu, Zn, Pb	Exchanger (3 g) used in columns of dimensions 200 mm × 7 mm and then pelletised Radionuclide XRF analysis	RSD ~ 1 – 18% Sample volume: 2 L	49

Retention Media	Samples	Analytes	Procedure details	Analytical characteristics	Ref.
Activated charcoal	Waste water	P	Analyte coprecipitated as phosphate with $Fe(OH)_3$, pH 9, and retained on activated charcoal (100 mg) Precipitate needs to coagulate for 3-6 h EDXRF determination	LOD = 0.9 mg P / g activated charcoal RSD = 3.9% Linear range: 0.09 – 3 mg P Counting time: 300 s Sample volume: 50 - 500 mL Recovery ~ 95%	53
MnO_2 loaded anion exchange resin (*Dowex 1-X8*)	Water	U	Anion exchanger Dowex 1-X8 (400 mesh) is loaded with 67% MnO_2 Resin mass: 2 g pH: 6.5 WDXRF determination	LOD = 0.3 ppb U Linear range: 12.5 – 125 ppm Counting time: 1000 s Sample volume: 15 L Recovery: 87% for 2 g of resin	52
Zr activated charcoal	Water	Cr^{III}, Cr^{VI}	Retention of Cr^{VI} on Zr activated charcoal at pH 4 Retention of Cr^{III} on Zr activated charcoal at pH 9, aided by coprecipitation with $Fe(OH)_3$ EDXRF determination	LOD = 0.01 – 0.04 mg L^{-1} RSD < 10% Linear range: 0 – 4.5 mg L^{-1} Counting time: 100 s Sample volume: 100 mL	54
Chelating agents retained on *Amberlite XAD* resins, 100-200 mesh	Synthetic samples	Ce, La, Pr	Mass of exchanger: 10 g pH: 7 WDXRF determination	RSD = 1 - 5% Linear range: 0 – 50 mg L^{-1} Counting time: 100 s Capacity: 0.05 mg Ce g^{-1} Recoveries > 97%	51

Retention Media	Samples	Analytes	Procedure details	Analytical characteristics	Ref.
Textile-bound polyacryloamidoxime chelating agent	Water	Cu, Pb	The *passive sampling* method is employed: Concentration of analyte expressed as a weighted function of the time of analysis The sampling times are long (days)	Sensitivity in the mg L^{-1} range Best RSD = 6% for Pb at 15 days Uptake rates: 600 mg/day for Cu and 200 mg/day for Pb	50
Activated alumina	Liquid hazardous waste	Br, Cl, I, P, S, Cr, Cu, Ni, V, Zn, As, Cd, Hg, Pb, Sb, Se, Sn, Tl	Mix 5 g of sample with 15 g of activated alumina in plastic bottle Equilibration time: 30 s Transfer directly into XRF sample cup EDXRF determination	LLOD = 3 – 17 mg kg^{-1} RSD < 10% for most elements Counting time: 50 – 150 s Recovery > 73% Total analysis time < 15 minutes for more than 20 elements	55

1.5 AIMS OF THE STUDY

Although XRF spectrometry is, in principle, an ideal technique for direct and rapid determinations, it is clear, as discussed in previous sections that the quantitative analysis for most common samples is far from simple. The use of solid retention media as a sample support for XRF offers the potential to overcome instrumental and sample limitations of the technique at the same time. In reality, many of the methods developed seem to overcomplicate an analytical procedure and many suggest a limited understanding of their real analytical boundaries.

It is evident that the physical and chemical characteristics of certain absorbers such as resins are still not fully understood. In order to overcome some of the problems encountered a greater emphasis in the use of wavelength dispersive instruments has been seen in the literature in preference to energy dispersive instruments.

Despite the characteristics of resin loaded paper filters being studied in great detail (mostly because of their 'apparent' status as the 'ideal sample preconcentration media for XRF analysis'), little is known of the characteristics of ion exchange and chelation resins in bulk; even those that are widely used as support for flow injection or chromatographic separations. This is, in part, because no in-depth physical / physico-chemical study has been performed under these conditions or with this presentation mode in mind. These resins may offer greater analytical capabilities than the filters with the added advantages of a larger capacity, improvements in homogeneity and a reduction of the very long equilibration times (ranging from hours up to several days). The selectivity of the resins towards metal and non-metal

species may be improved by i) operating at particular pHs, ii) utilising bound chelating agents and iii) using different particle size exchangers, which take advantage of the increased sensitivity of the technique without adding extra time or greater complexity to the analysis.

Therefore, the aims of this work were to i) investigate suitable, rapid methods of retention of trace metal species on commercially available ion exchange and chelating resins prior to their determination by x-ray fluorescence spectrometry; ii) to obtain and explain chemical and structural information of these retention systems, in order to acquire an understanding of their advantages and limitations as potential aids for XRF analysis; iii) to use this information for the development of new methodologies for extending the applications of those already existing, especially in the field of elemental speciation and iv) to study the possibility of direct determination of chemical species retained on ion exchangers after measuring their relative $K\alpha$ / $K\beta$ intensities by x-ray fluorescence spectrometry. The emphasis of the work was upon the use of energy dispersive x-ray fluorescence spectrometry as a rapid and multielemental detection system. However, wavelength dispersive XRF was also utilised in order to obtain additional data.

2. *INSTRUMENTATION*

Chapter 2. Instrumentation

2.1 Instrumentation for Energy Dispersive X-ray Fluorescence Spectrometric Analysis

This section describes the main features associated with the components of a typical energy-dispersive spectrometer, which is illustrated in Figure 2.1. Specific details of the two EDXRF instruments used in these investigations are displayed in Table 2.1. The instrumental parameters used in the analyses were selected after optimisation for each element on each sample type. When multielemental analysis was performed, compromise conditions were used.

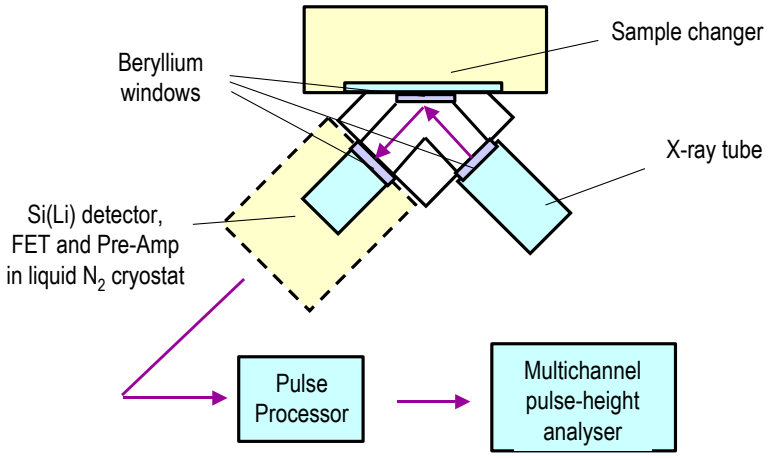

Figure 2.1 Schematics of an EDXRF spectrometer

Table 2.1 **Instrumentation for EDXRF spectrometry**[56, 57]

Instrument	
Philips PV9500/9100 XRF spectrometer (EDAX International Inc., Praire View, Illinois, USA).	
General	
Optics	Inverted
X-ray incidence angle	45°
Take-off angle	45°
Maximum irradiated sample surface	22 mm diameter
X-ray generator	
Voltage	0 - 50 kV
Current	0 - 500 μA
X-ray tube	
Target	Rh
Window	Be (125 μm)
Filters	
Three available	Rh, Ti, Ni
Detector	
Si(Li) crystal	
FET pre-amplifier	
Liquid N_2 Dewar	
Resolution	180 eV @ MnKα (5.9 keV)

Instrument	
Link Analytical XR300 XRF spectrometer (Link Analytical Ltd., High Wycombe, Bucks, UK)	
General	
Optics	Inverted
X-ray incidence angle	45°
Take-off angle	45°
Automatic sample changer	16 samples
X-ray generator	
Voltage	0 - 30 kV (Resolution: 1kV)
Current	0 - 500 μA (Resolution: 10 μA)
X-ray tube	
Target	Ag
Window	Be
Filters	
Five available	Ag (0.05 mm), Ag (0.125 mm), Cu, Al and cellulose
Detector	
Si(Li) crystal	
FET pre-amplifier	
Liquid N_2 Dewar	
Resolution	150 eV @ MnKα (5.9 keV)

2.1.1 ***X-ray tube***

As discussed in Chapter 1, x-ray fluorescence in elements may be induced by the bombardment of the specimen containing those elements with highly energetic particles. A variety of sources can be used for this purpose, e.g., high energy electrons, protons, synchrotron radiation and γ-rays. However, this section will concentrate on the source used for the production of EDXRF spectra in these investigations, i.e., the *x-ray tube*, also known as the *Coolidge tube*.

Schematics of this source can be seen in Figure 2.2. It consists basically of a highly evacuated tube containing a filament, often made of tungsten, which acts as a cathode. An electric circuit heats the filament causing it to emit electrons by a process known as *thermionic emission*[8]. This circuit enables control of the intensity of x-rays used for excitation. A high voltage is applied between the cathode and a metallic anode or target, in order to direct and accelerate the electrons towards the anode. A metallic screen called a *focusing cup* and kept at a more negative voltage, aids the process by directing electrons towards the anode. X-rays are produced at the anode from the collision. The energy of these x-rays is determined by the potential applied. The x-rays produced are emitted in all directions but may only leave the tube through a beryllium window, which is transparent to the radiation. The metal case of the tube absorbs the x-rays emitted in any other direction.

The production of x-rays is a highly inefficient process; only 1% of the electrical power is converted to radiant power. The remainder is degraded to heat.

Modern equipment overcomes this problem by operating with considerably lower powers and the use of significantly more sensitive detectors.

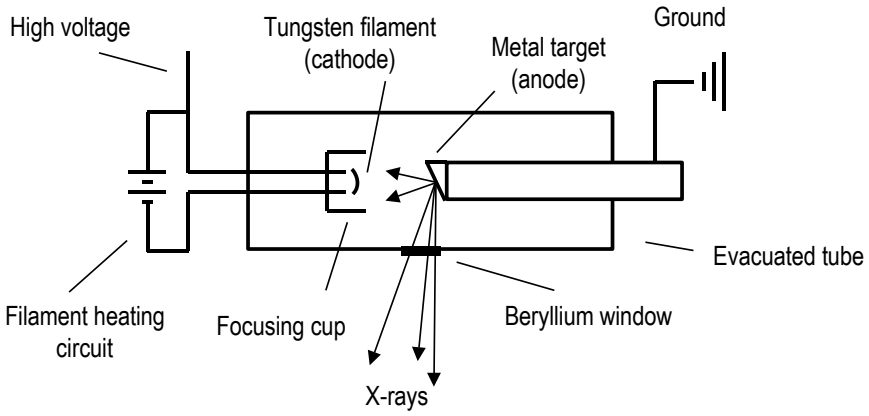

Figure 2.2 Schematics of an x-ray tube

2.1.2 Primary x-ray beam filters

The use of primary filters in EDXRF allows a reduction of the continuous emission from the tube that contributes to the scattered background underneath the analytes. This would improve the sensitivity of the determination, provided that the tube emission that excites the analytes is not too severely reduced at the same time. In this respect, the thickness of the filter is critical. It is often found that the best filter for improving the peak to background ratio on one element in a certain matrix reduces this ratio for another element. In this case compromise conditions or separate analyses would be required.

2.1.3 The Si(Li) detector

The *Si(Li) detector*, also known as *semiconductor* or *solid-state detector*, is the characteristic detection device of the energy dispersive x-ray spectrometer. It is based on the principle of the *photoelectric effect* and consists of three units: the Si(Li) crystal, a pre-amplifier and a cryostat.

2.1.3.1 The Si(Li) crystal

Intrinsic semiconductors, such as pure crystalline silicon, have a *valence band*, completely occupied with electrons and an empty *conduction band* of higher energy. The energy gap between the bands is small enough to allow conductivity under certain circumstances[8]. Thus, the existence of impurities such as Ga, As and boron (B) acting as electron donors and acceptors, increases the conductivity by adding electrons or creating electron gaps.

E.g.: As $\Rightarrow$ + 1 e^- $\Rightarrow$ *n-type* semiconductor

Ga $\Rightarrow$ - 1 e^- (electron gap) $\Rightarrow$ *p-type* semiconductor

The crystal used in the detector is a p-type semiconductor where the original acceptor impurities in the crystal (mainly B) are neutralised by drifting it with lithium, a very small atom that easily diffuses through Si. The Li atoms provide

donor bands that compensate for the electron gaps in the crystal, reducing its conductivity. Eventually, three layers will exist in the crystal, as seen in Figure 2.3: i) the original p-type Si layer that faces the x-ray source and is coated with gold film for electrical contact; ii) a central intrinsic Si(Li) region that has a high resistivity in comparison with the other two layers, because of Li ions being less mobile than the holes they displace and iii) a newly formed n-doped Si layer in which the Li concentration is high; this is an electron donor area[7].

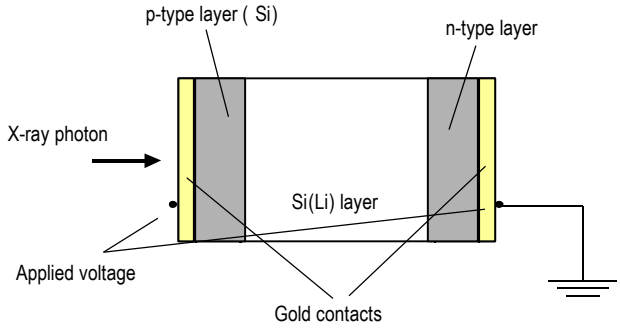

Figure 2.3 A schematic representation of a typical Si(Li) detector diode

When x-ray photons enter the Si crystal, electrons from the valence band 'jump' to the conduction band absorbing energy. The electron gap in the valence band behaves as a positive charge and enhances the conductivity of the silicon. Similarly, the conduction band electrons are mobile and can act as charge carriers. If a potential (~ 1000 V) is applied across the crystal, a charge pulse accompanies the absorption of each photon. The size of the pulse is directly proportional to the energy of the incident photons[9].

2.1.3.2 The pre-amplifier

The signal to noise ratio in Si(Li) detectors is still quite low and pre-amplification of the signal prior to conventional amplification is required. It is also necessary to convert the charge pulse originated in the crystal into a voltage pulse[57]. The field effect transistor (FET) is the most common type of pre-amplifier because of its low noise characteristics. It is kept inside the cryostat to reduce this noise further[8]. The FET integrates the charge coming from the crystal and produces an output voltage. To avoid increasing the background noise the method of *pulsed optical feedback* is used, which means the FET is not reset to zero after each pulse. Instead, successive pulses are accumulated until a voltage is reached at which non-linearity could occur. At this point, a light emitting diode (LED) is switched on and the FET returns to the baseline. A few x-ray photons may be missed during the reset time.

2.1.3.3 The cryostat

A pure Si crystal has a low intrinsic conductivity, which is essential for its use as a detector. When the conductivity increases, the applied voltage produces constantly flowing 'leakage' currents and therefore, high background signals. Keeping the Si(Li) detector inside a cryostat, at the temperature of liquid nitrogen (77 K), helps to reduce the conductivity, hence decreasing the electronic noise. Low

temperatures also avoid reverse drifting of the Li atoms[8]. Modern Si(Li) detectors only have to be cooled during use.

2.1.4 Pulse processing

The step-shaped pulses from the pre-amplifier are passed into the pulse processor for their final amplification and preparation for measurement. The original pulse is triplicated and sent in three different directions as shown in Figure 2.4.

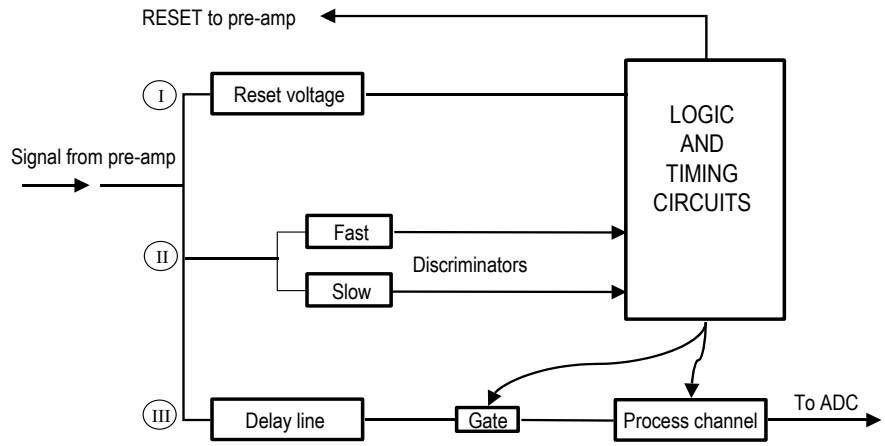

Figure 2.4 Schematics of the pulse processor

I. This is the *reset* line that sends a signal to the pre-amp when the output voltage has gone over a certain level.

II. The *fast* channel is the basis of the pile-up rejection circuit that ensures pulses are far enough apart to be measured accurately. It discriminates between pulses arriving at closer than 1μs intervals. The *slow* channel separates true signals from noise fluctuations.

III. This is the *processing* channel. It holds the pulse until signals from the slow and fast discriminators determine whether it should be measured or rejected. If the pulse is valid, the processing channel will integrate it for a fixed period of time and then hold it for measurement by the *analogue to digital converter* (ADC). The channel is then reset.

Certain operations in the pulse processor require that the measurement of pulses stops. This occurs while a pulse is being processed and also when the pulsed optical feedback device i.e., the LED, is in operation. The percentage of time for a given acquisition time that the processor is closed is known as *dead time* and it is proportional to the number of x-rays reaching the detector. For efficient operation, the dead time should be kept below 50%.

2.1.5 Pulse measurement

The processed pulses are measured as a function of time by the ADC. The ADC uses the principle that a high energy pulse will take longer to decay, at a constant rate, than a low energy pulse. In this manner, it measures the pulse amplitude and converts it to a digital number that corresponds to a location in the memory of a *multi-channel analyser* (MCA), commonly, a computer. Each time that

a pulse of the same ‘characteristics’ is measured, the MCA adds one count to that location. The number of counts can be stored simultaneously for 1024 separate energy channels, allowing acquisition of a whole spectrum.

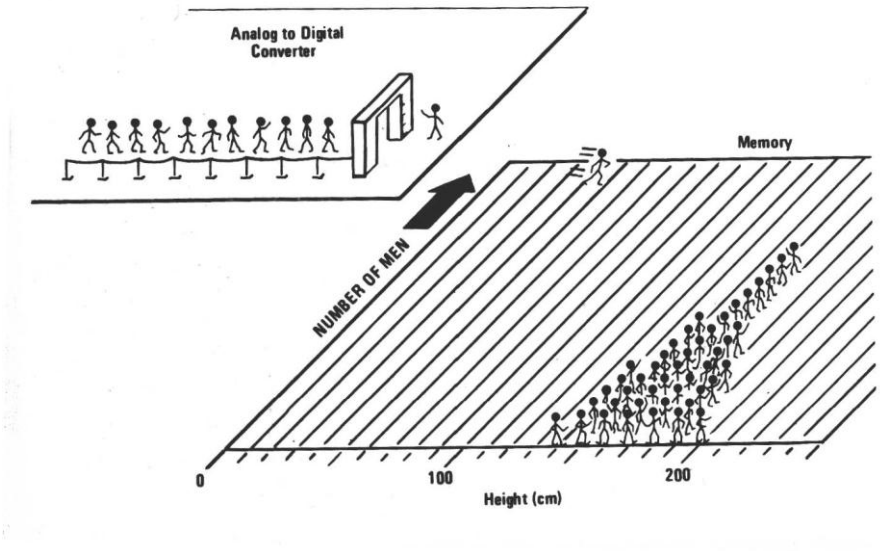

Figure 2.5 Analogy representing the pulse-height sorting function in the MCA[4]

The process can be easily explained by using the analogy shown in Figure 2.5. In the picture, men represent pulses that need to be classified according to their height. As the men arrive at the doorway, their height is measured and they are assigned to the appropriate lane in the square. Viewed from above, the histogram formed on the floor (number of men vs. height) is the equivalent of an x-ray spectrum.

2.2 OTHER INSTRUMENTATION

Determination of the analytes in aqueous solutions was performed using a Perkin-Elmer Optima 3000 Radial ICP-AE spectrometer (Perkin-Elmer Ltd., Beaconsfield, Bucks., UK). The instrument is equipped with an echelle grating optical system and a segmented-array charge-coupled-device detector (SCD). Descriptions of the dispersive device and the solid state detector can be found in the literature[58, 59]. Details of the instrumental set-up and typical operating conditions are shown in Table 2.2. By using compromise conditions and, as a result of the instrument featuring an echelle-based polychromator and a SCD, it is possible to acquire all the spectral data simultaneously, including background signals, which are necessary for the determination of the analytes. The wavelengths used in each analysis are shown in the relevant section.

When only a few elements had to be quantified and the sensitivity was sufficient, flame atomic absorption spectrometry was employed instead of ICP-AES. In this case, the analysis was performed using a GBC 902 flame atomic absorption spectrometer (GBC Scientific Equipment PTY Ltd., Victoria, Australia). Operating conditions varied depending on the analyte and will be listed as required in the following chapters.

Electron microscopy work was carried out using a JEOL 6100 scanning electron microscope (JEOL, Tokyo, Japan), equipped with a cryogenic cell CT1500 (Oxford Instruments, High Wycombe, Bucks., UK) and an Oxford Instruments ISIS 200 energy dispersive x-ray analyser for x-ray microanalysis and digital mapping (Oxford Instruments, High Wycombe, Bucks., UK). Images of the resins were also obtained using a JEOL 5300 scanning electron microscope (JEOL, Tokyo, Japan).

For additional XRF work, a Philips PW1404 wavelength dispersive XRF spectrometer (Philips Analytical X-Ray, Cambridge, UK) was used. The instrument is equipped with a fine collimator, LiF 200 dispersing crystal and both flow and scintillation detectors. Average operating conditions were 50 kV and 60 mA.

Table 2.2 **Operational parameters for the Perkin-Elmer Optima 3000 ICP-AES instrument**

RF Generator		
Frequency	40 MHz, free running	
RF Power	1000 W	
Sample Introduction System		
Peristaltic Pump	Gilson Minipuls 3, computer operated	Anachem, Luton, Beds., UK
Nebuliser	Cross-flow	Perkin-Elmer Ltd., Beaconsfield, Bucks., UK
	Ebdon v-groove (high solids)	P.S. Analytical Ltd., Kent, UK
Spray Chamber	Ryton Scott double-pass	Perkin-Elmer Ltd., Beaconsfield, Bucks., UK
Torch	Demountable quartz torch with 4 mm observation slot and 1.5 mm i.d. alumina injector	Perkin-Elmer Ltd., Beaconsfield, Bucks., UK
Argon Flow Rate		
Plasma	17 L min^{-1}	
Auxiliary	1 L min^{-1}	
Nebuliser	1 L min^{-1}	
Spectrometer		
Viewing Height	15 mm above load coil	

3. *PHYSICO-CHEMICAL STUDIES FOR THE CHARACTERISATION OF SOLID RETENTION MEDIA FOR EDXRF ANALYSIS*

Chapter 3. Physico-Chemical Studies for the Characterisation of Solid Retention Media for EDRXF Analysis

3.1 INTRODUCTION

The solid retention media used in these investigations are mainly synthetic resins consisting of a cross-linked organic polymer containing functional groups. These groups have the potential to be ionised and become active sites for the retention of the species of interest. The three ion-exchangers investigated, Dowex 50W-X8, Dowex 1-X8 and Chelex-100, share the same structural backbone where linear polystyrene has been cross-linked with 8% divinylbenzene (DVB). The resins are manufactured in the shape of small spheres, which are treated with different reagents in order to incorporate the desired functional group. This group is responsible for the properties of cation, anion and chelating exchange that each resin possesses.

Sharing the same organic structure makes the characteristics of the three resins very similar. This can be observed in Table 3.1, which presents a summary of data characteristic of the exchangers. However, any slight variation in these characteristics may be of paramount importance when selecting the appropriate resin for use in analysis. Aside from the different functional groups, other noticeable dissimilarities can be observed in the capacity and the moisture content of the resins.

Table 3.1 **Characteristics of the solid retention media used in this study**[60, 61, 62]

CHARACTERISTIC	Dowex 50W-X8	Dowex 1-X8	Chelex-100
Main structure	Divinylbenzene-polystyrene	Divinylbenzene-polystyrene	Divinylbenzene-polystyrene
Functional group	$-SO_3H$	$-CH_2NMe_3Cl$	$-CH_2N(CH_2COONa)_2$
Ionic form	H^+	Cl^-	Na^+
Bulk density (g mL^{-1})	0.80	0.71	0.73
True density* (g mL^{-1})	1.0 - 1.4	1.0 - 1.4	1.0 - 1.4
pH stability	0 - 14	0 - 14	2 - 14
Mesh range / Particle size (μm)	20 - 50 / 297 - 840 100 - 200 / 74 - 149 200 - 400 / 38 - 74	100 - 200 / 74 - 149	100 - 200 / 74 - 149
Total dry capacity (mEq g^{-1})	4.8	3.5	2.0
Moisture content (% by weight)	51 - 54	43 - 48	68 - 76

* The 'true density' values are the result of experimental measurements on the resins

A resin such as Chelex-100, which contains paired iminodiacetate ions, acting as chelating groups that bind polyvalent metal ions, has the main advantage of its high selectivity for transition metal ions[21]. Tables 3.2 and 3.3 show respectively the selectivity factors of Chelex-100 and Dowex 50W-X8 for some metal cations compared with the affinity of these resins for Zn(II).

It is apparent that the selectivity factors for Dowex 50W-X8 are very close, even for metal ions of totally different characteristics like Na^+ (1.29) and Mn^{2+} (1.18). Hence, the efficient separation of these metals, when Dowex 50W-X8 is used, is unlikely. The selectivity factors for Chelex-100 vary greatly depending on the

metal involved. This would result in quick and effective separations of certain elements, mainly transition metals, when using the chelating exchanger.

Table 3.2 **Selectivity factors for metal cations and Chelex-100[60]**

Hg^{2+}	1060	Zn^{2+}	1.00	Ba^{2+}	0.016
Cu^{2+}	126	Co^{2+}	0.615	Ca^{2+}	0.013
UO_2^{2+}	5.70	Cd^{2+}	0.390	Sr^{2+}	0.013
Ni^{2+}	4.40	Fe^{2+}	0.130	Mg^{2+}	0.009
Pb^{2+}	3.88	Mn^{2+}	0.024	Na^{+}	0.0000001

Table 3.3 **Selectivity factors for metal cations and Dowex 50W-X8[63]**

Li^{+}	0.65	Mg^{2+}	0.95	Mn^{2+}	1.18
H^{+}	0.82	Zn^{2+}	1.00	Ca^{2+}	1.49
Na^{+}	1.29	Co^{2+}	1.08	Sr^{2+}	1.88
K^{+}	1.88	Cu^{2+}	1.12	Pb^{2+}	2.86
Ag^{+}	5.54	Cd^{2+}	1.12	Ba^{2+}	3.32
UO_2^{2+}	0.70	Ni^{2+}	1.13	Cr^{3+}	1.65

However, the values shown in these tables should only be taken as a guideline and they may change for each real system considered depending on the pH, ionic strength and which species are present in the solution. Hence, it may be possible to change the conditions of the ion exchange process to facilitate a selective separation for certain metals. The effect of pH on the retention and separation of metals using ion-exchangers is experimentally studied and discussed in Chapters 4 and 6.

Selectivity is obviously not the only factor that needs to be considered when choosing or making use of an ion exchanger. In terms of the capacity of the exchanger, i.e., the number of milliequivalents of the metal that will be retained per gram of exchanger, Dowex 50W-X8 (4.8 mEq g^{-1})[61, 62] may be preferable to Chelex-100 (2.0 mEq g^{-1})[60]. Furthermore, the high moisture content in Chelex-100 (68-76%)[60] makes it absolutely necessary to ensure that the resin is dried before its use for XRF analysis. Wet resins may cause inaccurate results, poor precision in the analysis and increase the risk of exceeding the capacity of the exchanger. Experimental studies on the capacity and moisture content of the ion-exchangers are examined in Chapters 4 and 6.

Despite their importance in the application of ion-exchangers as solid retention media for XRF analysis, the characteristic parameters described above are not always evaluated. Furthermore, no examples are seen in the literature of full and critical assessments of the physico-chemical characteristics of the resins and how they may affect the determination.

This chapter investigates those characteristics of the resins and the possible effects associated with their application as substrates for XRF analysis. The parameters studied included the distribution of active sites and collected ions in the exchangers, the effect of the particle size, the effect of the retention method used (batch or column) and the effect of the sample volume. The effect of other characteristics such as pH, exchange capacity and the relationship between intensity of fluorescence and mass of resin were also investigated and the results discussed in following chapters.

3.2 CHARACTERISATION OF SOLID RETENTION MEDIA BY SCANNING ELECTRON MICROSCOPY, X-RAY ANALYSIS AND DIGITAL DOT MAPPING

3.2.1 Introduction

Although the resins Dowex 50W-X8, Dowex 1-X8 and Chelex-100 have been commercially available for several decades, there is only a limited amount of data regarding their physical characteristics and structure. Most of this information is general and not specific to the resin types used in the analysis. In order to have a greater understanding of the phenomena involved in the exchange of metal ions and their x-ray determination on and in the resin beads, there is a need for further and more tailored information.

Scanning electron microscopy was the technique chosen to obtain structural data of the ion-exchangers. Electron microscopy can be defined as the science and technology of using an electron beam to form magnified images of specimens[64]. When compared with optical microscopy, it has the advantage of a thousand-fold increase in resolving power, as well as improvements in depth of field and depth of focus[65].

A scanning electron microscope works by moving a beam of focused electrons across the surface of a specimen and using the electrons emitted by the sample (commonly secondary electrons are monitored) to form a three-dimensional image of the object on a monitor[64, 65].

It must be noted that, as explained in Chapter 1, the interaction of x-rays with matter is not a surface phenomenon, because a certain degree of penetration into the specimen occurs. Therefore, it is not sufficient to obtain information regarding the

outer layer of the resin beads. It is also necessary to investigate the core of these particles and to establish whether their nucleus is only an inert support for the exchanging material on the surface, or whether ion exchange occurs also inside the bead. The experimental work completed to obtain this information is reported in the following sections.

3.2.2 Experimental

3.2.2.1 Chemicals and reagents

AnalaR grade $Ni(NO_3)_2.6H_2O$, $CrCl_3.6H_2O$, $K_2Cr_2O_7$ and $CuSO_4$ were all obtained from Merck (Poole, Dorset, UK). The water used was of ultra pure grade, Milli-Q, 18MΩ cm (Millipore, Bedford, Massachusetts, USA). Whatman filter paper No 1 was used to separate solid retention media from solutions.

The ion exchange resins Dowex 50W-X8 (H) and Dowex 1-X8 (Cl), 100 – 200 mesh, were obtained from Merck. The chelating resin Chelex-100, sodium form, 100 – 200 mesh, was purchased from Bio-Rad Laboratories (Hemel Hempstead, Herts, UK).

The embedding methacrylate resin was an in-house preparation obtained from Mr Paul Russell, Dept. of Biological Sciences, University of Plymouth, UK. The composition of this resin is described in section 3.2.2.5.

3.2.2.2 Instrumentation

Images of the resins were obtained using a JEOL 5300 scanning electron microscope (JEOL, Tokyo, Japan).

Electron microscopy work on analyte saturated resins was carried out using a JEOL 6100 scanning electron microscope (JEOL, Tokyo, Japan), equipped with a cryogenic cell CT1500 (Oxford Instruments, High Wycombe, Bucks., UK) and an Oxford Instruments ISIS 200 energy dispersive x-ray analyser for x-ray microanalysis and digital mapping (Oxford Instruments). The operating conditions used for the qualitative analysis are shown in Table 3.4.

Table 3.4 **Instrumental parameters used on the JEOL 6100 scanning electron microscope and the Oxford Instruments ISIS 200 energy dispersive x-ray spectrometer**

Voltage	*Beam Current*	*Working distance*	*Magnification*	*Acquisition time*
20 kV	1.5×10^{-9} A	39 mm	× 950	50 s

3.2.2.3 Sample preparation for obtaining images of the resins

For this experiment, approximately 10 g of sample resin (Chelex-100, Dowex 50W-X8 and Dowex 1-X8) were freeze-dried in order to remove the water that is attached to the exchangers in relatively high proportions (Table 3.1). The elevated

moisture content would hamper the acquisition of relevant information from the resins.

The samples were then mounted on to metals stubs, using adhesive paper and gold coated in a sputter coater to make them conductive.

The metal stubs containing the samples were placed on a multi-holder and introduced to the Jeol 5300 SEM. The sample chamber was then evacuated. A good image was obtained for each resin by adjusting contrast, brightness, focus and magnification. The image was then recorded photographically by means of the Polaroid® camera attached to the microscope.

3.2.2.4 Sample preparation and analysis of metal-loaded resins

The samples were prepared by stirring saturated solutions of Cr(III) as $CrCl_3.6H_2O$, Cr(VI) as $K_2Cr_2O_7$, and Cu(II) as $CuSO_4$ in ultra pure water with 5.0 g of Dowex 50W-X8, Dowex 1-X8 and Chelex-100 respectively. The mixtures were stirred for approximately 10 minutes. The resins were then separated from the aqueous phase by filtration, dried at 40 ^oC overnight and transferred to plastic containers.

Small quantities of the resins were placed on metal stubs and gold coated in the sputter coater. The specimens were then introduced to the JEOL 6100 scanning electron microscope. Images of the resins were taken and qualitative x-ray microanalysis and digital mapping performed on these samples.

3.2.2.5 Sample preparation and analysis of sections of the metal-loaded resins

Three resins (Dowex 50W-X8, Dowex 1-X8 and Chelex-100) were saturated, following the procedure described in the preceding section, with the exception of Dowex 50W-X8 which was saturated with a solution of Ni, as $Ni(NO_3)_2.6H_2O$, in order to make this resin more easily identifiable. A very small amount of each saturated ion-exchange resin was then embedded in methacrylate resin. The purpose of this was to offer support during ultramicrotomy and to retain the spatial organisation of the specimen section[65].

The embedding mixture consisted of two solutions A and B. Solution A is prepared by mixing 2-hydroxyethyl methacrylate (80 mL), 2-butoxy ethanol (15 mL) and benzoyl peroxide (0.5 g). Solution B acts as a catalyst for the methacrylate resin and is a combination of polyethylene glycol 400 (10 mL) and n,n-dimethylaniline (1 mL). The embedding preparation consists of solution A and B in proportions 50:1 A:B.

To complete the procedure, small amounts of the ion-exchange resins (tip of spatula) were placed into plastic moulds. The moulds were then filled with the embedding mixture (approximately 0.8 mL). The lids of the moulds were closed and the preparation was left to settle for 4 to 10 hours.

Once the blocks of resin were formed, ultrathin (< 100 nm) sections of the specimen were cut using an ultramicrotome equipped with a sharp glass knife. The

sections obtained were transferred to a glass slide, fixed with a drop of water and allowed to dry.

The specimens were carbon coated using a carbon string evaporator. This was preferred to gold coating because of carbon's low absorption of x-rays and to avoid peak overlaps from the gold L-series. Once in the JEOL 6100 scanning electron microscope, images of the sections were obtained and qualitative x-ray analysis and digital mapping performed.

3.2.3 Results and discussion

3.2.3.1 Resin images

Plates 3.1 (a) and 3.1 (b) show the close ups of photographic images obtained for Chelex-100 and Dowex 50W-X8 resins. A picture of Dowex 1-X8 is shown in Plate 3.1 (c). The images obtained from Dowex resins were identical and showed smooth surfaces, whereas those of Chelex-100 were rough and resembled a ball of wool. This indicates that, although the backbone of the three exchangers is the same, there are obvious morphological differences between them. These differences are likely to arise from the way in which the resin beads are prepared.

Experimental measurements of the diameter of the resins' beads, based on the SEM images, fell within the particle size range given by the manufacturers (75 – 150 μm). This can be observed in Plate 3.1 (c).

a)

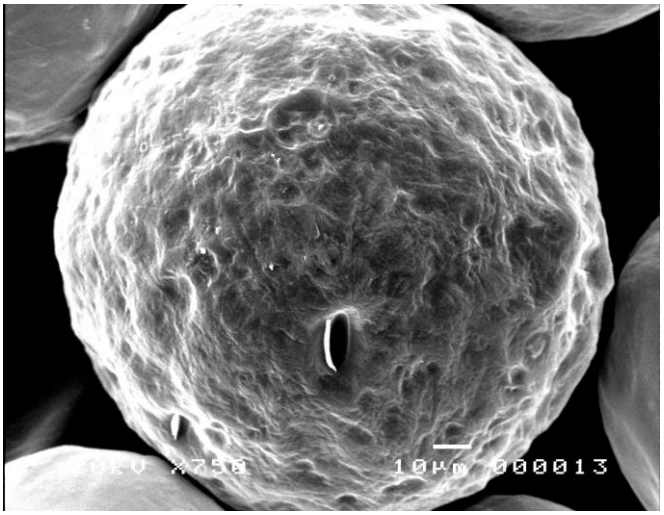

b)

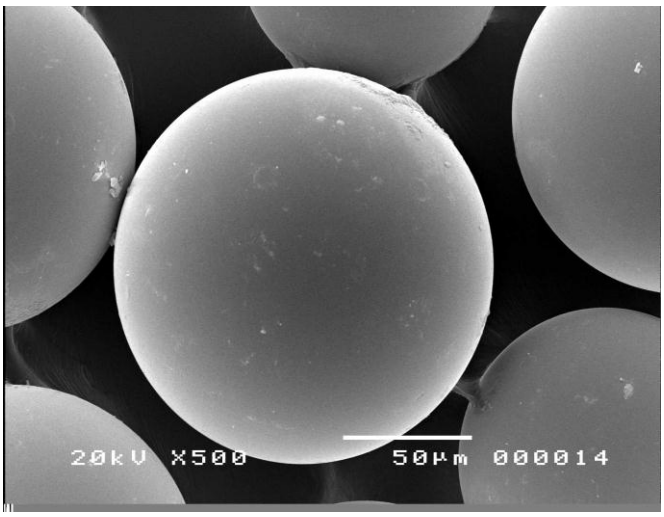

c)

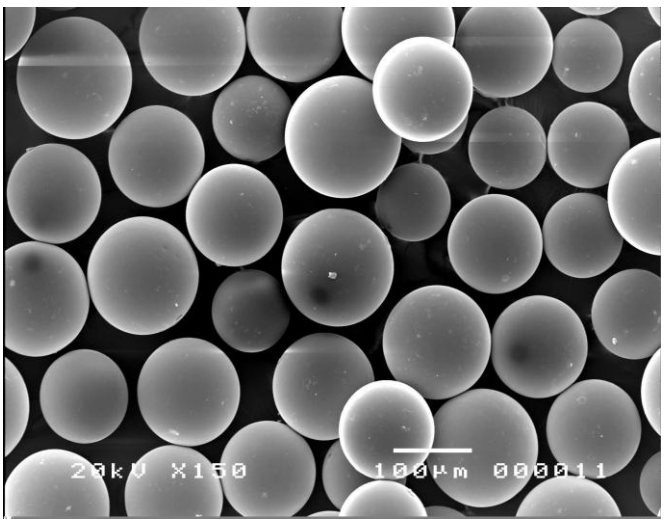

Plate 3.1 **Photographic images of a) Chelex-100, b) Dowex 50W-X8 and c) Dowex 1-X8 obtained by scanning electron microscopy**

3.2.3.2 Analysis of saturated resins

Plate 3.2 shows the digital dot maps from samples of resins that had been loaded to saturation with metals. The surface of Dowex 50W-X8 is evenly covered by chromium ions [Plate 3.2 (a)], that have been retained on the functional groups of the resin. These functional groups ($-SO_3H$) are identified by sulphur, one of the elements in their structure, [Plate 3.2 (b)]. The density of dots obtained for sulphur is higher than that of Cr. This may be explained by the excitation and detection efficiency for S being higher than that of Cr. Another contributing factor would be the presence of various Cr(III) species in the saturated solutions[66], i.e., $Cr(H_2O)_6^{3+}$, $CrOH^{2+}$ and $Cr(OH)_2^{+}$, which will displace respectively three, two or only one H^+.

Plate 3.2 (c) also shows an even distribution of Cr atoms on Dowex 1-X8. In this case it is not possible to monitor any of the elements in the functional groups of the resin, as they all have low atomic numbers. The x-ray spectrum for Dowex 1-X8 showed that the majority of Cl^- ions originally attached to the resin had been replaced by Cr(VI) anions. However, it was not possible to establish whether smaller quantities of Cl^- were still present because of the proximity of Au L-lines.

A uniform dispersion of copper on the surface of Chelex-100 was also observed and is shown in Plate 3.2 (d). As in the case of Dowex 1-X8 it is not possible to establish the position of the functional groups of the resin because of the low atomic number of the elements involved [$-CH_2N(CH_2COONa)_2$]. However, the presence of sulphur on the surface of Chelex-100 was noted from the x-ray spectrum of the resin. The distribution of this element is also homogeneous as shown in Plate 3.2 (e) and its origin is thought to be in the sulphate ions from the copper compound used to saturate the resin.

a)

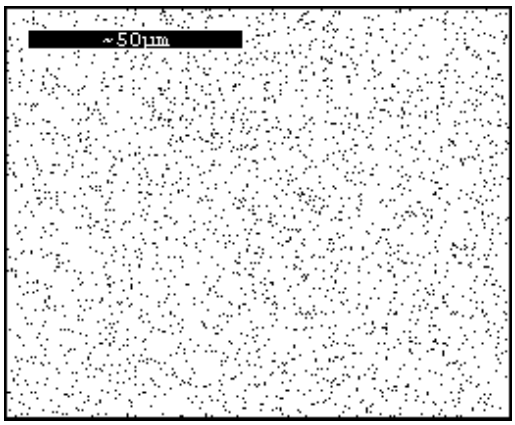

b)

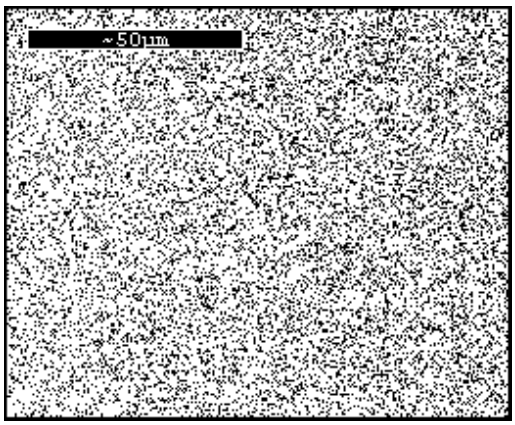

c)

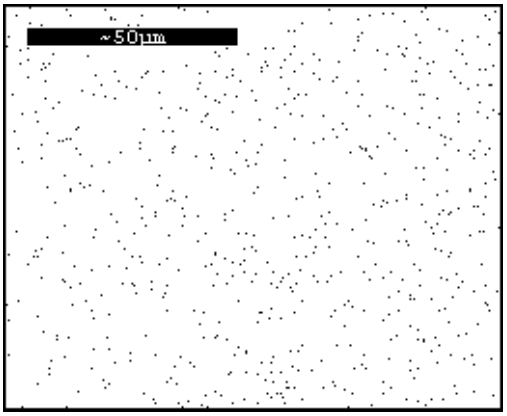

a) Chromium atoms on Dowex 50W-X8

b) Sulphur from Dowex 50W-X8

c) Chromium atoms on Dowex 1-X8

d) Copper atoms on Chelex-100

e) Sulphur atoms on Chelex-100

d)

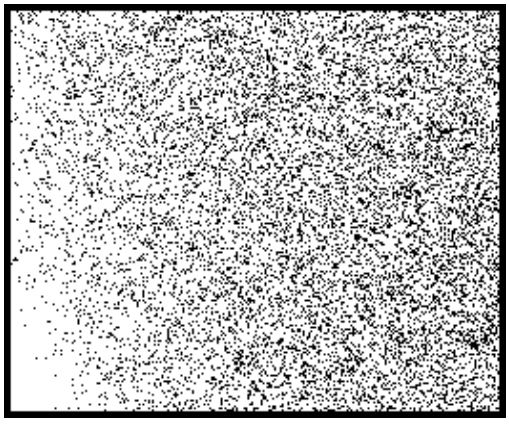

e)

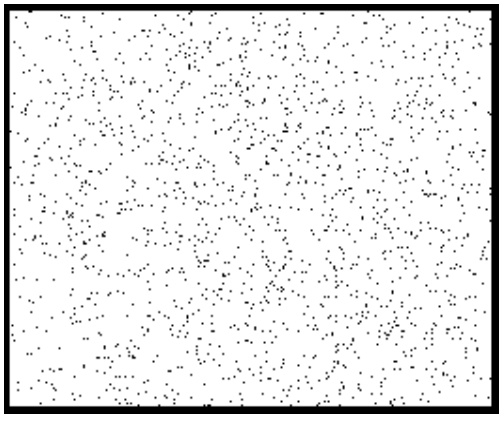

Plate 3.2 Digital dot maps of saturated ion-exchange resins beads

3.2.3.3 Internal structure of the resins

To study the inner structure of the resins, cryofracturing first was performed. This was achieved by placing small quantities of the resins on a metal support and immersing them in liquid nitrogen before introducing them to the cryogenic unit of the Jeol 6100 SEM. However, it soon became clear that once the resin bead had been fractured, this technique did not allow the interior of the resin beads to be distinguished from the surface layers with absolute certainty. This is shown in Plate 3.3. Thus, it was decided to obtain thin sections of the resin beads by using ultramicrotomy, as described in section 3.2.2.5.

The x-ray spectra obtained from the analysis of the sections with the energy dispersive system are shown in Figure 3.1. These spectra served to identify the metals in the samples to be used for digital mapping. With carbon coating on the samples, it was possible to see traces of Cl^- still present in Dowex 1-X8 [Figure 3.1 (c)], although the dot maps obtained show the chloride present in the section of the resin to be indistinguishable from the background [Plate 3.4 (e)].

Plates 3.4 (a), (d) and (g) show photographic images of the sections from the three resins analysed, i.e., Dowex 50W-X8, Dowex 1-X8 and Chelex-100, with little difference between them. Plate 3.4 (b) shows the even distribution of sulphur over an internal layer of Dowex 50W-X8. The spread of nickel is also uniform, as shown in Plate 3.4 (c) and these results are in agreement with those reported in the preceding

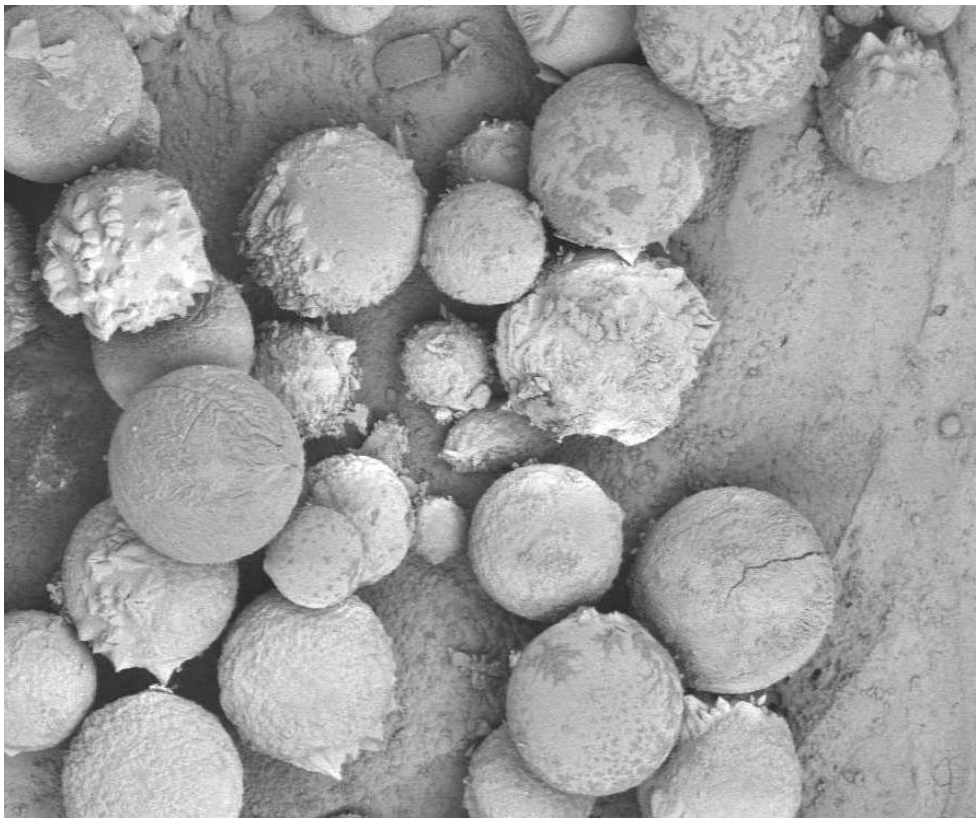

Plate 3.3 Close up of freeze-fractured beads of Dowex 50W-X8

a)

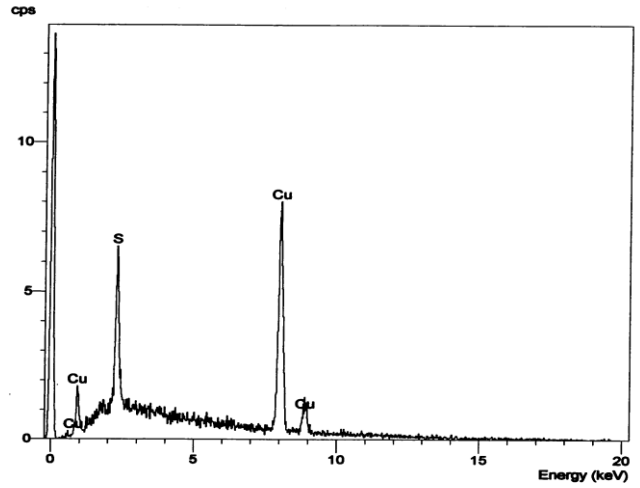

b)

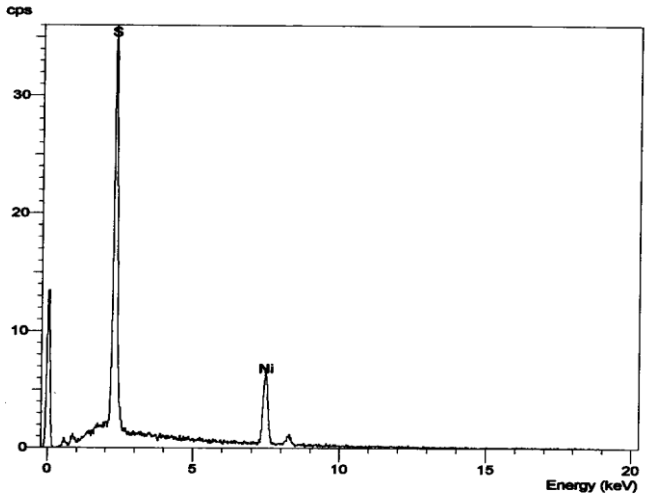

c)

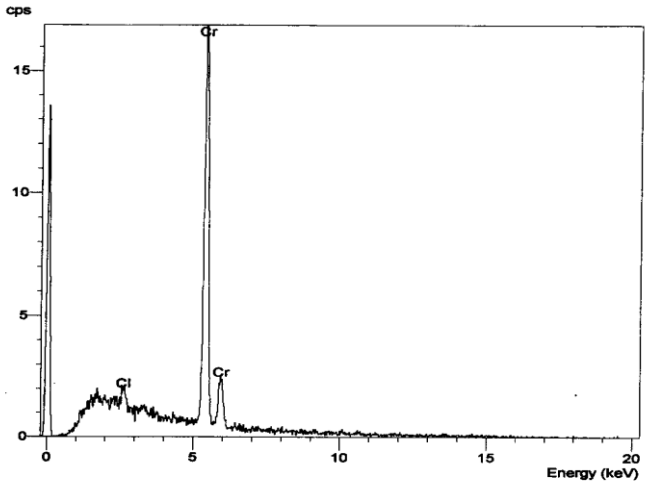

Figure 3.1 **X-ray spectra obtained from the microanalysis of sections of a) Chelex-100, b) Dowex 50W-X8 and c) Dowex 1-X8**

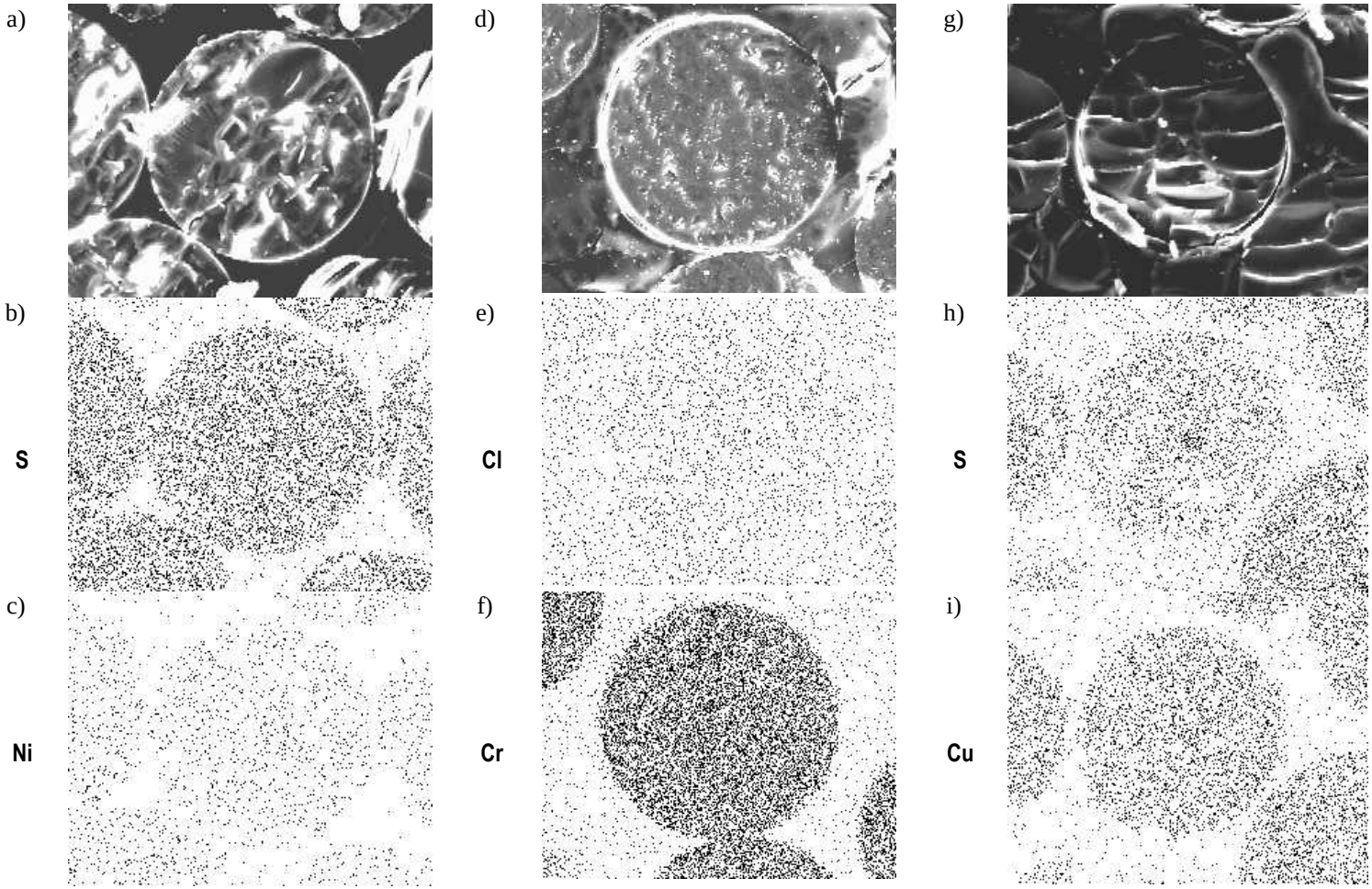

Plate 3.4 **Images and dot maps from the inner cores of the ion exchange resins Dowex 50W-X8 (a, b, c), Dowex 1-X8 (d, e, f) and Chelex-100 (g, h, i)**

section. The same patterns are found when looking at the dispersion of Cr(VI) on sections of Dowex 1-X8 [Plate 3.4 (f)] and Cu on sections of Chelex-100 [Plate 3.4 (i)] Thus, it is possible to say that the exchange of cations is not an exclusively surface phenomenon, but that there is retention of the analytes inside the resin beads. As was the case when looking at whole resin beads, sulphur was identified in the x-ray spectrum of the Chelex-100 sections [Figure 3.1 (a)]. Mapping of this element on the resin section is shown in Plate 3.4 (h). The dot maps visually display an image density for target elements in the resins, which correlate with the relative peak intensities from the spectra obtained using x-ray microprobe analysis.

The uniform distribution of active sites and retained metals on and inside the resins is of paramount importance, as it ensures the homogeneity of the presentation for EDXRF analysis.

3.2.4 Conclusions

Structural and distribution information regarding the solid retention media Dowex 50W-X8, Dowex 1-X8 and Chelex-100 was obtained by scanning electron microscopy, x-ray microanalysis and digital mapping.

Images of resin beads show morphological dissimilarities between the Dowex resins and Chelex-100.

The digital dot maps of saturated resin beads demonstrate that the distribution of functional groups and retained metal species on the surface of the resins is

homogeneous. The maps can also be used to obtain preliminary information on the proportionality between the number of active sites and the number of ions held by these sites.

Methacrylate resin embedding and ultramicrotomy sectioning proved to be successful procedures in the production of sample specimens, used to obtain information of the internal structure of the resins.

The microanalysis and mapping of the resin sections also shows uniform spread of functional groups and retained ions. It has been concluded that there is no qualitative difference between the surface and inner structure of the retention media and that ion-exchange occurs throughout the whole resin bead.

3.3 COMPARISON OF BATCH AND MINI-COLUMN SYSTEMS

3.3.1 Introduction

As discussed in Chapter 1, the most popular method for analyte retention on loose resins is the batch technique. For those applications that use paper or membrane bound resins, alternative techniques are employed. Several examples of the batch procedure when applied to different ion exchangers before their use in XRF analysis can be found in the literature[19-23, 45, 67]. Although less common, examples of the use of resins packed inside columns are also available[18, 24]. Some authors[20, 45, 67] state the reasons why use of the resins in batch form is more convenient to that of running the samples through resin columns. The benefits mentioned include faster

collection, smaller quantity of resin required and homogeneous distribution of the analytes on the resin. However, these statements have little or no experimental support. The lack of a comparative study that shows the advantages and limitations of both methods makes it difficult to assess critically which is the more efficient analytical approach to take, considering the final measuring technique of x-ray fluorescence.

In this investigation, the determination of copper on Chelex-100 by EDXRF was performed using batch and mini-column systems. The results obtained for these methods are then compared. The effect of the sample volume in the selection of the retention method is also discussed.

3.3.2 Experimental

3.3.2.1 Chemicals and reagents

Aristar grade concentrated nitric acid, sodium hydroxide pellets and glacial acetic acid, AnalaR grade sodium acetate and Spectrosol grade standard stock solution (1000 mg L^{-1}) of Cu were all obtained from Merck. Standard solutions of 5 mg L^{-1} Cr(VI) were prepared by dissolving 70.7 mg of $K_2Cr_2O_7$ (Merck) in 5000 mL of 0.01M HNO_3.

Whatman filter paper No 1 was used to separate ion exchange media and solutions. The sample cups and Mylar film were obtained from Philips Analytical X-ray (Cambridge, UK). The water used was of ultra pure grade, Milli-Q, 18MΩ cm (Millipore, Bedford, Massachusetts, USA).

Chelex-100, 100-200 mesh, Na^+ form was obtained from Bio-Rad Laboratories (Hemel Hempstead, Herts, UK). Dowex 1-X8, 100-200 mesh was obtained from Merck.

3.3.2.2 Instrumentation

The EDXRF analysis was performed using a Link Analytical XR300 XRF spectrometer (Link Analytical Ltd., High Wycombe, Bucks., UK). The operating conditions employed are shown in Table 3.5.

Table 3.5 **Instrumental parameters used on the Link Analytical XR300 XRF spectrometer for the analysis of Cu on Chelex-100 resin**

Voltage	*Current*	*Vacuum*	*Filter*	*Acquisition time*
20 kV	120 μA	off	none	100 s

Measurement of metal concentrations in aqueous solutions for the calculation of recovery data was achieved using a GBC 902 FAA spectrometer (GBC Scientific Equipment PTY Ltd., Victoria, Australia). The operating conditions used are shown in Table 3.6.

Table 3.6 **Instrumental parameters for the GBC 902 flame atomic absorption spectrometer**

Element	**Cr**	**Cu**
Wavelength	357.9 / 425.4 nm	324.7 nm
Band pass	0.5 nm	0.5 nm
Lamp current	6 mA	5 mA
Flame	Air-Acetylene (reducing)	Air-acetylene (oxidising)

3.3.2.3 Procedure

The mini-columns were prepared by slurry loading empty PTFE tubes (0.3 cm i.d. × 8.5 cm) with Chelex-100 in ultra-pure water using a plastic syringe. The columns were closed at both ends with plugs of glass wool and small portions of pump tubing. The PTFE tubes were weighed before and after adding the resin so the mass of Chelex-100 entrapped in each column could be determined. On average the columns contained 0.72 ± 0.02 g of wet Chelex-100 (n = 5). All the mini-columns were conditioned by pumping through 10 mL of 0.5 M sodium acetate and 12.5 mL of water.

A series of Cu standards with concentrations 0, 10, 20, 40 and 80 mg L^{-1} was prepared by appropriate dilution of a 1000 mg L^{-1} Cu standard stock solution to 50 mL with 0.2 M sodium acetate buffer. Aliquots of 25 mL were transferred into beakers and the pH of the solutions was adjusted to 5.0 ± 0.1 with NaOH and acetic acid. Each standard was pumped at 1.5 mL min^{-1} through a Chelex-100 mini-column

into a PTFE bottle that was kept for determination of the efficiency of the retention by comparison with the remaining 25 mL of standard by FAAS. Once all the solutions had passed through the resins the end plugs were removed from the columns and the contents emptied onto paper filters. The resins were then dried overnight in a drying cabinet at 40 ^{o}C, transferred into XRF sample cups fitted with Mylar film and analysed by EDXRF measuring the Cu Kα line.

To make the batch experiment comparable to the use of mini-columns in terms of concentration of Cu retained on the resin, a column with the same dimensions used before (0.3 cm i.d. × 8.5 cm) was filled five times with slurried Chelex-100 and then emptied into five beakers. The resin was mixed with standards prepared in the same manner and with the same concentrations as before. The pH was then adjusted to 5.18 ± 0.05 with NaOH and acetic acid and the mixtures stirred for 10 minutes. The resins were separated by filtration, dried at 40 ^{o}C and transferred into XRF sample cups. The filtrates were kept for analysis by FAAS.

3.3.3 Results and discussion

3.3.3.1 Comparison of batch and mini-column systems applied to the retention of copper on Chelex-100 and its determination by EDXRF

Figure 3.2 shows the calibration graphs obtained for the determination of Cu standards on Chelex-100 prepared in batch (a) and using mini-columns (b) by EDXRF. Each standard was analysed five times. The data shown in the graphs is the

mean value of the five replicates. Error bars for one standard deviation are also included in the figure, but are too small to be seen.

The excellent linearity obtained when using the batch system is seen in Figure 3.2 (a). However, this linearity deteriorates when the standards are prepared in mini-columns. This was not a result of the efficiency of the chelation process, which proved to be close to 100% when filtrates and eluates, collected after mixing 25 mL aliquots of the standards with the resins, were analysed by FAAS against the original standards. The precision in the measurement of the standards was between 1.5 and 2 times better when using the batch process.

The reason why the deviation from linearity becomes manifest when using mini-columns was attributed to the lack of homogeneity observed when the Cu^{2+} ions are being retained by the packed resin. As the Cu^{2+} solution was pumped through the column, interaction between the analyte and the functional sites started to occur and these were occupied in a sequential manner. At the front of the column, all the sites were occupied, whereas at the end they were all empty as shown in Table 3.7. As a consequence, it was necessary to mix the resin beads physically once they had been removed from the column and dried and the accuracy of the XRF readings depended on how efficient this mixing step was.

In comparison, Cu^{2+} ions are retained homogeneously on Chelex-100 when the solution and the resin are mixed in batch using a magnetic stirrer to ensure contact between the analyte and the functional sites of the exchanger. The difference between the two systems is illustrated with the diagrams in Figure 3.3.

(a)

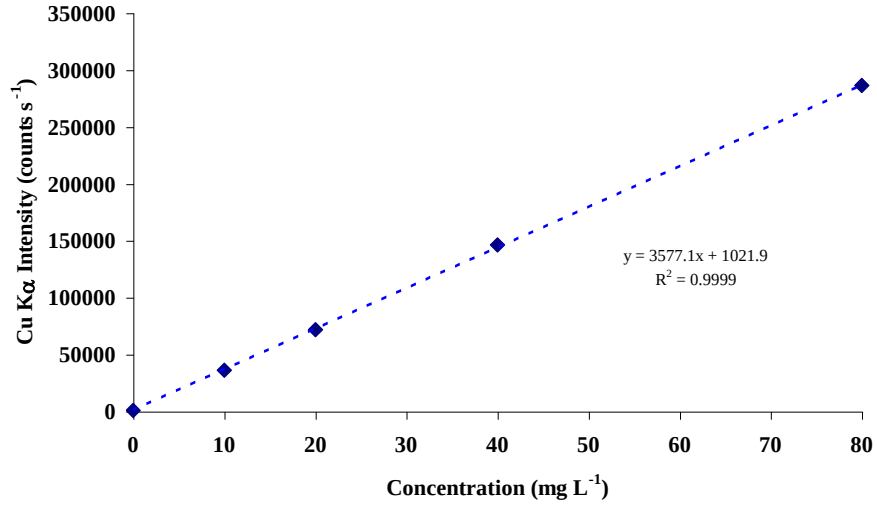

(b)

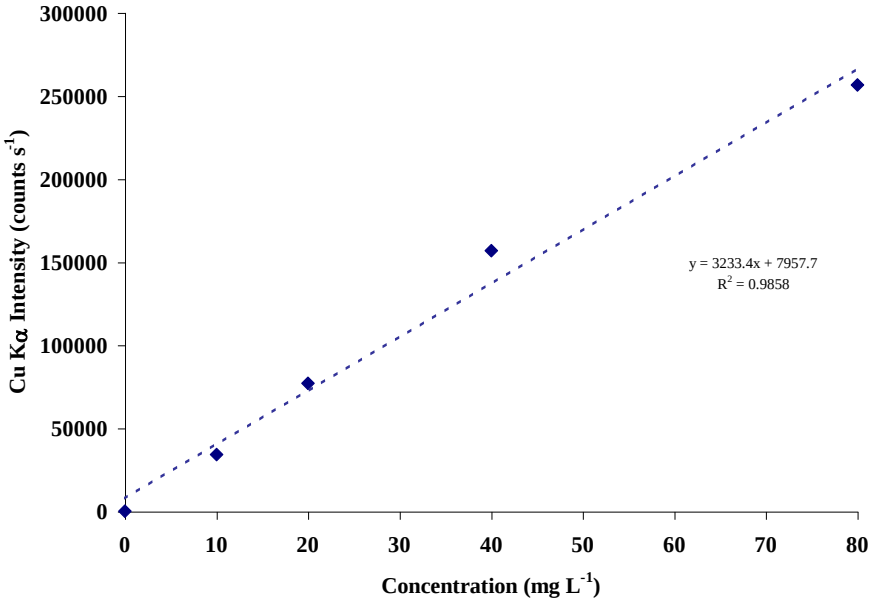

Figure 3.2 Calibration graphs for Cu^{2+} retained on Chelex-100 using (a) batch system and (b) mini-columns

Table 3.7 **Distance occupied by Cu^{2+} in Chelex-100 mini-columns when 25 mL of different concentrations of the analyte are pumped through (distance measured from the beginning of the column)**

Standard Concentration (mg L^{-1})	*Column No*	*Occupied Length of the Column (cm)*
0	1	0
10	2	1.5
20	3	1.8
40	4	2.4
80	5	3.4

(a)

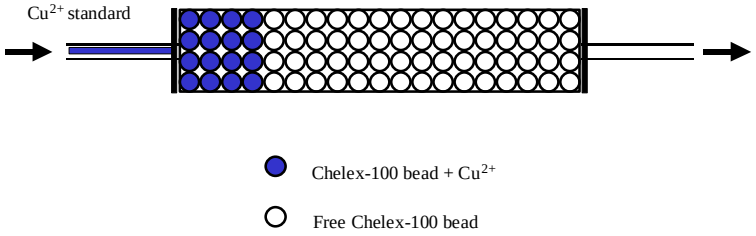

(b)

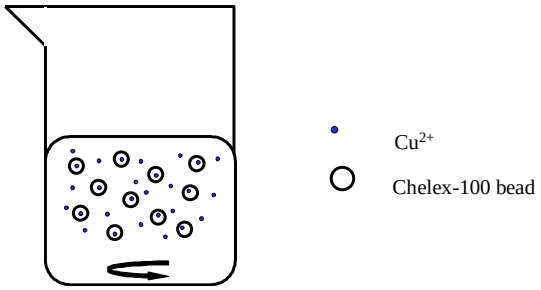

Figure 3.3 **Mechanisms of the retention of Cu^{2+} on Chelex-100 when using (a) mini-columns and (b) batch systems**

3.3.3.2 Effect of the volume of sample in batch systems

It is important to note that, although in the majority of applications studied in this work, the use of resins in batch is more convenient than utilising microcolumns, batch systems may not be adequate when dealing with a large volume of sample. The effect of sample volume (for volumes between 25 and 500 mL) on the efficiency of the retention for chromium species on Dowex exchangers is studied in Chapter 6. In this case, the recoveries obtained are independent of the volume. However, if a larger preconcentration factor was required, the efficiency of retention could drop. When 5000 mL of 5 mg L^{-1} Cr(VI) in 0.01 M HNO_3 were mixed with 1g of Dowex 1-X8, recoveries for the analyte on the resin may go down to 60 % as Figure 3.4 shows. These recoveries remain relatively stable during the period of time studied (20 minutes).

These findings can be explained by referring to the mechanism of the ion exchange or chelation process. Considering a sulphonic acid resin in the sodium form and a solution of any other metal M^+ that are mixed in batch by stirring them inside a beaker, the exchange will occur until equilibrium is achieved[63]:

$$R\text{-}Na + M^+ \rightleftharpoons R\text{-}M + Na^+$$

In actual fact, this process occurs in five steps as described in Figure 3.5:

1. Diffusion of M^+ towards the resin
    a. Transport through the solution. This is aided by stirring.
    b. Transport through the stationary liquid film around the resin. The thickness of the film (10^{-2} to 10^{-3} cm) depends on the stirring rate.
2. Diffusion of M^+ inside the resin towards the active site.

3. Chemical ion exchange between R-Na and M^+.
4. Diffusion of Na^+ inside the resin towards the surface.
5. Diffusion of Na^+ in the solution.
    a. Across the stationary film.
    b. Diffusion through the solution.

According to the Electroneutrality Principle, steps 1 and 5 must occur simultaneously and at the same rate. The same rule applies to steps 2 and 4. The exchanging rate will be controlled by the slowest step and, as the exchange of the mobile ions in the functional groups is usually fast, ion exchange can be considered mainly a diffusion phenomenon. Although the stirring speed neutralises the differences in concentration of the solution, it has no effect inside the bead or across the liquid film where transport takes place only by diffusion.

In effect, two steps determine the speed of the exchange: i) diffusion of the mobile ions inside the exchanger (*particle diffusion*) and ii) diffusion of the mobile ions in the liquid film (*film diffusion*). The slowest process is the controlling step, depending mainly on the external concentration, although other factors such as particle size and diffusion coefficients also have an influence. Figure 3.6 shows the effect of the concentration of the solution on the exchanging rate. When $C < 0.01$ N, diffusion through the film is the slowest step. In this case, the exchange rate can be accelerated by increasing the stirring speed, as this reduces the thickness of the film. However, there is a limit below which augmenting the agitation speed will not reduce the width of the film further. If $C > 0.1$ N diffusion through the resin bead is the controlling step[68, 69].

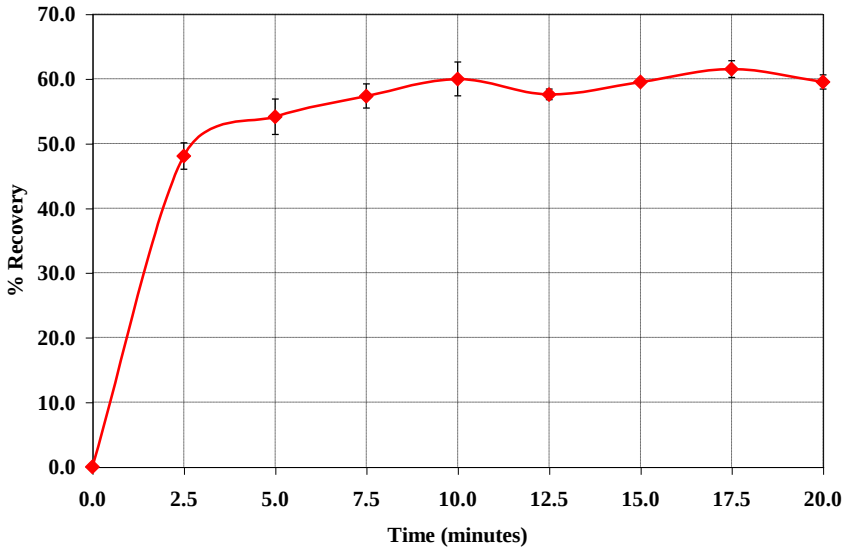

Figure 3.4 **Recoveries for the retention of 25000 µg of Cr(VI) from a large volume (5000 mL) on 1 g of Dowex 1-X8**

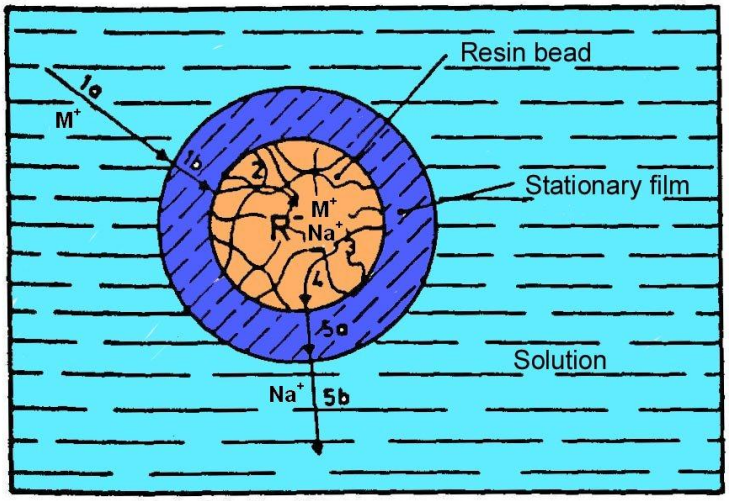

Figure 3.5 **General mechanism of ion exchange**[63]

In the experimental case studied, the concentration of Cr(VI) in the external solution was 5 mg L^{-1} which, expressed as molarity, would be 0.0001 M. Considering that the exchange takes place with Cr(VI) in the form $HCrO_4^-$, only one equivalent is involved and molarity equals normality. A solution being 0.0001 N certainly falls within the area of the graph (Figure 3.6) where the exchange rate is controlled by film diffusion. Hence, the importance of the stirring step rises because, as the sample volume increases from the usual 25 mL to 5000 mL, the stirring speed is not high enough to keep the thickness of the liquid film sufficiently low and the whole process becomes kinetically slow. However, the preconcentration of the analyte from such a large volume (5 L) on the exchanger packed into a mini-column, although efficient, would also be extremely slow (125 hours at 1.5 mL min^{-1}) and, as described previously, the analyte is likely to be distributed unevenly throughout the resin.

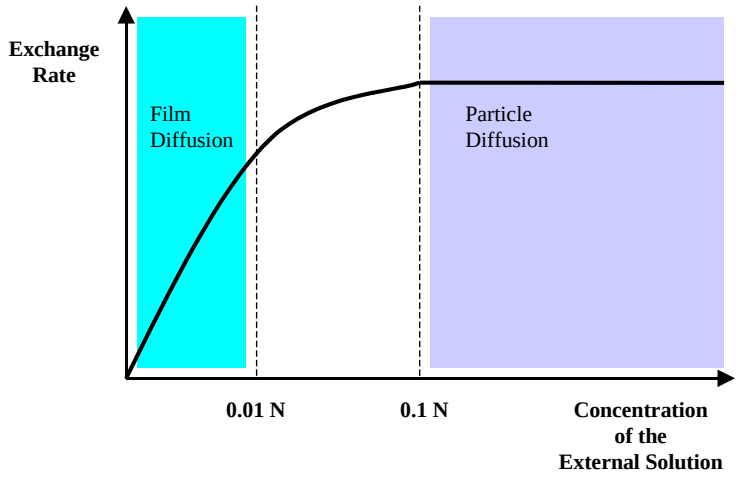

Figure 3.6 Effect of the ionic concentration of the solution on the exchange rate and, therefore, in the controlling step of the exchange rate

3.3.4 Conclusions

The retention of Cu(II) on Chelex-100 was employed to compare the use of solid retention media for XRF analysis in batch and column systems. The best results in terms of accuracy and precision were achieved when using the batch process. As a result, significantly better calibration graphs were also obtained. This is a consequence of the homogeneous mixture of resin beads and Cu(II) ions in solution. The batch method is also fast and simple and it has therefore been selected as the ion-exchange procedure to be used in these investigations.

When using very large sample volumes, batch systems may become less efficient, because of the ion exchange rate being controlled by the diffusion of the ions through the stationary film that surrounds the resin bead. In this case, utilising mini-columns may be a more convenient compromise, but at the expense of exceptionally long, if not prohibitive, sample preparation times.

3.4 PARTICLE SIZE EXPERIMENTS

3.4.1 Introduction

General considerations regarding the effect of the particle size on the intensity of fluorescence emitted by the elements in a sample have been discussed in section 1.2.4. Therefore, this section will consider only the effect of the particle size when using ion-exchangers as a sample analyte support.

Allen and Rose[12] studied the effect of the ion-exchange resin particle size on the determination of copper on Dowex A-1 by XRF analysis. These authors based their studies on the generally accepted fact that the intensity of fluorescence will increase with decreasing particle size. The results of their experiments match the general model described in section 1.2.4 and show dramatic changes in the measured intensities with the size of the ion-exchanger. The use of particle sizes below 50 μm was recommended.

Since these results were reported, in 1972, other researchers have used this size-related effect as an accepted starting point for their work. To date, no confirmatory, in-depth investigation has been found that tests the conclusions of this seminal work.

The following experimental sections describe how Dowex 50W-X8, with three different particle size ranges, was used to retain Cr(III). The samples obtained were analysed by EDXRF. The effects of using resins of particular size ranges upon the Cr Kα fluorescence are studied and discussed.

3.4.2 Experimental

3.4.2.1 Chemicals and reagents

Aristar grade concentrated nitric acid and Spectrosol grade standard stock solution (1000 mg L^{-1}) of chromium (III) nitrate were both obtained from Merck (Poole, Dorset, UK).

Whatman filter paper N^{o} 1 was used to separate ion exchange media and solutions. The plastic sample cups and Mylar film were obtained from Philips Analytical X-Ray (Cambridge, UK). Milli-Q doubly deionised water, 18 MΩ cm (Millipore, Bedford, Massachusetts, USA) was used throughout the study.

The Dowex 50W-X8 ion exchange media were all obtained from Merck. Three particle size varieties of this resin were used with mesh size being 20-50, 100-200 and 200-400. Table 3.8 shows the equivalence between mesh size and particle size for commercially available Dowex resins.

Table 3.8 **Equivalence between mesh size and particle size (µm) for Dowex resins**

Mesh size	***Particle size (µm)***
20 - 50	297 - 840
50 - 100	149 - 297
100 - 200	74 - 149
200 - 400	38 - 74

3.4.2.2 Instrumentation

The work was performed using a Link Analytical XR300 energy dispersive XRF spectrometer. The conditions under which this instrument was operated are shown in Table 3.9.

Table 3.9 **Instrumental parameters used on the Link Analytical XR300 XRF spectrometer for the analysis of Cr(III) standards on Dowex 50W-X8 resins (different particle sizes)**

Voltage	*Current*	*Vacuum*	*Filter*	*Acquisition time*
20 kV	150 μA	off	none	100 s

Measurement of metal concentrations in aqueous solutions for the calculation of recovery data was achieved using a GBC 902 FAA spectrometer with operating conditions as shown in Table 3.10.

Table 3.10 **Instrumental parameters used on the GBC 902 flame atomic absorption spectrometer for the analysis of Cr**

Wavelength	*Band pass*	*Lamp current*	*Flame*
357.9 / 425.4 nm	0.5 nm	6 mA	Air-Acetylene (reducing)

3.4.2.3 Sample preparation procedure for studies on the effects of the particle size of Dowex 50W-X8 on the determination of Cr(III) by EDXRF

Known volumes (0.125, 0.250, 0.500 and 1.000 mL) of Cr(III) standard stock solution (1000 mg L^{-1}) were diluted to 50 mL with 0.01M HNO_3, to give a solution

of approximately pH 2. At this pH, the most stable chemical form of Cr(III) is $Cr(H_2O)_6^{3+}$, favouring the retention of the species on a cation exchanger[66].

From each new standard, 25 mL were taken and mixed with 0.5 g of dry Dowex 50W-X8 100-200 mesh. The samples were mixed using a magnetic stirrer for 10 minutes. The resins were then separated from the solutions using a filter paper, dried at 40 ^oC in a drying cabinet and transferred to XRF sample cups fitted with Mylar film for analysis by EDXRF. The conditions used are shown in Table 3.9. The filtrates were kept for FAAS analysis in order to obtain recovery data. An identical procedure was used for Dowex 50W-X8 200-400 mesh and Dowex 50W-X8 20-50 mesh on which Cr(III) was retained and determined.

3.4.2.4 Sample preparation procedure for the study of the effect of the mass of resin on the intensity of fluorescence using different particle sized Dowex 50W-X8

A series of standards with the same concentration of Cr(III) retained on Dowex 50W-X8 100-200 mesh (1000 $\mu g\ g^{-1}$) but employing different masses of resin (125-2000 mg) was prepared by mixing 100 mL of 50 mg L^{-1} Cr(III) solution in 0.01M HNO_3 with 5 g of dry resin. The mixture was stirred for 30 minutes. The resin, now with Cr(III) retained on its surface was separated from the solution by filtration and dried in a drying cabinet at 40 ^oC. Various amounts of loaded resin, between 125 and 2000 mg, were weighed into XRF sample cups and analysed. The same procedure was followed for Cr(III) on Dowex 50W-X8 200-400 mesh and Dowex 50W-X8 20-50 mesh.

3.4.3 Results and discussion

3.4.3.1 Studies on the influence of the particle size of Dowex 50W-X8 on the determination of Cr(III) by EDXRF

The results of the experiments to study the influence of the particle size of the resin beads on the linearity of the relationship between intensity of fluorescence (net) and concentration are displayed in Figure 3.7.

No apparent effect was observed on the linearity when varying the particle size of the exchanger in the range of concentrations studied (0 – 2000 μg g^{-1}). The datasets obtained for Dowex 50W-X8 200-400 mesh, 100-200 mesh and 20-50 mesh are virtually identical. This equivalence can be better visualised using Figure 3.8, where the Kα intensities obtained from the EDXRF determination of each mesh size have been paired and represented in x-y graphical form. The lines have correlation coefficients better than 0.999. The slopes obtained are, in the three cases, very close to unity and the intercepts are negligible in comparison with the magnitudes measured. This presentation shows the close correlation of the datasets.

The only difference observed in the use of different particle sizes in this manner was in the overall sulphur signal (Figure 3.7). This element, always present in the resin as part of the sulphonic functional group, was determined in order to monitor any anomalous effects that might arise from the use of different particle sizes that may not be apparent by simply looking at chromium. The signal obtained for sulphur should be constant throughout the concentration range studied. It should also be the same for the three exchangers, assuming that the number of functional groups (i.e. capacity) is the same. However, a slightly lower signal is observed for

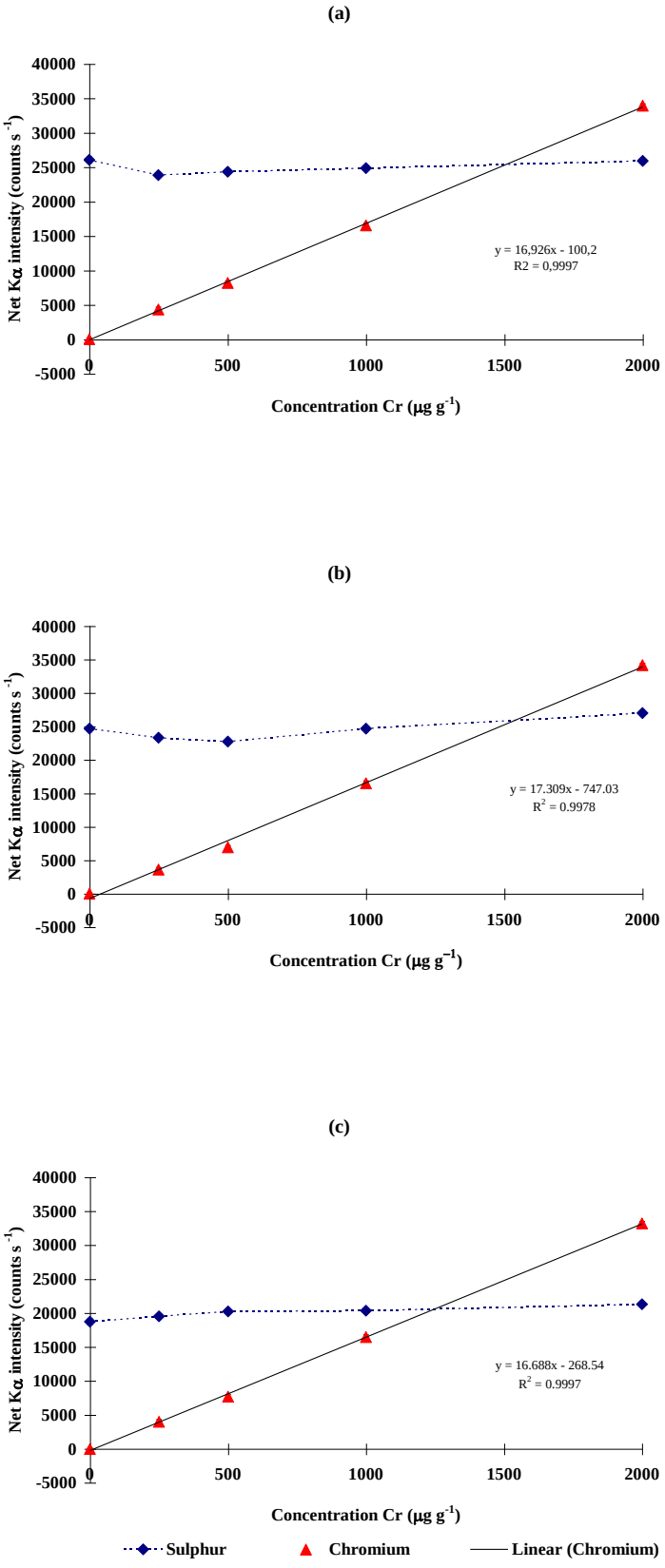

Figure 3.7 Calibration graphs (net intensities) for Cr(III) retained on Dowex 50W-X8 with different particle sizes: (a) 200-400 mesh, (b) 100-200 mesh and (c) 20-50 mesh

(a)

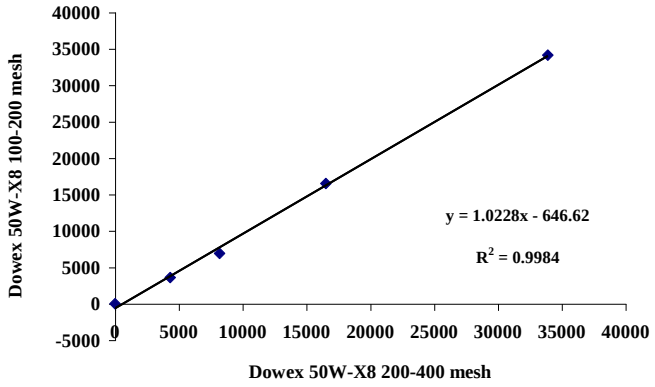

(b)

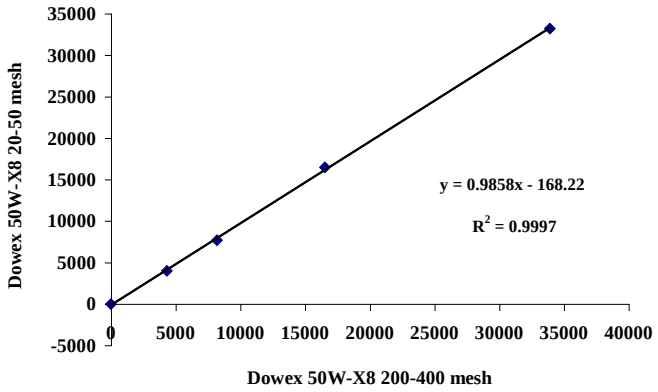

(c)

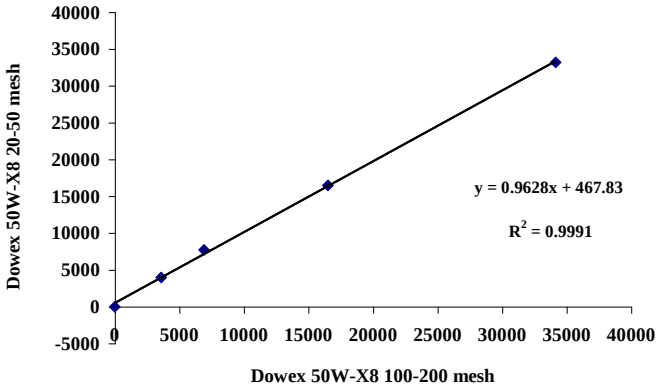

Figure 3.8 Compared Kα intensities (counts s^{-1}) from standards of Cr(III) retained on Dowex 50W-X8 with different particle sizes

sulphur on Dowex 50W-X8 20-50 mesh when compared with the smaller particle sizes. One obvious explanation is that there is a lower number of active sites in the large particle size exchanger. Dow Chemical Co., the manufacturers of Dowex resins, quote total exchange capacity values for each resin type, regardless of the particle size[61, 62]. However, it is logical to expect lower capacities for resins with fewer active sites. In this experiment, full recoveries for Cr were obtained with all the resins used. Nevertheless, a reduced number of active sites could obviously affect the retention of the analytes when their concentrations are high or when there is a high proportion of competitive interferents in the sample. Thus, it is important to ensure that the exchange capacity of the resin selected as sample support is measured experimentally, before the application of the method to the analysis of real samples is attempted.

The results of this experiment are clearly at variance with the findings reported by Allen and Rose for Cu retained on Dowex A-1[12]. Although different analytes have been used (Cr and Cu, respectively) the backbone of the resin in both this study and that of Allen and Rose is essentially the same, i.e., a polystyrene DVB framework, and would not justify the disparity. These investigations have shown that the intensity of fluorescence measured for the CrKα depends only on the concentration of Cr retained on Dowex 50W-X8 and is independent of the particle size of the resin used in the range studied. It is noted however that a different sample matrix, i.e., a different resin with different analytes, would result in intensity vs. concentration curves with different slopes. Allen and Rose describe dramatic effects for particle sizes larger than 112 μm (average for mesh size 100-200). In the present

work, particle sizes up to 800 μm (20-50 mesh) have been used with no apparent effect on the intensity of fluorescence.

It is difficult to establish the exact cause for the discrepancy, for several reasons. For example, the work by Allen and Rose was performed using wet resins and the influence of excess water in the samples was not evaluated. In addition, the intensities of fluorescence are given as normalised figures, without further explanation regarding the composition of the reference standard. Background correction was achieved subtracting the intensity from an "unloaded resin sample" from all other standards, including the reference standard. However, it is unlikely that samples with different particle size or even, different matrix, would give identical background intensities, therefore, their methodology is one possible source for their seemingly erroneous results. Furthermore, the effect of the particle size reported by Allen and Rose, which was studied using a wavelength dispersive instrument, could be affected by the peak integration system used; the authors do not specify whether the results obtained were based on measuring the peak area or height.

Finally, the authors quoted the infinite thickness of their sample as 30.9 μm, which agrees with the results of their experiment. Again, there is no information on how this value was calculated. Table 3.11 shows the results of theoretical calculations to determine the infinite thickness or critical penetration depth (d_c) of the resins used in these investigations based on 99% absorbance. The basis for these calculations and a worked example are shown in Appendix A. It has been considered that the resins were completely saturated with the analyte and that the density of the resins is 1.2 g cm^{-3}. From the results shown in Table 3.11, it can be seen that the

infinite thickness depends upon the element retained on the resin, increasing with the mass of this element. Although different concentrations of analyte would give rise to different values for the infinite thickness, it is also apparent that the results obtained are, at least, one order of magnitude larger than the value quoted by Allen and Rose. It has also been noted that the theoretical infinite thickness for Dowex 50W-X8 (approximately 500 μm) falls in the middle of the particle size range of this exchanger for mesh size 20-50, i.e., 297-840 μm. This suggests that the rules of classic sample presentation methods for XRF analysis may not directly apply to the use of resins as sample support as it was initially proposed in their paper. A theoretical model that helps to explain the reasons behind these and other differentiating effects is discussed in section 3.5.

Table 3.11 **Calculated infinite thickness (d_c) for saturated Dowex and Chelex-100 resins with different analytes**

Resin	*Analyte*	d_c (*μm*)
Chelex-100	Cr	1460
Chelex-100	Mn	1810
Chelex-100	Cu	3691
Dowex 50W-X8	Cr	428
Dowex 50W-X8	Mn	504
Dowex 1-X8	Cr	1006
Dowex 1-X8	Mn	1160

In summary, the results shown in this section suggest that previous information found in the literature regarding the relationship between the intensity of

fluorescence and the particle size of ion-exchangers is far from conclusive. In the case of the determination of Cr on Dowex 50W-X8, all the particle sizes studied behave similarly, although the use of 20-50 mesh could result in lower exchange capacities.

3.4.3.2 Effect of the mass of resin on the intensity of fluorescence for different particle sized Dowex 50W-X8

Figure 3.9 shows the effect of the mass of resin on the intensity of fluorescence (expressed as net intensity) for three different particle sizes of Dowex 50W-X8. Again, there is good agreement between the results obtained from 100-200 mesh and 200-400 mesh resins for the Cr Kα line [Figure 3.9 (a)]. The curve for the 20-50 mesh resin shows poorer intensity, but still the same optimum mass at 500 mg of exchanger. Using less resin would mean not reaching the maximum possible intensity and using more would involve diluting the analytes in the sample. Dowex 50W-X8 100-200 mesh barely excels the other two exchangers in terms of total intensity, although this difference is narrowed when the results are plotted as 'net intensity to background ratio versus mass of resin' [Figure 3.10 (a)]. In this case, the three curves converge.

Figures 3.9 (b) and 3.10 (b) show equivalent plots for the Cr Kβ and, as could be expected from the poorer sensitivity and precision, indicate the need for a greater mass of resin (at least 1 g) if this line is to be measured for quantitative analytical purposes.

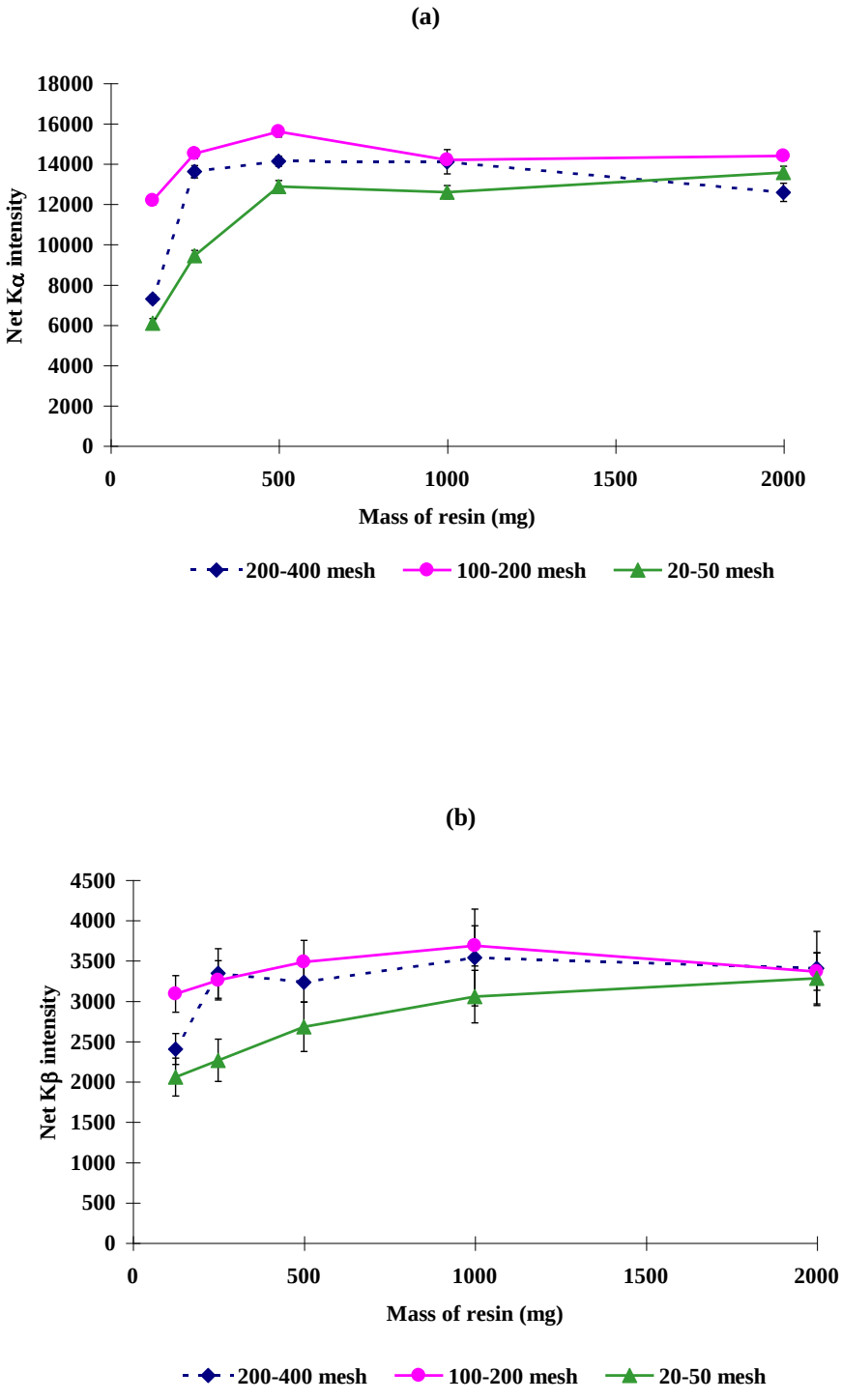

Figure 3.9 Effect of the mass of resin on the net intensity of fluorescence [(a) Kα and (b) Kβ] from Cr(III) retained on different particle sizes of Dowex 50W-X8

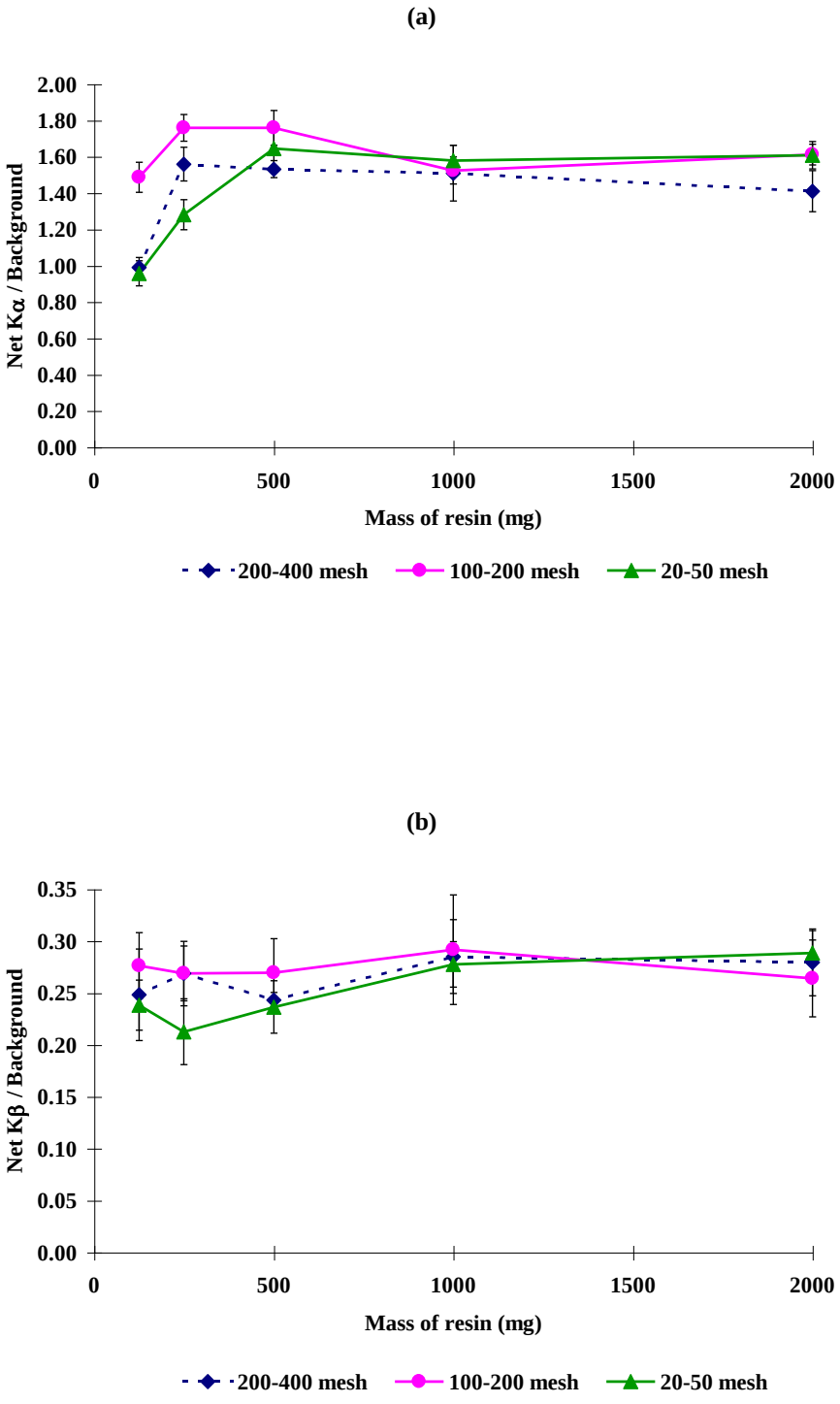

Figure 3.10 Effect of the mass of resin on the net intensity [(a) Kα and (b) Kβ] to background ratio from Cr(III) retained on different particle sizes of Dowex 50W-X8

3.4.4 Conclusions

Standards of Cr(III) on Dowex 50W-X8 with different particle sizes ranging from 38 μm up to over 800 μm were prepared and analysed by EDXRF. When the linearity of the relationship between intensity of fluorescence and concentration was studied, no effect from the three ranges of particle size used was observed. The Cr Kα intensities obtained from the three sets of standards were virtually identical. This suggests that the ion-exchanger could be used directly without any need for grinding to achieve smaller particles as previously suggested in the literature. Nevertheless, it would be preferable to avoid the use of Dowex 50W-X8 with mesh size 20-50, as a reduced number of active sites would result in lower exchange capacities.

The effect of the particle size on the optimum mass of resin presented to the EDXRF sample chamber is also minimal, especially when this parameter is optimised for net Kα intensity to background ratio. In the measurement of the Cr Kα intensity, the ideal mass of resin was 500 mg irrespective of the particle size used.

In comparison with Kα, the measurement of Kβ intensities showed poor sensitivity and poorer precision. For the same concentration of Cr, a larger amount of resin (at least 1 g) would be required for an accurate measurement of this line.

The results of theoretical calculations of the infinite thickness of the resins used in these investigations support the experimental findings reported, i.e., the effect of the particle size in determinations of metals retained on resins by EDXRF being minimal. The values obtained are in hundreds or thousands of micrometers.

3.5 PROPOSED THEORETICAL MODEL FOR THE CHARACTERISTICS OF THE RETENTION OF METAL IONS ON RESINS THAT AFFECT EDXRF ANALYSIS

A theoretical model for the retention of metal ions on Dowex 50W-X8, Dowex 1-X8 and Chelex-100 resins has been formulated in order to link and explain the advantageous properties of the resulting specimens observed during these investigations. Some of these characteristics, such as homogeneity, long linear ranges and reduced particle size effects have already been discussed in this Chapter. Other features include diminished inter-element effects and lower limits of detection and will be discussed in following sections.

For this model, a resin bead has been considered to be the sphere represented in Figure 3.11. From the data obtained by SEM and x-ray microanalysis it is possible to say that the distribution of active sites and retained ions is uniform throughout the sphere. However, in agreement with probability laws, the assumption has been made that those sites on the surface of the sphere will be occupied first. As external sites become unavailable, inside layers will also be gradually occupied.

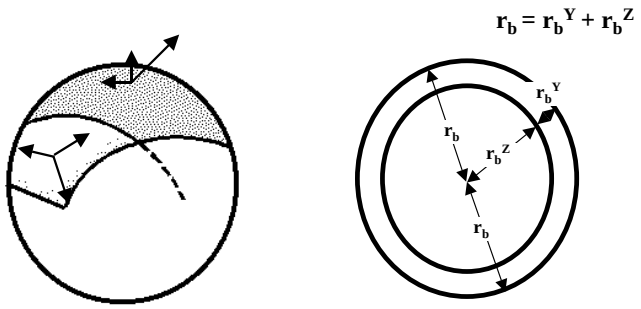

Figure 3.11 Theoretical representation of a resin bead as a sphere and its cross-section

By a series of calculations (displayed, in full, in Appendix B) that are based on the fundamental characteristics of the resins, it has been possible to determine the theoretical thickness of the layer where all the active sites are occupied by the analyte metal ions (r_b^Y):

$$r_b^Y = r_b \cdot \left[1 - \left(1 - \frac{c_s.V_s.n}{C_r.m_r.W} \right)^{\frac{1}{3}} \right] \qquad (3\text{-}1)$$

where r_b is the radius of the resin bead, c_s is the concentration of the solution containing the analyte, V_s is the volume of solution, n is the ion charge, C_r is the capacity of the resin, m_r the mass of resin and W is the relative molar mass.

It is possible to link the thickness of the layer of retained atoms to the percentage of absorbed or transmitted fluorescent radiation by using equation 3-2, which is a variation of equation 1-6 and has already been used in the calculation of the critical penetration depth (Appendix A).

$$d = -\frac{\mathrm{Ln}\frac{I}{I_o} \cdot \sin\psi}{\mu_r \cdot \rho_r} \qquad (3\text{-}2)$$

where I_o is the initial fluorescent radiation, I is the emerging fluorescent radiation, ψ is the radiation take-off angle, μ_r is the mass absorption coefficient of the resin and ρ_r is the density of the resin.

Figure 3.12 has been obtained using the same procedure shown in Appendix A and varying the values of I and I_o between 1 and 99. The resins have been considered to be saturated with Mn.

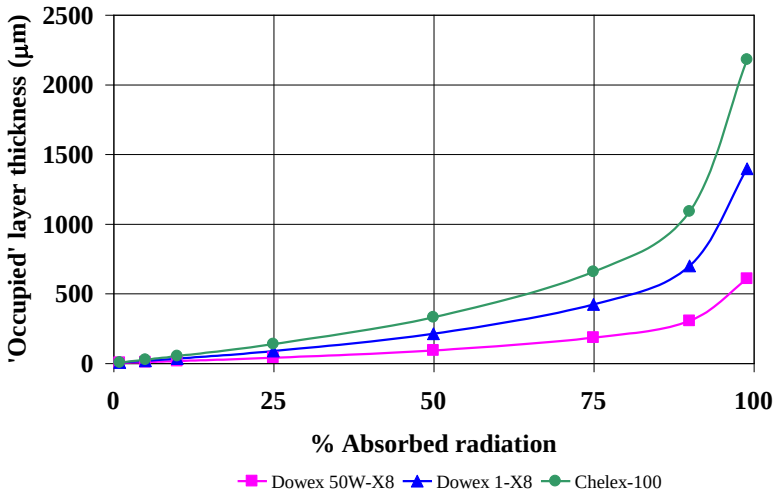

Figure 3.12 Variation of the thickness of the layer of retained manganese ions on the resin with the percentage of absorbed radiation

It is suggested from these theoretical values that an 'occupied' layer of thickness below 1 µm, would give approximately 1% absorbance, i.e., 99% transmitance of the fluorescent radiation for Dowex 50W-X8. For Dowex 1-X8, the layer thickness would have to be below 3 µm and for Chelex-100, below 5 µm in order to obtain the same result. Thus, if the thickness of the layer of ions retained of the resin is below 1 µm, the matrix would absorb only 1% of the fluorescent radiation and the inter-element effects would be greatly reduced. The theoretical determination of the thickness of the layer of ions on the resins (Appendix B) has

shown that in the majority of experiments performed in these studies, r_b^Y was below 1 μm. Only when the concentration of metal was above 50000 μg g^{-1}, greater values of r_b^Y would be expected. However, even in this extreme case, the thickness of the layer would still be below 10 μm, giving rise to only 5% absorbed radiation.

Using similar principles an equation has also been obtained that allows the determination of the average distance between active sites in a resin bead:

$$x = \left(\frac{6}{\pi} \cdot \frac{1}{\rho_r \cdot C_r \cdot N_A} \right)^{\frac{1}{3}} \qquad (3\text{-}3)$$

where N_A is *Avogadro's number.*

The distance between active sites may also have an important part in explaining the lack of particle size and matrix effects. This parameter is inversely proportional to the capacity and the density of the resin. For a fixed density and values of capacity between 0.5 and 5 mEq g^{-1}, the distance between active sites varies between 8.1 and 17.4 Å. When the capacity is kept constant and the density of the resin varies between 1.00 and 1.50 g cm^{-3}, the change in x is very small (8.7 – 10.0 Å). These figures are in agreement with theoretical data[70] that sets ionic radii between 0.07 and 2.94 Å. They also show that the distance between active sites and, therefore, between retained ions is large (compared with their 'ionic' size) and constitutes a relatively free path for the fluorescent x-rays.

With all this information, it is possible to gain a deeper understanding of the reasons behind some of the experimental results observed in these investigations. The structure of the resins provides a sample support which is totally different from

conventional specimens. The combination of an 'open' framework and a 'thin layer' distribution contributes to a reduction in inter-element and self-absorption effects. And, as a result of these minimised effects, longer linear ranges and lower limits of detection are achieved.

A worked example of the determination of r_b^Y and x for 1000 μg g^{-1} of Cu retained on Dowex 50W-X8 has been included in Appendix B.

4. *DETERMINATION OF TRACE METALS IN BIO-ENVIRONMENTAL SAMPLES BY RETENTION ON RESINS AND EDXRF DETECTION*

Chapter 4. Determination of Trace Metals in Bio-Environmental Samples by Retention on Resins and EDXRF Detection.

4.1 INTRODUCTION

The combination of ion exchangers and EDXRF can be employed not only to target different chemical species of the same element, but also several multielemental species present in the sample, providing a simple, inexpensive and rapid method for the determination of metals in bio-environmental matrices. The literature has many examples of the application of solid retention media to the separation and preconcentration of trace metals from a variety of samples, the majority of these being waters or aqueous solutions[15, 16, 24, 28, 35, 36, 38, 39, 43, 49, 52, 55].

However, nearly fifty years after Grubb and Zemany[14] used ion-exchange membranes for the first time as a sample support for x-ray analysis, the application of this and similar methods to geological and, especially biological and bio-environmental materials are still few. The reasons for this are attributable to the complexity of the samples and the existence of alternative, well established analytical techniques that may offer rapid and reliable results, once the samples have been dissolved. However, in many cases, the rapid and accurate analysis by FAAS, ICP-AES or ICP-MS can be limited by the analytes of interest, their concentrations and any spectral and matrix interferences that may be present. Preconcentration and / or

separation techniques may also be required, with the result that no advantage would be gained from their use over EDXRF.

In this study, two commercially available resins, the cation exchanger Dowex 50W-X8 and the chelating resin Chelex-100 were used to separate trace metal analytes from their matrix (the acid digest of certified sewage sludges) and present them for measurement by EDXRF spectrometry. The characteristics of the resins, such as pH dependence, capacity and optimum mass were determined and critically assessed in an evaluation of their performance for the determination of trace analytes in complex matrices. In this manner the limitations of the methods were identified.

The methods developed were not expected to compete directly with other atomic spectroscopy techniques, but to provide an alternative to them, based on the use of EDXRF spectrometry. In addition, the aim was to broaden the use of XRF spectrometers in standard research and routine laboratories.

4.2 DETERMINATION OF TRACE METALS IN SEWAGE SLUDGE BY RETENTION ON DOWEX 50W-X8 AND EDXRF DETECTION

4.2.1 Experimental

4.2.1.1 Chemicals and materials

ARISTAR grade concentrated nitric acid, sodium chloride, sodium hydroxide pellets and ammonia solution; AnalaR grade potassium nitrate (2.526 g to 100 mL to obtain a 10000 mg L^{-1} K standard stock solution) and Spectrosol grade standard

stock solutions of either 1000 or 10000 mg L^{-1} Ti, V, Cr, Mn, Fe, Co, Ni, Cu, Zn, Pb, Mg and Ca were all obtained from Merck (Poole, Dorset, UK). The 30% hydrogen peroxide solution was obtained from Aldrich Chemical Co. Ltd. (Dorset, U.K.). Whatman filter paper No 1 was used to separate cation exchanger and solutions. The sample cups and Mylar film were obtained from Philips Analytical X-ray (Cambridge, UK). The water used was of ultra pure grade, Milli-Q, 18 MΩ cm (Millipore, Bedford, Massachusetts, USA).

The cation exchange resin Dowex 50W-X8 (H), 75-150 μm particle size, was obtained from Merck.

The certified reference materials 'Trace Elements in a Sewage Sludge' were obtained from the Community Bureau of Reference (BCR No 144 and No 145).

4.2.1.2 Instrumentation

EDXRF measurements were performed using a *Link Analytical* XR300 XRF spectrometer operated using the conditions shown in Table 4.1. These conditions had been optimised to achieve the best net intensity to background ratio for the main analytes maintaining the 'dead time' in the range 45-48%.

As part of the mass balance measurements, the analytes left in solution after absorption onto the resin were determined using a *Perkin-Elmer* Optima 3000 ICP-AE spectrometer. The instrumental parameters employed are shown in Table 4.2.

Table 4.1 **Instrumental parameters used on the Link Analytical XR300 XRF spectrometer.**

Voltage	*Current*	*Vacuum*	*Filter*	*Acquisition time*
25 kV	120 μA	off	aluminium	100 s

Table 4.2 **Instrumental parameters used on the Perkin-Elmer Optima 3000 ICP-AE spectrometer.**

RF Power	1000 W
Viewing height	15 mm (above load coil)
Nebuliser	Cross-flow
Argon flow rate	
Plasma	17 L min^{-1}
Auxiliary	1 L min^{-1}
Nebuliser	1 L min^{-1}
Wavelength of analyte	
Al	308.215 nm
Ca	317.933 nm
Co	228.616 nm
Cr	357.869 nm
Cu	224.700 nm
Fe	259.940 nm
K	766.491 nm
Mg	279.079 nm
Mn	294.920 nm
Ni	232.003 nm
Pb	220.353 nm
Ti	334.941 nm
V	292.402 nm
Zn	202.548 nm

4.2.1.3 Determination of the optimum pH for the use of Dowex 50W-X8

Investigations were performed to determine the optimum pH for the retention of several metals on Dowex 50W-X8. The complex, multicomponent synthetic sample solutions (5000 mL) were prepared in admixture by dilution of 10000 mg L^{-1} standard stock solutions to 10 mg L^{-1} with 2% HNO_3. Aliquots (50 mL) were separated into beakers and the pH adjusted to the desired value within the range 1-12 using solutions of NaOH and HNO_3. Any precipitate formed was separated from the solution by filtration. A 25 mL aliquot of each solution was taken and analysed by ICP-AES in order to determine the concentration of metal left in solution and, by difference, the concentration left in the precipitate ('% Solid' in Figures 4.1 and 4.2). The remaining 25 mL in each beaker were mixed with 1.00 g of Dowex 50W-X8 and left stirring for 5 minutes. The loaded resin was then separated and the second filtrates were analysed by ICP-AES. The concentration of metals in solution, after precipitation and retention on the resin, was determined. The concentration of the metals on the resin ('% on Resin' in Figures 4.1 and 4.2) was also calculated by difference.

4.2.1.4 Sample preparation procedure for the preliminary investigation of interelement effects affecting metals retained on Dowex 50W-X8

The possibility of interelement effects occurring on resins was initially studied by preparing a set of standards in which the concentration of two elements, Zn and Mn, increased steadily (0 - 1000 μg g^{-1}) while the others (Cr, Fe, Cu and Pb)

remained constant at 250 μg g^{-1}. The standards were analysed by EDXRF using the compromise conditions shown in Table 4.1.

4.2.1.5 Sample preparation procedure for the determination of trace metals in sewage sludge using Dowex 50W-X8 as retention support

Two certified reference materials, BCR No 144 and BCR No 145, 'Trace elements in sewage sludge', were used for this analysis. Two sets of samples were prepared by accurately weighing, approximately 0.5000 g of the certified reference materials into microwave *Teflon*® bombs (Savillex Corporation, Minnesota, USA) and adding (i) 5 mL of 'aqua regia' to the first set and (ii) 4 mL of concentrated nitric acid and 1 mL of 30% H_2O_2 to the second set. This would allow a comparison to be made of the cation exchange efficiency of the resins in the presence of chloride anions which may form metal chloro-complexes with analytes of interest. The bombs were capped, loosely, and left to stand overnight. After sealing, the samples were digested in a domestic microwave oven (*PRO Line* SM 11, 750 W) for 3 minutes at medium power. After cooling, the digests were transferred into beakers, the volume increased to 25 mL with ultrapure water and the pH raised to 2 with 10% m/v sodium hydroxide solution. A pH of 2 had previously been determined as optimum for retention of the metals. A procedural blank was prepared in the same manner for each set of samples.

Both sets of samples and a series of multi-elemental, matrix-matched standards were mixed with two quantities of the cation exchanger, Dowex 50W-X8, i.e., 1.00

and 0.50 g respectively. While the optimum mass of resin has been shown to be 0.50 g, as stated in section 3.4.3.2, this mass was increased to 1.0 g to ensure that the final cation concentrations were well bellow the capacity of the resin (3.2 mEq g^{-1}, as shown in section 6.3.2). The mixtures were stirred for 10 minutes and, then, the adsorbing media were separated by filtration, dried at 40 ^{o}C and transferred to 32 mm XRF sample cups. The filtrates were analysed by ICP-atomic emission spectrometry to obtain recovery data.

Standards and samples were measured by EDXRF spectrometry using the Kα radiation for all the elements except for lead; for which the Lα line was employed. An aluminium filter was used in order to remove characteristic lines of the x-ray tube and, more importantly, to reduce the background under the area of interest with only minor reduction of the analytes' peak intensity. The filter's optimum energy range (3.0 – 8.0 KeV)[57] covers the elements of interest with exception of Zn, whose Kα line appears at 8.63 KeV. However, the compromise conditions of analysis proved to be adequate for the concentration levels of Zn found in the samples. Peak overlaps were corrected by using the Kβ/Kα ratios of the analytes obtained from pure resin standards (Table 4.3). No other computing facilities were needed apart from those that allowed the integration of the peaks.

Table 4.3 **Kβ/Kα line intensity ratios used for the correction of peak overlaps in the analysis of trace metals on Dowex 50W-X8 by EDXRF**

Cr	*Mn*	*Fe*	*Cu*	*Zn*
0.172	0.149	0.128	0.169	0.135

4.2.2 Results and discussion

4.2.2.1 Effect of the pH on the determination of metals on Dowex 50W-X8

The results of this experiment are shown in Figures 4.1 and 4.2. The metals studied can be placed in four different groups according to their reaction to changes in the pH:

1) K, Ca and Mg show a maximum retention on the resin in the range of 40 – 50 % recovery. The percentage retention for K is stable throughout the pH interval studied. However, for Ca and Mg, the recoveries on the resin dropped when the pH was higher than 7.

2) Trace metals Mn, Ni, Co, and Zn show an average recovery on the resin of 70% when the pH is between 1 and 8 (between 1 and 7 for Zn). Over pH 8, no metal species are recovered on the resin as nearly 100% of the analytes had already been collected as part of the precipitate in the first part of the experiment. Copper can also be included in this group although, unexpectedly, the highest recovery obtained for this metal on Dowex 50W-X8 was 60% between pH 1 and 3 with the retention falling rapidly at higher pH. However, previous studies showed that 70% recoveries were also achievable for this metal on Dowex 50W-X8 at pH 2.

3) Cr and Pb reach recoveries of 90% on the resin at low pH but the retention quickly falls when the pH is higher than 3 as metal hydroxy species precipitate.

4) Finally, Ti and V show very poor recoveries (< 40%) which are only maintained when working at low pH. As in the previous case, for pH higher than 3 the formation of insoluble species occurs.

In the range studied, pH 2 displayed the optimum retention for the transition metals Mn, Ni, Co, Zn, Cu, Cr and Pb with recoveries between 70 and 90%. Higher pH would still allow the retention of most of these metals but formation of insoluble hydroxy species would also occur. These species, although retainable on filtration, would cause homogeneity problems in the presentation of the samples for XRF analysis and are, therefore, not desirable. Another advantage of keeping the pH low is that a smaller volume of 10% NaOH solution is used to increase the pH of the samples (acid digests). This helps to keep the ionic strength of the solutions low and facilitates the ion exchange between the solution and the resin.

The recoveries for the unwanted possible interferents (the site competitive alkali and alkaline earth elements) were lower than those of the target analytes. However, these metals are still likely to cause competition problems when in high concentrations. Transition metals Ti and V would be difficult to determine using this method as their recoveries are quite low (< 40%) even at low pH.

Further investigations on the physico-chemical characteristics of Dowex 50W-X8 are discussed in Chapters 3 and 6.

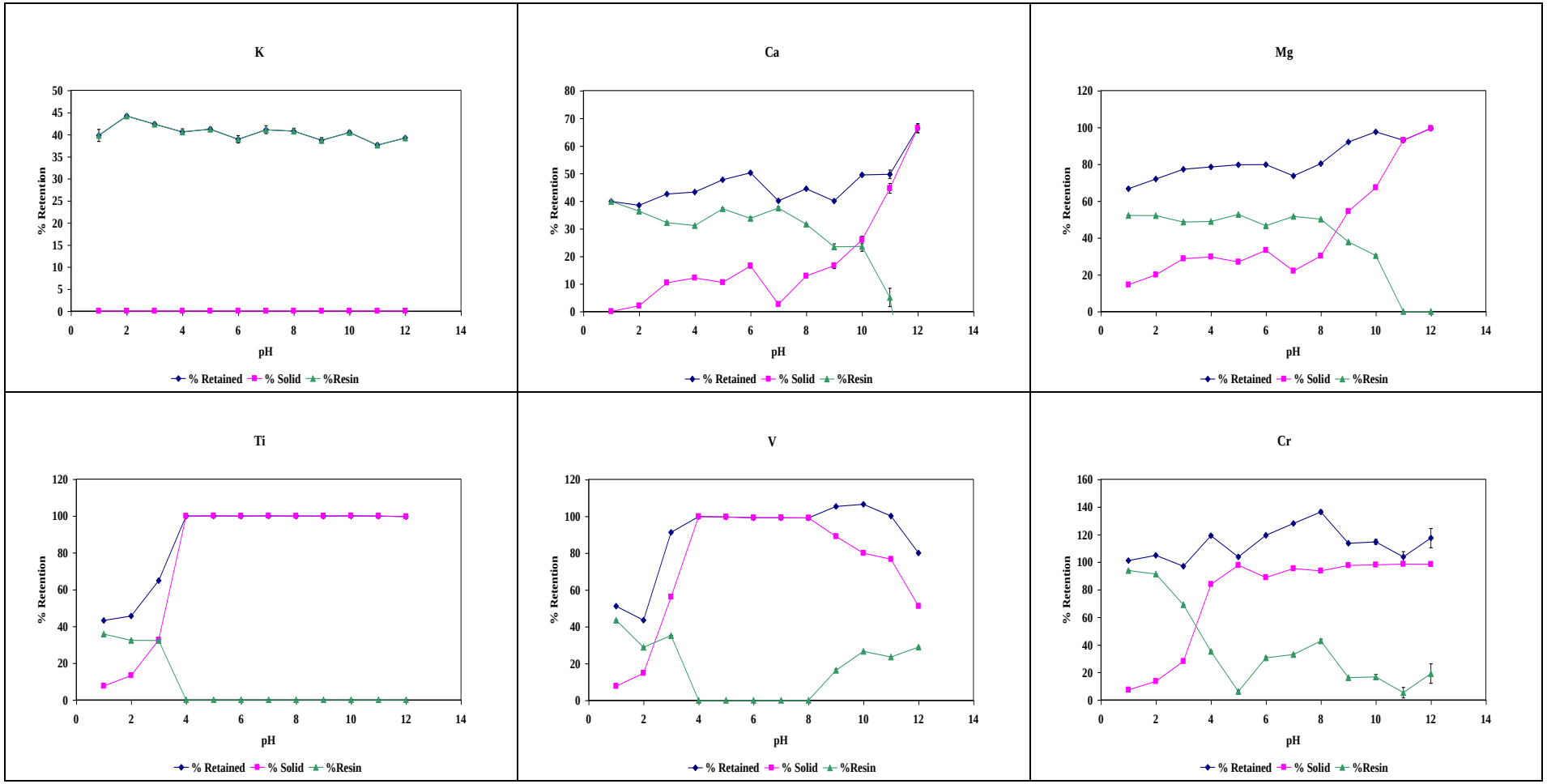

Figure 4.1 **Effect of pH on the retention of K, Ca, Mg, Ti, V and Cr on Dowex 50W-X8. Note: %Retained = % on Resin + % Solid (in Precipitate)**

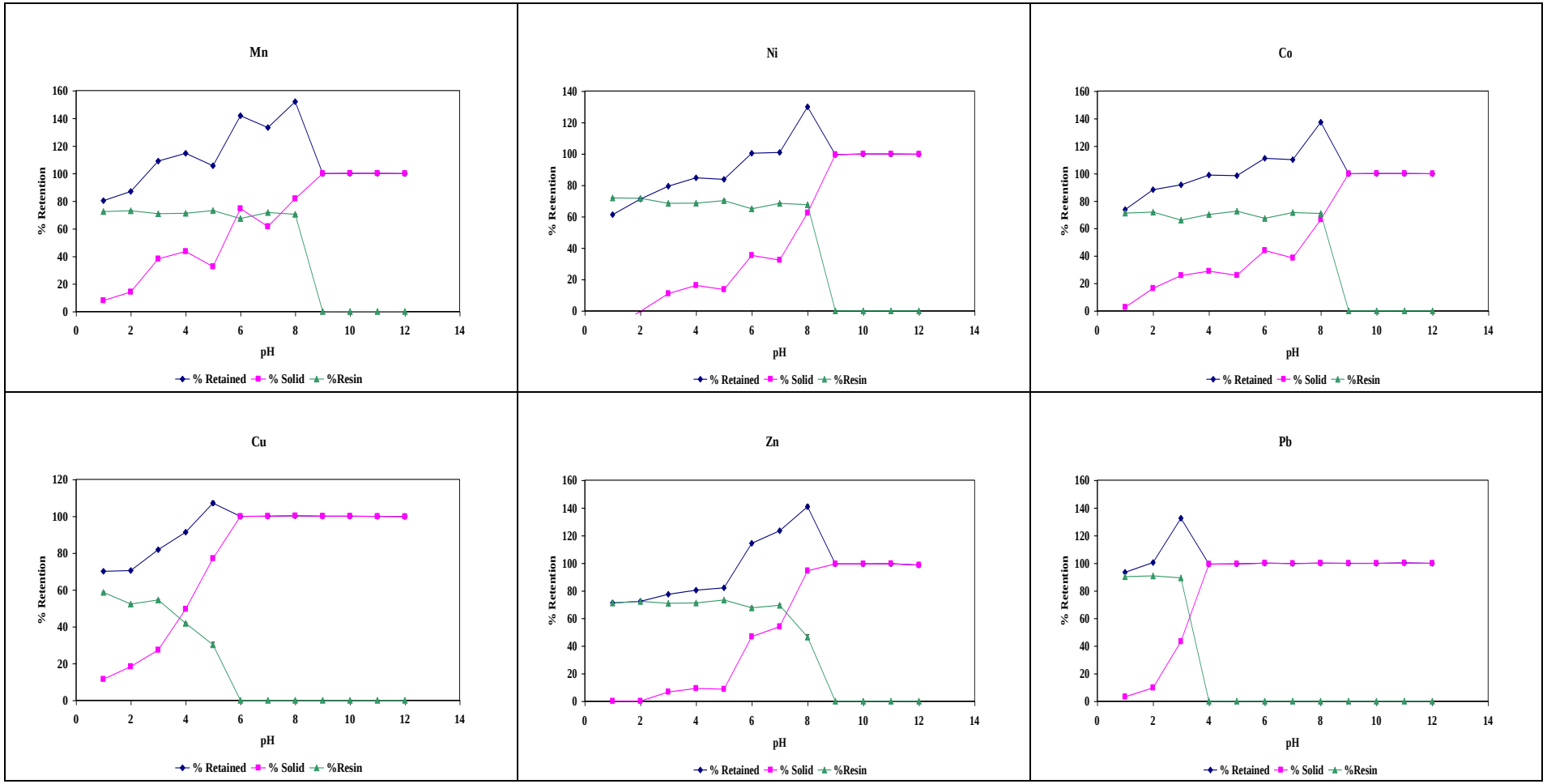

Figure 4.2 Effect of pH on the retention of Mn, Ni, Co, Cu, Zn and Pb on Dowex 50W-X8 Note: %Retained = % on Resin + % Solid (in Precipitate)

4.2.2.2 Limits of detection

The equations and correlation coefficients of the calibration graphs obtained when a series of five multielemental resin standards were analysed under the optimum conditions are shown in Table 4.4. The lowest limit of detection (LLOD) has been defined as the concentration equivalent to 2 standard deviations of the background. This is represented by equation 4-1.

$$\text{LLOD} = \frac{3}{\text{m}} \cdot \sqrt{\frac{\text{b}}{\text{t}}} \qquad (4\text{-}1)$$

where m is the sensitivity, b the counting rate for the background and t the counting time which, in this case, is 100 s.

Table 4.4 **Figures of merit for the determination of metals on Dowex 50W-X8**

Parameter	*Mn*	*Fe*	*Ni*	*Cu*	*Zn*	*Pb*
Working linear range / μg g^{-1}	0 - 1000	0 - 25000	0 - 1000	0 - 1000	0 - 2000	0 - 1000
Sensitivity (m) / counts s^{-1} μg^{-1} g	15	21	27	22	23	7
Background (b) / counts s^{-1}	961	1147	573	517	109	326
Correlation coefficient	0.9984	0.9996	0.9972	0.9974	0.9938	0.9919
Lowest limit of detection/ μg g^{-1}	0.62	0.48	0.27	0.31	0.14	0.77

However, in practise, it was not possible to distinguish concentrations in the ppb range. It was therefore necessary to determine the working instrumental limits of detection. For this purpose, pure elemental standards adsorbed on Dowex 50W-X8 (250 μg g^{-1}) were measured seven times and the limit of detection (LOD) calculated as:

$$LOD = \frac{C \cdot 3\sigma}{I} \qquad (4\text{-}2)$$

where C is the concentration of the standard (in μg or μg g^{-1} of resin), I is the intensity of the Kα or Lα line and σ is the standard deviation of the line intensity. The limits of detection obtained using this equation are shown in Table 4.5 and are now in the ppm range. This more realistic value for the LOD, takes account of both the instrumental noise and repeatability from an analyte that is present at a concentration around its limit of determination (approximately 10-12 times the standard deviation). The confidence level being set at 99.7%.

Table 4.5 **Limits of detection for the determination of metals on Dowex 50W-X8**

Element	*Detection limit (μg g^{-1})*	*Detection limit (μg)*
Cr	17	9
Mn	20	10
Fe	24	12
Ni	40	20
Cu	42	21
Zn	35	18
Pb	114	56

4.2.2.3 Preliminary study on interelement effects and their influence in the analysis of metals retained on Dowex 50W-X8

The experiments suggest that, at these concentrations, no interelement effects occurred. The intensities measured for Cr, Fe, Cu and Pb remained the same throughout the experiment indicating that increasing concentrations of Zn and Mn had no effect (Figure 4.3). A linear response of the intensity against the concentration was obtained for both Zn and Mn (Figure 4.4) indicating the absence of any enhancement or absorption arising from the matrix.

4.2.2.4 Determination of trace metals in sewage sludge by retention on Dowex 50W-X8 and EDXRF detection

The results obtained for the CRM BCR No 144 are shown in Table 4.6. The recoveries ranged from 50 to 100% depending upon the metal. These values were a consequence of the efficiency of retention of the analytes on the resin and did not arise from instrumental limitations of EDXRF, as confirmed by ICP-AES.

The second CRM analysed, BCR No 145 (Table 4.7), produced similar results for all the elements. However, it was not possible to determine nickel in this CRM, because the certified reference concentration of the element in the original sample, 40 $\mu g\ g^{-1}$, is at the limit of detection for this analyte.

The determination of Fe indicated that recoveries were very low (2 - 20%). This could be regarded as a problem if iron was the analyte. However, this element is

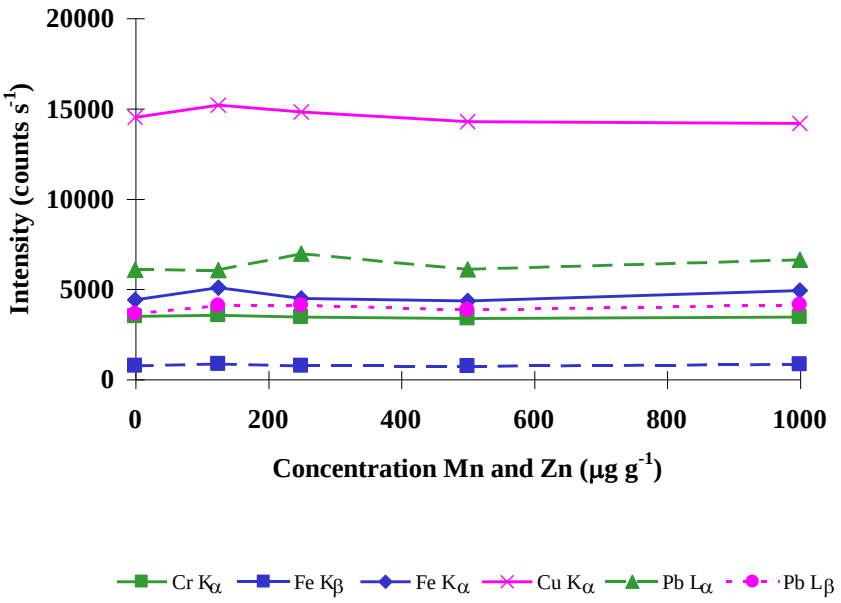

Figure 4.3 **Response of different metal lines to increasing concentrations of Mn and Zn**

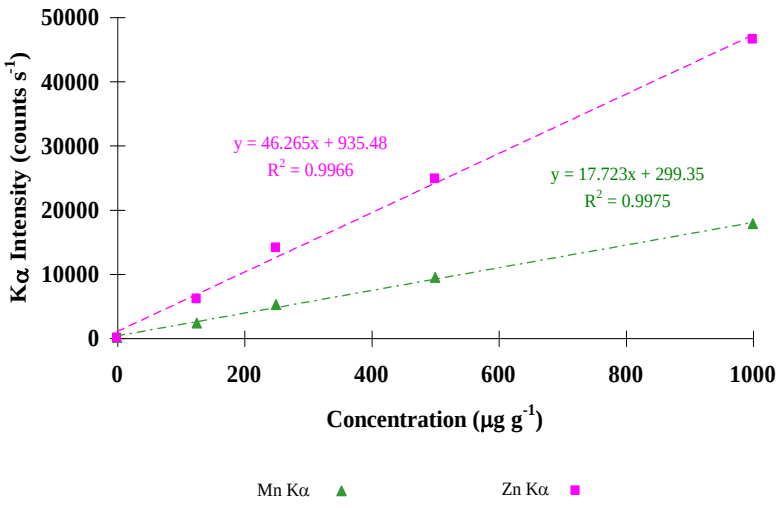

Figure 4.4 **Calibration curves for Mn and Zn in the presence of 250 µg g^{-1} Cr, Fe, Cu and Pb**

a major constituent of the CRMs, with concentrations between 1 and 5%. Therefore, iron has been treated as a matrix constituent in the determination of trace analytes and its low recovery can be regarded as an advantage. Reduced concentrations of Fe on the ion-exchanger will diminish any interference effects exerted on the determination of the other metals. Furthermore, since much of the iron precipitates as a hydroxy compound, there is less competition for the functional groups of the resin, hence increasing the recovery of the analytes. There is, however, a possibility of co-precipitation of analytes and, therefore, the process is in equilibrium.

In terms of repeatability and reproducibility, the method worked generally well for the trace metals in the sample, with the exception of Pb. This element continually gave irreproducible results (possibly linked to those effects described for Fe) and was subsequently removed from the study. The remaining analytes repeatedly produced recoveries that fell within a 25% relative error interval.

In general terms, the results obtained for the set of samples digested with ‘aqua regia’ agreed with those from the nitric-peroxide digestion. It was concluded that any formation of metal chloro-complexes, under the conditions used does not present a major problem. Thus, future experiments would employ the simpler and easier to handle nitric-peroxide digestion on a routine basis.

Table 4.6 **Analysis of metals in sewage sludge (BCR No 144) after retention on Dowex 50W-X8**

Element	*HNO_3 / H_2O_2 digestion*			*'Aqua regia' digestion*		
	Found [a] *$\mu g\ g^{-1}$*	*Reference* [b] *$\mu g\ g^{-1}$*	*% Recovery*	*Found* [a] *$\mu g\ g^{-1}$*	*Reference* [b] *$\mu g\ g^{-1}$*	*% Recovery*
Mn	364 ± 52	449 ± 13	81.1	374 ± 14	449 ± 13	83.3
Fe	9802 ± 29	44332[c]	22.1	8870 ± 130	44332[c]	20.0
Ni	574 ± 58	942 ± 22	60.9	574 ± 18	942 ± 22	60.9
Cu	364 ± 14	713 ± 26	51.1	456 ± 84	713 ± 26	64.0
Zn	1624 ± 52	3143 ± 103	51.7	1680 ± 112	3143 ± 103	53.5

[a] Determined value with 1s confidence interval, n=5.
[b] Certified value with 95% confidence interval.
[c] Not certified.

Table 4.7 **Analysis of metals in sewage sludge (BCR No 145) after retention on Dowex 50W-X8**

Element	*HNO_3 / H_2O_2 digestion*			*'Aqua regia' digestion*		
	Found [a] *$\mu g\ g^{-1}$*	*Reference* [b] *$\mu g\ g^{-1}$*	*% Recovery*	*Found* [a] *$\mu g\ g^{-1}$*	*Reference* [b] *$\mu g\ g^{-1}$*	*% Recovery*
Mn	224 ± 18	241 ± 12	92.9	204 ± 96	241 ± 12	84.6
Fe	1789 ± 64	9090[c]	19.7	764 ± 48	9090[c]	8.4
Ni	< LOD	41.4 ± 2.4	-	< LOD	41.4 ± 2.4	-
Cu	270 ± 64	429 ± 10	62.6	214 ± 100	429 ± 10	50.0
Zn	1722 ± 132	2843 ± 64	60.7	1076 ± 88	2843 ± 64	37.8

[a] Determined value with 1s confidence interval, n=5.
[b] Certified value with 95% confidence interval.
[c] Not certified.

4.2.3 Conclusions on the determination of trace metals in sewage sludge by retention on Dowex 50W-X8 and EDXRF detection

From the pH studies performed with synthetic sample solutions containing the elements of interest and possible interferents, the best recoveries were achieved when the digested samples were mixed with resins at pH 2. The limits of detection for the analytes were between 10 and 21 μg and the LLODs, which can be obtained only under ideal conditions, were approximately two orders of magnitude lower.

No evidence of matrix effects was found and the determinations were simplified by preparing multi-elemental resin standards, customised to cover the linear range in which the concentrations of the analytes were expected. For the analysis of unknown samples the linear range covered by the standards could be extended to the analysts convenience, as long as the capacity of the resin is not exceeded.

The determination of Mn, Ni, Cu, and Zn in sewage sludge was accomplished using the cation exchanger Dowex 50W-X8 to retain the metal species from digests prior to XRF analysis. Two microwave digestion methods were compared (HNO_3-H_2O_2 and 'aqua regia') yielding similar results. Good recoveries were obtained for the determination of Mn (80-90%), whereas for the other metals, the recoveries were lower (around 60%), but repeatable.

Although high concentrations of Fe in samples are an impediment to obtaining better recoveries, the method works well within its limits and, since no complicated software or costly equipment is necessary, the method is inexpensive and does not

require further modifications in order to be used with instruments of different characteristics to the one described in this work.

4.3 DETERMINATION OF TRACE METALS IN SEWAGE SLUDGE BY RETENTION ON CHELEX-100 AND EDXRF DETECTION

4.3.1 Experimental

4.3.1.1 Chemicals and materials

Aristar grade concentrated nitric acid, sodium acetate, sodium hydroxide pellets and glacial acetic acid and Spectrosol grade standard stock solutions of 1000 and 10000 mg L^{-1} V, Cr, Mn, Co, Ni, Cu, Zn, Pb, Mo, Hg and Cd were all obtained from Merck. The 30% hydrogen peroxide solution was obtained from Aldrich Chemical Co. Ltd. (Dorset, U.K.).

Whatman filter paper No 1 was used to separate chelation exchange resin and solutions. The sample cups and Mylar film were obtained from Philips Analytical X-ray (Cambridge, UK). The water used was of ultra pure grade, Milli-Q, 18 MΩ cm (Millipore, Bedford, Massachusetts, USA).

The certified reference materials 'Trace Elements in a Sewage Sludge' were obtained from the Community Bureau of Reference (BCR No 144 and No 145).

The chelating resin Chelex-100, 75-150 μm particle size, was obtained from Bio-Rad Laboratories.

4.3.1.2 Instrumentation

EDXRF work was again performed using a *Link Analytical* XR300 XRF spectrometer operated using the conditions shown in Table 4.8 after optimisation of the net intensity to background ratio for the analytes, keeping the 'dead time' in the range 45-48%.

Table 4.8 **Instrumental parameters used on the Link Analytical XR300 XRF spectrometer.**

Voltage	***Current***	***Vacuum***	***Filter***	***Acquisition time***
20 kV	100 μA	off	aluminium	100 s

The concentrations of the analytes left in solution were determined using a *Perkin-Elmer* Optima 3000 ICP-AE spectrometer using the same instrumental conditions shown in Table 4.2. Additional elements were determined at the following lines: Hg (253.652 nm), Cd (226.502 nm) and Mo (202.030 nm).

4.3.1.3 Optimum pH for the use of Chelex-100

A similar study to that described in section 4.2.1.3 was performed to determine the optimum pH for the retention of certain metals on Chelex-100. A synthetic solution containing 10 mg L^{-1} of each element in admixture in 0.2 M sodium acetate was prepared from 10000 mg L^{-1} standard stock solutions. The pH of 50 mL aliquots was adjusted to specific values in the range 3 – 12 using 10% NaOH and acetic acid. Each synthetic sample solution was mixed with 1.00 g of dried Chelex-100 resin, with stirring for 10 minutes. The resin was separated and dried at 40 ^{o}C, prior to direct analysis by EDXRF. In addition, the filtrates were analysed by ICP-AES and the concentrations on the resin determined by difference.

4.3.1.4 Determination of the maximum retention capacity of Chelex-100

Three microcolumns were prepared by slurry loading empty *Teflon*® tubes (4.2 ± 0.2 cm × 0.3 cm i.d.) with Chelex-100, 100 – 200 mesh (approximately 0.22 ± 0.01 g of resin) in ultra pure water using a plastic syringe. The columns were conditioned with 0.5 M sodium acetate (10 mL) and rinsed with 12.5 mL of ultra pure water.

Each column was connected on-line with an ICP-AE spectrometer to give three replicate measurements of the capacity of Chelex-100. The distance between the end of the column and the plasma was kept to a minimum to reduce dead volume and dispersion effects. A solution of copper in ultra pure water with a concentration of

500 mg L^{-1} was prepared and passed through the column at a flow rate of 1.57 ± 0.06 mL min^{-1}. The copper signal was monitored continuously by the ICP-AES instrument and the process timed in order to determine the moment at which saturation occurred. The experimental average maximum capacity of Chelex-100 was then calculated from the response curves.

4.3.1.5 Determination of the optimum mass of resin

Standards with the same concentration of Cu on Chelex-100 (1000 μg g^{-1}) and different mass of resin (500 – 2000 mg) were prepared by diluting a standard stock solution of Cu (1000 mg L^{-1}) to the appropriate concentration in 50 mL, adjusting the pH to 5.0 ± 0.2 with sodium acetate and mixing the solutions with the resin in batch. The Cu Kα line was measured by the XRF spectrometer. The optimum resin mass was selected from 'net intensity' vs. 'mass of Chelex-100' graphs.

4.3.1.6 Sample preparation procedure for the investigation of interelement effects affecting metals retained on Chelex-100

Two resin calibration series for Cu (0 – 2000 μg g^{-1}) in the presence of different concentrations of Co (500 and 2000 μg g^{-1}) were prepared and measured by EDXRF, in order to study the multielemental effects occurring on Chelex-100. The choice of

metals was based on copper being one of the main target analytes in this investigation and cobalt a very strong absorber of the CuKα line.

4.3.1.7 Sample preparation procedure for the determination of trace metals in sewage sludge using Chelex-100 as retention medium

As previously reported in section 4.2.1.4 the certified reference materials BCR No 144 and BCR No 145, 'Trace elements in sewage sludge' were the subjects of the analysis. The samples were prepared by weighing approximately 0.5000 g of certified reference material accurately into microwave *Teflon*® bombs (Savillex) and adding 4 mL of concentrated nitric acid and 1 mL of 30% H_2O_2. The bombs were capped loosely and left to stand overnight. The following day, they were sealed and microwaved at medium power for 3 minutes in a domestic microwave oven (*PRO Line* SM 11, 750 W).

The digests were filtered through Whatman paper N^o 1 to remove any solids remaining in the bombs. The solutions were transferred into beakers, the volume increased to 25 mL with ultrapure water and the pH raised to 4 with 10% m/v sodium hydroxide solution. This pH had been shown to be the optimum for the retention of the target metals. A procedural blank was prepared in the same way as the samples.

One gram of Chelex-100 was then added to each sample digest and the pH checked and readjusted, if necessary, with sodium hydroxide solution or acetic acid. A series of multi-elemental, matrix-matched standards was also prepared by mixing

aqueous standard solutions with 1.00 g of chelating resin. The mixtures were stirred for 10 minutes, the adsorbing media were then separated by filtration, dried at 40 ^{o}C and transferred to 32 mm XRF sample cups.

Standards and samples were measured by EDXRF spectrometry using the Kα line radiation of the elements of interest (Ni, Cu and Zn). Any peak overlaps were corrected by using the Kβ/Kα ratios of the analytes obtained from pure resin standards (Table 4.9). The filtrates were analysed by ICP-atomic emission spectrometry to obtain recovery data.

Table 4.9 **Kβ/Kα line intensity ratios used for the correction of peak overlaps in the analysis of trace metals on Chelex-100 by EDXRF**

Co	***Ni***	***Cu***	***Zn***
0.130	0.119	0.139	0.167

4.3.2 Results and discussion

4.3.2.1 Effect of the pH in the determination of metals on Chelex-100

It is apparent from the results shown in Figure 4.5 that it is possible to reach 100% recovery for the majority of these metals on Chelex-100 when the pH is kept between 4 and 5. The analytes can be grouped according to their behaviour in the pH range studied:

1) Ni, Co, Cu, Zn and Cd show a similar trend with recoveries that reach 100% when the pH is 4 or 5 and remain constant for the rest of the pH range investigated. However, the results reported in section 4.2.2.1 show that, for these metals, insoluble hydroxy species started to precipitate at pH 6-7. It has already been stated that these species are not desirable because the retention on solid media method is based on the metal ions being homogeneously distributed on the surface of the exchanger. Precipitated species would also be collected on a filter, but it would be impossible to guarantee their distribution with the resins and it would also introduce another matrix into the measurements. Therefore, it would be recommended to work at a pH lower than 5 and reduce any solubility problems to a minimum.

2) The response to change in pH for Cr and Pb is similar to that described for group 1, above. However, recoveries reach an optimum at pH 4 and decrease at pH 5 (60-70%), then, increase again in retention at pH 6 (close to 100%). This can be explained by the formation of species, e.g. $Cr(OH)_2^+$, that neither have the adequate structure to be retained on Chelex-100, nor precipitate out of solution (although they would at a slightly higher pH). For these two metals it would be necessary to use a pH not higher than 4.

3) Mo and V reach 100% retention very quickly (pH 3-4) but this value drops dramatically as the pH increases.

4) Finally, Mn and Hg show similar behaviour with low recoveries (20-60%) at pH 3-5 which indicate that it would not be possible to determine these metals directly on Chelex-100 without prior modification of the samples.

From these results, it was decided to work at pH 4, when possible, in solutions prepared in 0.2 M sodium acetate and using sodium hydroxide and acetic acid to fix the pH when necessary.

It should be noted that acetate ions in solution reduce precipitation by forming acetate complexes. However, the stability constants for complex formation with iminodiacetic groups are higher and retention on Chelex-100 occurs preferentially.

4.3.2.2 Maximum retention capacity of Chelex-100

The working capacity of the Chelex-100 was determined from plots similar to that shown in Figure 4.6. The maximum retention capacity has been defined as the capacity at which the resin is 50% saturated. The working capacity of Chelex-100 was calculated as 0.67 ± 0.07 mEq g^{-1} (average of 3 measurements). This value is one third of the average capacity quoted for the resin by Bio-Rad[60] (2.0 mEq g^{-1}). Working concentrations in this study are below the maximum capacity of the resins.

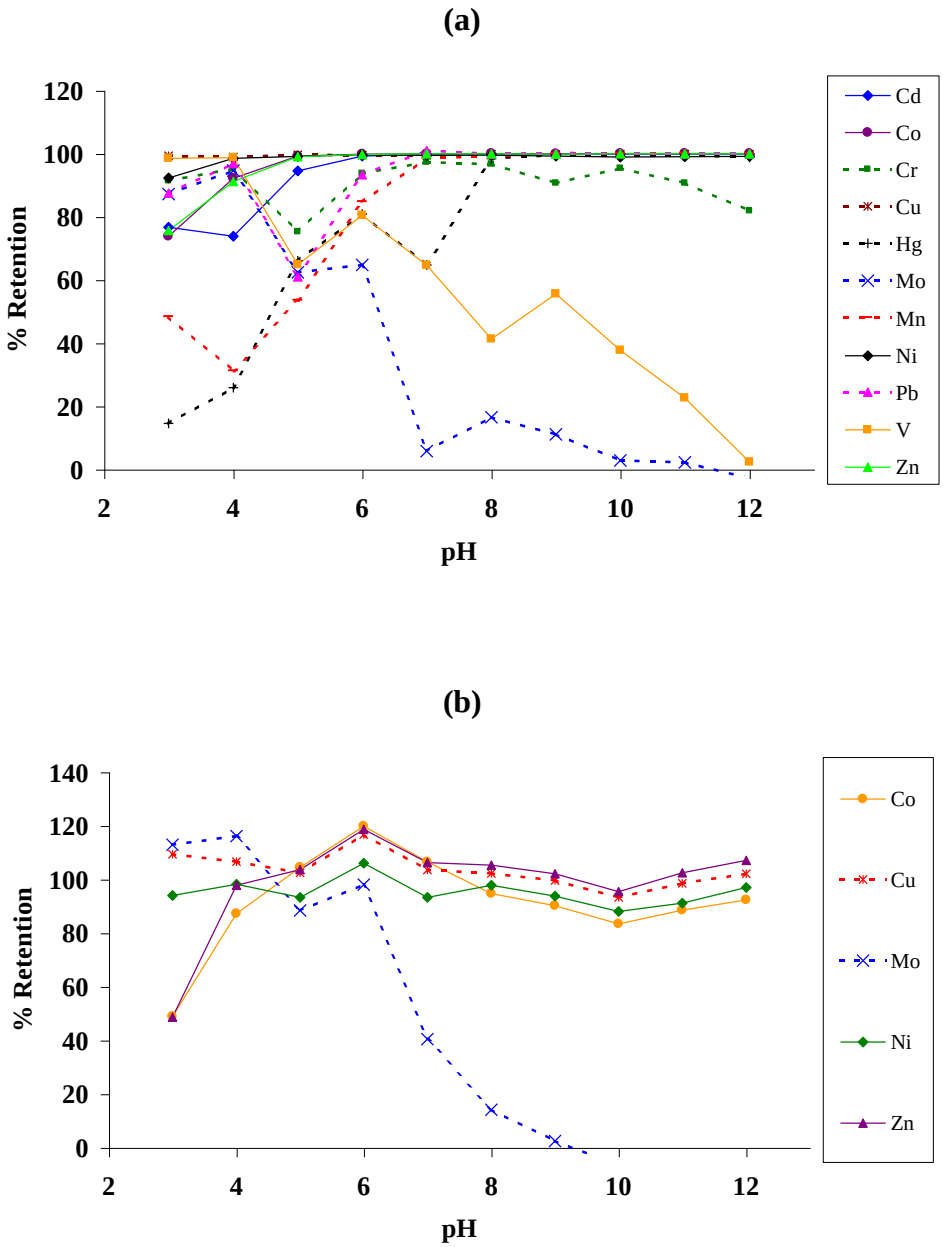

Figure 4.5 **Effect of pH on the retention of metals on Chelex-100. Data from (a) ICP-AES and (b) EDXRF determinations**

Looking at the shape of the saturation curve in Figure 4.6, it is apparent that the reaction between Cu and the functional groups in the resin is slow and therefore, under kinetic control. The 'apparent' saturation of the resin is a consequence of this kinetic process (with 100% saturation occurring at an average total time of 20 minutes) in which continuous and increasing breakthrough occurs. The shape of this curve is totally different to that obtained for the Dowex resins (Figure 6.6). The resins quantitatively adsorb the analyte without any breakthrough for a long period of time (15-20 minutes), then saturation occurs rapidly. One reason for this discrepancy may be that the functional group in Dowex 50W-X8 is a strong acid whereas, in Chelex-100, it is a weak acid that may lead to slow equilibration rates[22]. The problem of breakthrough from Chelex-100 has been tackled by using the resin in batch. Quantitative recoveries are obtained after ten minutes stirring. Column and batch systems for Chelex-100 have been discussed in more detail in Chapter 3.

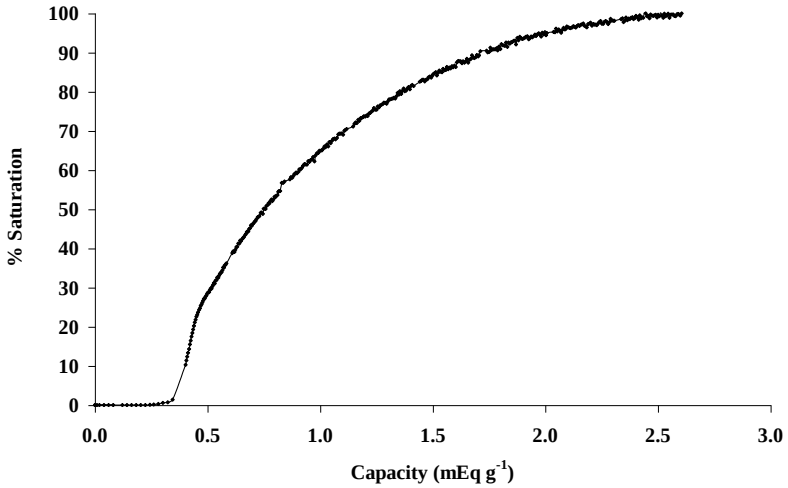

Figure 4.6 Determination of the maximum retention capacity for Chelex-100

4.3.2.3 Optimum mass of resin

The results shown in Figure 4.7 show that in order to obtain a response in net intensity of fluorescence that is proportional to the concentration of analyte in the sample, in this case Cu, a minimum mass of 1500-2000 mg of resin (not dried) is required. This will ensure that factors such as specimen thickness and physical distribution in the sample cup have no significant influence on the intensity of fluorescence and do not contribute to inaccuracy and poor precision. Using greater resin mass is not desirable because this will lead to lower preconcentration factors.

Taking into consideration that the experiment was performed using un-dried, natural resin, the moisture content of Chelex-100 was experimentally determined as 79% by weight (the moisture content of the resin is given as 68-76% by Bio-Rad[60]) and the optimum mass of dry resin calculated as 315-420 mg. In agreement with these findings and for convenience, a mass of 500 mg of dry resin was set as optimum in the remaining experiments. This was increased to 1.00 g of dry Chelex-100 when dealing with sample digests that might exceed the capacity of the resin.

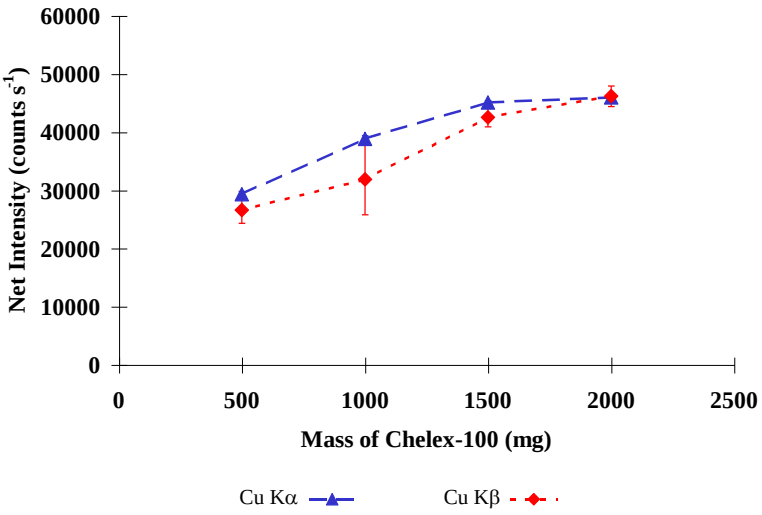

Figure 4.7 **Determination of optimum mass of Chelex-100. (Note: The Cu Kβ series has been normalised to fall in the same intensity range as the Cu Kα)**

4.3.2.4 Multielemental effects and their influence in the analysis of metals on Chelex-100

Figure 4.8 shows the typical response to changes in concentration from the Cu Kα and Cu Kβ lines when a series of resin standards was prepared by mixing aqueous standards of Cu and Chelex-100. In this example, the calibration curves were linear up to 2000 μg g^{-1} of the metal on the resin although further research has shown that it is possible to achieve a linear range up to at least 10000 μg g^{-1}. Analogous curves were found for other elemental standards analysed (Co, Ni, Zn and Mo). These findings

would suggest that, at the concentration levels required for the analysis of trace metals in sewage sludge, there is no deviation from linearity caused only by the matrix itself, i.e. by the chelating resin Chelex-100.

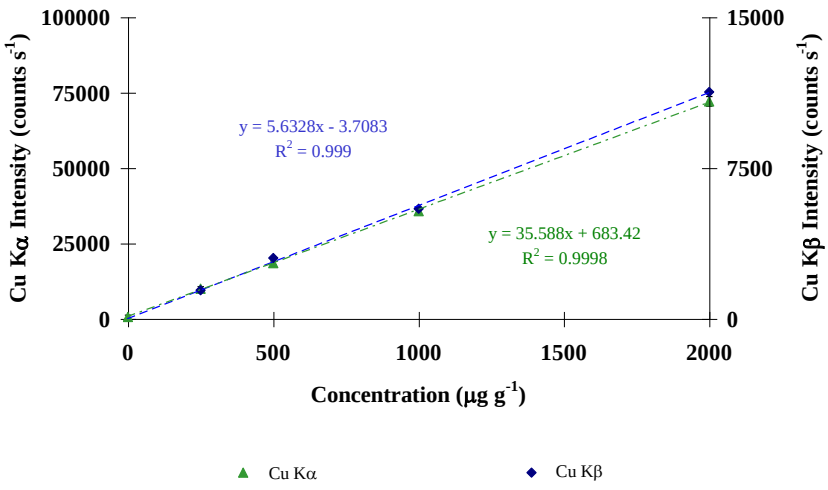

Figure 4.8 Typical calibration curves for a single element (Cu) retained on Chelex-100

However, theoretical calculations based on mass absorption coefficients have shown that when a second element is retained on the resin, deviations from linearity of up to 12.5% may occur for concentrations of the interferent element between 250 and 2000 µg g^{-1}. This would be the case, for example, when copper is to be determined on Chelex-100 in the presence of a strong absorber of the Cu Kα line, such as cobalt (Figure 4.9).

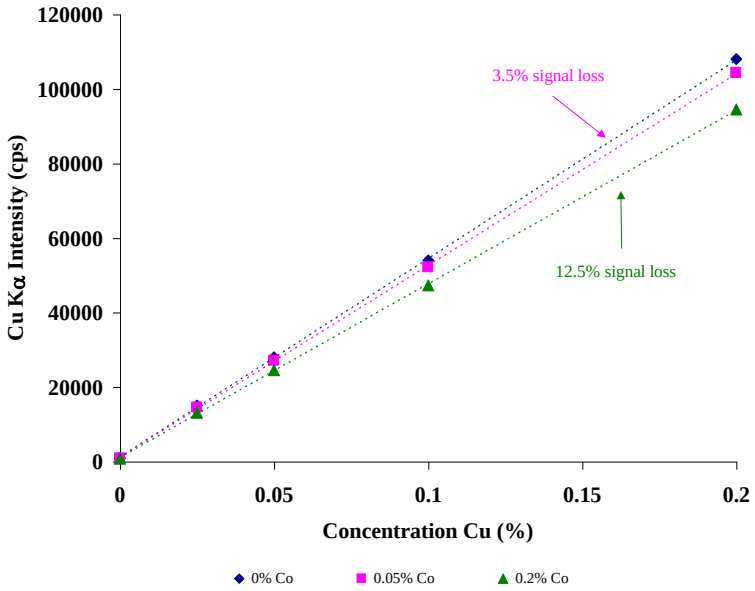

Figure 4.9 **Theoretical changes in the Cu Kα line intensity due to absorption by Co. Calculations based on mass absorption coefficients**

For this reason, it was decided to investigate experimentally the possible absorption effect by a second element retained on Chelex-100. No deviation from linearity was observed for a concentration of Co of 500 μg g^{-1}, as shown in Figure 4.10 (a). When the concentration of Co on the resin was set at 2000 μg g^{-1}, there was a drop in the slope of calibration curves, as displayed in Figure 4.10 (b). This variation is however small (1.3% in the Cu Kα and 1.0% in the Cu Kβ) and well within the precision of the technique with a RSD for both lines being at best 0.5%. In these circumstances, the absorption effects are minimal and it would not be necessary to introduce further corrections to the method. Furthermore, the Co Kα line can be used to normalise the Cu intensity resulting in better calibration curves (Figure 4.11).

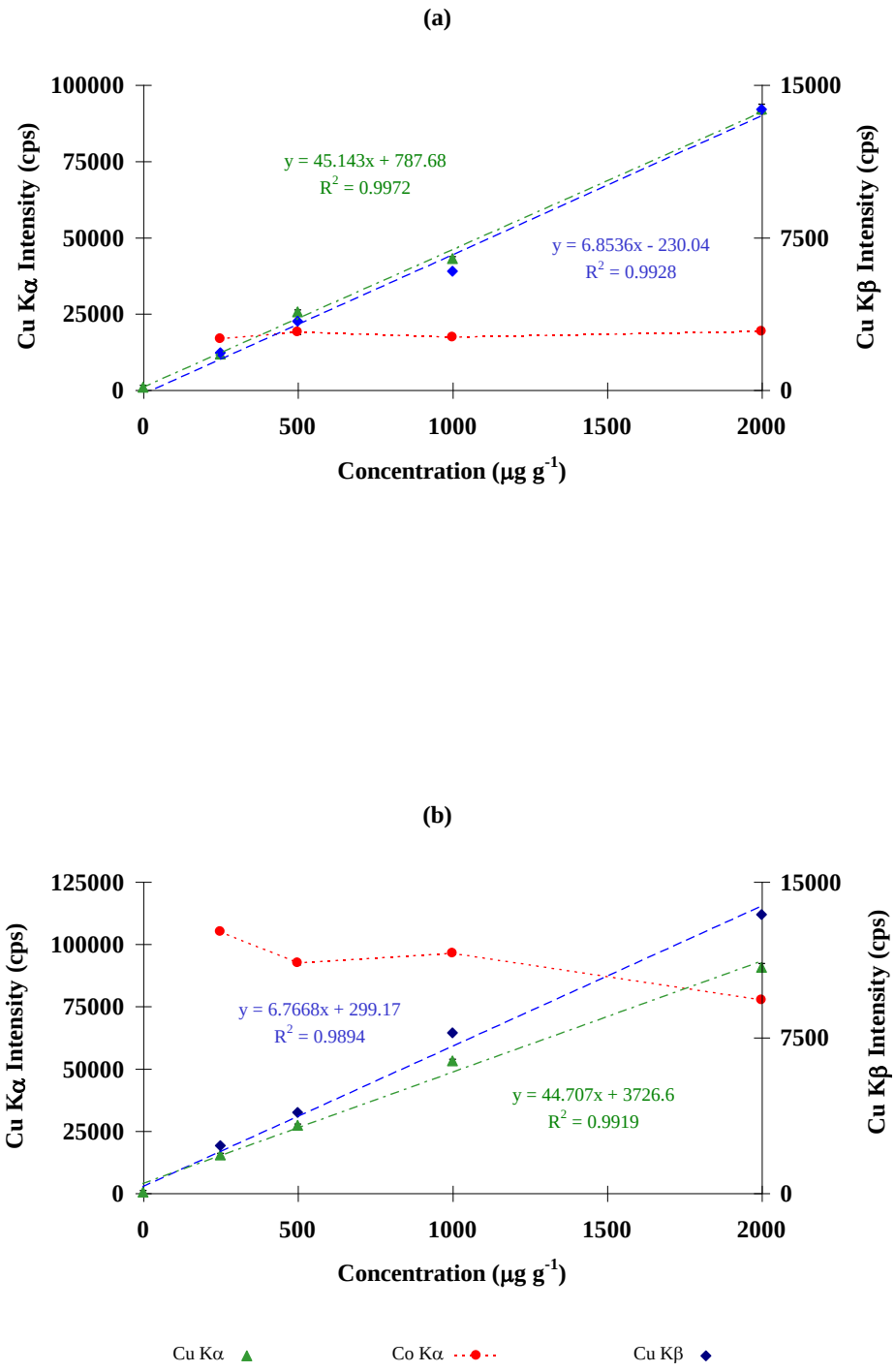

Figure 4.10 **Studies of the influence of cobalt at the (a) 500 µg g^{-1} and (b) 2000 µg g^{-1} concentration levels on the intensity of fluorescence of copper**

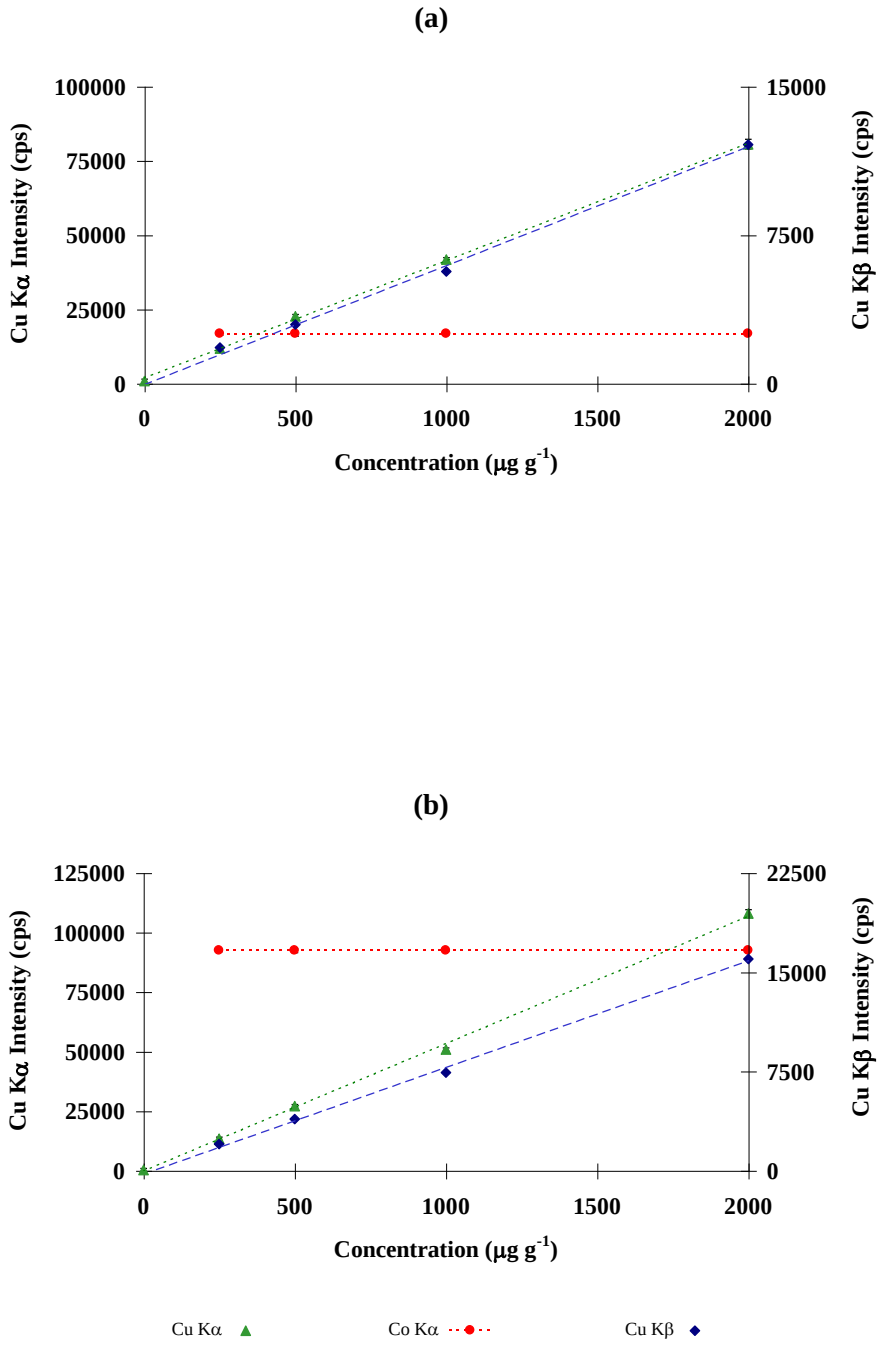

Figure 4.11 **The use of the Co Kα line from (a) 500 μg g^{-1} Co and (b) 2000 μg g^{-1} Co to standardise instrumental fluctuations in the determination of Cu**

These results have been reproduced for the other target elements of the study and, while matrix effects are difficult to predict when more than two elements are involved, no evidence of such effects was found. This was apparent even when using multi-elemental standards in the working concentration range. All calibration curves were found to be linear and reproducible, thereby allowing for the preparation of customised standards in every single determination. A model that explains this and other characteristic effects of the resins has been proposed and discussed in Chapter 3.

Taking advantage of the flexibility offered by the resin, multi-elemental or pure elemental standards were prepared depending on the requirements of the analyses. Multi-elemental standards were used for the quantification of trace elements in sewage sludge. Pure elemental standards were used for the determination of detection limits and for the determination of Kβ/Kα ratios employed for the correction of peak overlaps.

4.3.2.5 Limits of detection

Table 4.10 shows typical figures of merit for the analysis of a series of multi-elemental standards on Chelex-100 using optimum conditions. The LLODs found when working with Chelex-100 fall within the same range as those encountered with Dowex 50W-X8, even though the sensitivity is, overall, higher when using the chelating resin (approximately four times for Ni, Cu and Zn). This indicates that the

limiting factor for detection, under the different conditions and resin matrix employed, is background generated.

However, as discussed previously, a more realistic approach is to determine the 'working limits' of detection (LOD) by preparing and analysing pure elemental standards on Chelex-100 (250 μg g^{-1}). After seven replicate measurements, the LODs were calculated as three times the standard deviation of the net signal, providing the results shown in Table 4.11. As seen when working with Dowex 50W-X8, the limits of detection are higher than the so called LLODs by approximately one order of magnitude. Only when working under ideal instrumental conditions of stability, with a totally homogeneous matrix would it be possible to consider the levels indicated by the LLODs.

Table 4.10 **Figures of merit for the determination of metals on Chelex-100**

Parameter	*Co*	*Ni*	*Cu*	*Zn*	*Mo*
Working linear range / μg g^{-1}	0 - 2000	0 - 2000	0 - 2000	0 - 2000	0 - 2000
Sensitivity (m) / counts s^{-1} μg^{-1} g	48	62	51	45	4
Background (b) / counts s^{-1}	4414	5403	4859	5108	153
Correlation coefficient	0.9965	0.9972	0.9965	0.9947	0.9980
Lowest limit of detection/ μg g^{-1}	0.42	0.36	0.41	0.48	0.93

Table 4.11 **Limits of detection for the determination of metals on Chelex-100**

Element	*Detection limit ($\mu g\ g^{-1}$)*	*Detection limit (μg)*
Co	11	11
Ni	8	8
Cu	49	49
Zn	9	9

4.3.2.6 Determination of trace metals in sewage sludge

Table 4.12 shows the results obtained for the determination of Ni, Cu and Zn in the CRMs BCR No 144 and BCR No 145 after microwave digestion and retention on Chelex-100. Recoveries for Cu and Zn match or are superior to those obtained by using Dowex 50W-X8 for both CRMs. It is apparent that the high concentration of Fe in the samples affects the efficiency of retention for other analytes as was evident when using Dowex 50W-X8. When the concentration of Fe in the CRM decreases from 5% (BCR 144) to 1% (BCR 145) the recoveries for both Cu and Zn increase by approximately 30%.

Table 4.12 **Analysis of metals in sewage sludge digest after retention on Chelex-100**

Element	*BCR No 144*			*BCR No 145*		
	Found [a] $\mu g\ g^{-1}$	*Reference* [b] $\mu g\ g^{-1}$	*% Recovery*	*Found* [a] $\mu g\ g^{-1}$	*Reference* [b] $\mu g\ g^{-1}$	*% Recovery*
Ni	124 ± 32	942 ± 22	13	< LOD	41.4 ± 2.4	-
Cu	390 ± 11	713 ± 26	55	361 ± 9	429 ± 10	84
Zn	2372 ± 87	3143 ± 103	75	2987 ± 96	2843 ± 64	105

[a] Determined value with 1s confidence interval, n=5.
[b] Certified value with 95% confidence interval.

When using Chelex-100 as retention support, the Fe in the sample causes another problem, in addition to those described in section 4.2.2.3. Because the pH for use of this resin needs to be higher than that used for Dowex 50W-X8 (pH 4 instead of pH 2), the amount of Fe that precipitates is also greater. An experimental study of pH vs. solubility (Figure 4.12) shows how the proportion of soluble Fe drops dramatically after pH 3 for an initial solution containing 10 mg L^{-1} Fe and is in agreement with literature values[71]. This means that, when using Chelex, not only part of the active sites of the resin are going to be taken by free Fe ions but also, part of the metal will precipitate and be collected alongside the resin contributing to the dilution of the specimen prior to its analysis by EDXRF. As a result both the accuracy and the precision of the determination may be affected.

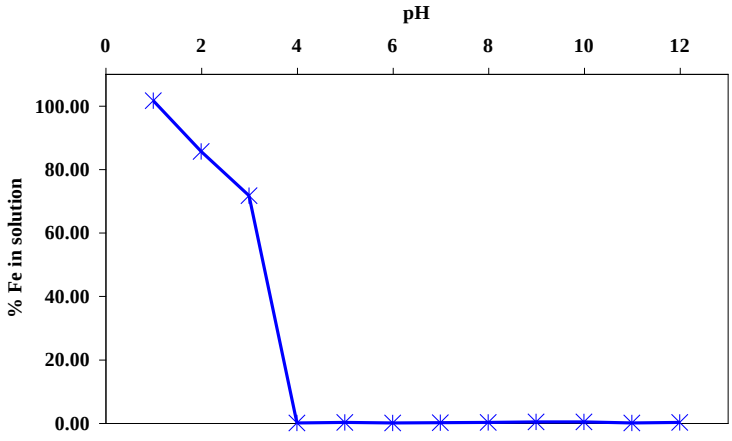

Figure 4.12 Effect of pH on the solubility of Fe in aqueous solution

In order to minimise the effect of the Fe on the determination of the trace metals, several different modifications to the original method were attempted.

i) The precipitate formed at pH 4 was separated prior to the addition of Chelex-100. This gave lower recoveries, presumably because coprecipitation of the trace analytes is aided by the formation of active iron hydroxy species.

ii) The Fe(III) was reduced to Fe(II) with sodium sulphite and with ascorbic acid, in order to diminish the effect of Fe based on Fe(II) being more soluble and having less affinity for Chelex-100 than Fe(III). Again, recoveries were low and also erratic. Further experiments showed that the reducing agents hamper the retention of the trace metals on Chelex-100 as much as they impede the precipitation and retention of Fe.

iii) Finally, NaF was added to digests to complex the metals in solution, including Fe that would form a negatively charged fluoride. The solution was then passed through a Dowex 50W-X8 column with the intention of retaining the trace metals while the iron fluoride complex was sent to the waste. Unfortunately, the breakthrough of the trace metals was too high to allow the use of this method quantitatively.

Nevertheless, the Chelex-100 method provided greater recoveries for Cu and Zn when compared with those obtained with Dowex 50W-X8, especially in the analysis of the CRM BCR No 145 (> 84%). The results were repeatable with RSDs between 2 and 4%. The analysis of Ni yielded very poor results that could not be improved to allow quantitative determination in any subsequent attempts. An absorption effect from Fe on the Ni Kα line can be expected but experimental work showed that this effect did not influence the determination of the metal on Dowex 50W-X8.

It is clear that the use of a chelating resin to determine trace metals in such a complex matrix presents the advantage of a greater selectivity for the analytes, providing better recoveries. Conversely, the conditions in which Dowex 50W-X8 is used allow the determination of a larger number of metals with reasonable recoveries for many of them. In practise, both methods could be combined to target the widest possible range of elements without having to compromise other important factors of the analysis severely, such as cost, preparation and determination time.

4.4 CONCLUSIONS

It was possible to quantitatively determine Cu and Zn in sewage sludge by using the chelating resin Chelex-100 and EDXRF analysis. The pH studies performed showed that a higher compromise pH (pH 4) than that used for Dowex 50W-X8 (pH 2) was necessary to achieve the highest recoveries with Chelex-100 for a range of analytes. The maximum retention capacity was determined as 0.67 ± 0.07 mEq g^{-1} and the optimum mass of resin for the analysis was found to be 0.50 g. However, 1.00 g was used when working with digested sewage sludge to minimise competition problems.

Instrumental multi-elemental effects were not observed during the determinations at the concentration levels used. Multi-elemental standards were employed successfully in the same manner as that described for Dowex 50W-X8.

The limits of detection for analytes using Chelex-100 (between 8 and 49 μg) were similar to those achieved with Dowex 50W-X8. The LLODs were, again, approximately two orders of magnitude lower.

Although good recoveries were obtained for the determination of Cu and Zn in BCR No 145 (80-100%), the influence of Fe when using Chelex-100 seems to have an even greater effect than in the case of Dowex 50W-X8. The recoveries obtained for BCR No 144, which has the higher Fe concentration (5% vs. 1%), are lower. Nevertheless, the use of Chelex-100 is recommended when a higher selectivity is required and there is potential for extension of the method to the determination of other metals, such as Mn by using high pH. As stated previously for Dowex 50W-X8, the simplicity of the method is one of its greater advantages.

5. *STUDY OF THE ANALYTICAL POTENTIAL OF THE Kβ/Kα INTENSITY RATIO IN THE DETERMINATION OF METAL SPECIES BY XRF SPECTROMETRY*

Chapter 5. Study of the Analytical Potential of the Kβ/Kα Intensity Ratio in the Determination of Metal Species by XRF Spectrometry

5.1 INTRODUCTION

The characteristic emission spectrum of an element comprises a series of lines, known as *characteristic lines*. It is possible to predict those lines expected in a particular spectrum and to distinguish between normal transitions (diagram lines), satellites and forbidden transitions depending on whether or not the lines observed follow certain selection rules. The basis for this is that the energy state of an atom can be predicted by means of its electronic configuration. This can be described in terms of four parameters known as *quantum numbers*[2]. These numbers are:

- *n*, the *principal quantum number* which can only take the values of a positive integer, starting with $n = 1, 2, 3$, etc. It defines the shell in which the electron resides (K, L, M, etc.).

- *l*, the *angular quantum number* which has values from 0 to $(n - 1)$. It defines the type of orbital for an electron (s, p, d, f, etc.).

- *m*, the *magnetic quantum number* which can take values from $-l$ to $+l$ and specifies the orbital that the electron will occupy.

- *s*, the *spin quantum number* which only has values of $\pm 1/2$ and determines the direction of the electron *spin*.

The electronic configurations of the first four shells of the atom are shown in Table 5.1. In the ground state, electrons occupy the lower energy orbitals such that in accordance with the *Pauli exclusion principle*, no two electrons in the same atom can have the same four quantum numbers[72].

When discussing polyelectronic atoms, as is always the case in x-ray spectrometry, it is necessary to consider the interactions between electrons. The *spin-orbit coupling* which occurs between the quantum numbers *l* and *s* is one of the most important of these interactions. The vector sum of the '*l* and *s'* moments is known as *j*, the *total momentum* and is a positive number from which the so-called *transition levels*, listed in Table 5.2, originate. Using the quantum numbers and the total moment, it is possible to formulate three *selection rules* that define whether a transition is allowed[2]:

$$|\Delta n| \geq 1 \qquad \Delta l = \pm 1 \qquad \Delta j = 0, \pm 1$$

The characteristic lines that follow these rules (*normal transitions*) are grouped in series and identified as K, L, M, etc.; named after the shell in which the electronic transition ends. Certain transitions give rise to more than one line. For example, a transition from the L shell to the K shell has two possibilities that satisfy the selection rules:

$L_{III}\ (2p^{3/2}) \rightarrow K\ (1s)$ *K-L₃ line* $\qquad\qquad$ $L_{II}\ (2p^{1/2}) \rightarrow K\ (1s)$ *K-L₂ line*

Although the currently accepted nomenclature for characteristic lines is the *IUPAC notation* used above, the *Seigbahn notation*, where the strongest line in each series is called the α line and the remaining lines are called β, γ, δ, etc., is still widely

used in the literature. Thus, in order to be consistent with the publications referred to in this Chapter, the Seigbahn notation (e.g., Kα and Kβ) has also been adopted.

Table 5.1 **Electronic configurations of atoms in the first four shells**[2]

Shell	Quantum number				Orbital	Maximum number of electrons
	n	*l*	*m*	*s*		
K	1	0	0	±1/2	1s	2
L	2	0	0	±1/2	2s	
		1	+1	±1/2		
		1	0	±1/2	2p	8
		1	-1	±1/2		
M	3	0	0	±1/2	3s	
		1	+1	±1/2		
		1	0	±1/2	3p	
		1	-1	±1/2		
		2	+2	±1/2		18
		2	+1	±1/2		
		2	0	±1/2	3d	
		2	-1	±1/2		
		2	-2	±1/2		
N	4	0	0	±1/2	4s	
		1	+1	±1/2		
		1	0	±1/2	4p	
		1	-1	±1/2		
		2	+2	±1/2		
		2	+1	±1/2		
		2	0	±1/2	4d	32
		2	-1	±1/2		
		2	-2	±1/2		
		3	+3	±1/2		
		3	+2	±1/2		
		3	+1	±1/2		
		3	0	±1/2	4f	
		3	-1	±1/2		
		3	-2	±1/2		
		3	-3	±1/2		

Table 5.2 **Transition levels in the first four shells**[2, 3]

Transition level	*l*	*s*	*j*	*Quantum notation*
K	0	1/2	1/2	$1s_{1/2}$
L_I	0	1/2	1/2	$2s_{1/2}$
L_{II}	1	-1/2	1/2	$2p_{1/2}$
L_{III}	1	1/2	3/2	$2p_{3/2}$
M_I	0	1/2	1/2	$3s_{1/2}$
M_{II}	1	-1/2	1/2	$3p_{1/2}$
M_{III}	1	1/2	3/2	$3p_{3/2}$
M_{IV}	2	-1/2	3/2	$3d_{3/2}$
M_V	2	1/2	5/2	$3d_{5/2}$
N_I	0	1/2	1/2	$4s_{1/2}$
N_{II}	1	-1/2	1/2	$4p_{1/2}$
N_{III}	1	1/2	3/2	$4p_{3/2}$
N_{IV}	2	-1/2	3/2	$4d_{3/2}$
N_V	2	1/2	5/2	$4d_{5/2}$
N_{VI}	3	-1/2	5/2	$4f_{5/2}$
N_{VII}	3	1/2	7/2	$4f_{7/2}$

In a characteristic spectrum, it is also possible to encounter lines that do not correspond to normal transitions. *Satellite lines* originate from transitions following double ionisation of the atom, as is seen with the Auger effect, which has been discussed in section 1.2.2.2. *Forbidden transitions*, i.e., those that do not follow the selection rules, are also possible but are generally very weak.

Those factors that condition the intensity of the emitted x-radiation, such as their absorption by matter, the Auger effect and scattering criteria have been discussed in Chapter 1. There is, however, another factor that needs to be taken into

account. The *transition probability*, governed by the *j* quantum number, allows the prediction of the relative intensities of characteristic lines, with a high degree of accuracy. However, this prediction of intensities decreases in accuracy in the order K, L, M, etc.; a consequence of the increased complexity of the spectra[3].

When unfilled, hybridized and, in general, molecular orbitals are to be considered, the calculations are not so straight forward and *j* is not sufficient to explain the characteristic spectrum. The coupling needs to be described more specifically and *Russell-Saunders coupling* and *j-j coupling* are used to this effect[72].

Even with the above corrections, it is important to emphasise that the transition probabilities may be different from the measured intensity ratios because these depend on the experimental conditions. Nevertheless, many authors have taken an interest in characterising this so-called 'chemical effect'. Intensity ratios and energy shifts of the peaks, both a consequence of the unique electronic environment of each atom, have been measured and the information obtained has been used mainly to research the structure of many compounds. Examples of this include the study of titanium[73], boron[74], aluminium and silicon[75] compounds by x-ray emission (XRE) and qualitative speciation of S in solid compounds[76], coal[77] and magmas[78] by XRE and electron microprobe (EMP) methods. Other related applications cover the determination of valence ionisation energies of Ni, Co and Fe compounds by XRE[79, 80] and the investigation of the origin of the chemical effect on the Kβ/Kα ratios from V, Cr and Mn compounds by XRE with WD and ED instrumentation[81]. The determination of electronic structures by photoelectron and x-ray spectroscopy (PAX) has been discussed extensively by Urch[82, 83].

These same principles, i.e., the effect of chemical environment upon the characteristic x-ray spectrum of an element, have also been used (to a lesser extent and with varied success) for the quantitative determination of a species. Some of the recent applications in this field include the speciation of selenium[84] and uranium[85] in soils by x-ray absorption (XAS). Species of Cr have also been determined in solid compounds by extended x-ray absorption fine structure spectroscopy (EXAFS)[86] and in solid particulate matter from air collected in membrane filters by WDXRF[87].

To date, those publications which have covered the determination of element species based on their chemical form or environment with x-ray methods, have concentrated upon relatively pure solids or well characterised mixtures. In this phase, it is difficult to distinguish the chemical effects originating from the lattice of the molecular structure surrounding the analyte from those effects arising from, for example, the oxidation state of the analyte. As a result, those variations observed in intensity ratios or peak shifts are difficult to assign unequivocally. If it was possible to separate the analyte species from that environment, the contributing effect of the oxidation state could be isolated and quantified. One possible route to attaining this separation is from the use of cation and anion exchange resins like Dowex 50W-X8 and 1-X8. The resins will collect the ionic metal species from solutions presenting them to the XRF spectrometer free of their original matrix and in a relatively common 'frame' or environment. Furthermore, it should be possible to evaluate the effect of the oxidation state at lower concentration levels than has previously been attained using EDXRF. In addition, the study may be extended to a comparison with species in solution, where different bonds exist.

Although the majority of the work in this field of x-ray analysis has been performed with WDXRF instrumentation, EDXRF spectrometry has been selected because of the unique presentation properties of the resins. The results obtained will however be supported and compared with WDXRF determinations.

The metals Cr and Mn have been selected for this investigation because they exist in two stable oxidation states with a relatively large difference in electronic charge, Cr(III)/Cr(VI) and Mn(II)/Mn(VII) respectively, and they are both easily retained on ion exchangers.

The aim of this study was to investigate the XRF intensity ratios from different chemical species of the same metal that had been separated from their normal environment onto resins and to evaluate the possibility of using any systematic differences in these ratios for analytical purposes.

5.2 EXPERIMENTAL

5.2.1 Chemicals and materials

Potassium chromate and dichromate, both AnalaR grade, chromic potassium sulphate, chromium trioxide, chromium metal and Spectrosol grade standard stock solution (1000 mg L^{-1}) of chromium (III) nitrate were all obtained from Merck. Standard stock solution of 1000 mg L^{-1} Cr(VI) was prepared by dissolving 0.283 g of $K_2Cr_2O_7$ (Merck) in 100 mL of ultra pure grade water. Chromium (III) chloride

hexahydrate was obtained from Aldrich Chemical Co. Ltd. and chromium (III) oxide was obtained from Johnson Matthey (Royston, Herts, UK).

Potassium permanganate and manganese (II) chloride tetrahydrate (AnalaR grade) and concentrated nitric acid, ARISTAR grade, were obtained from Merck.

Whatman filter paper N^{o} 1 was used to separate ion exchange media and solutions. The plastic sample cups and Mylar film were obtained from Philips Analytical X-Ray. Milli-Q doubly deionised water, 18 MΩ cm was used throughout the study.

The ion exchange resins, Dowex 50W-X8 (100-200 mesh) and Dowex 1-X8 (100-200 mesh) were both obtained from Merck.

5.2.2 ***Instrumentation***

Measurement of metal concentrations in aqueous solutions for the calculation of recovery data was achieved using a Perkin-Elmer Optima 3000 Radial ICP-AE spectrometer or, sensitivity permitting, a GBC 902 FAA spectrometer with operating conditions as shown in Table 5.3.

The XRF work was performed using Philips PV9500/9100 and Link Analytical XR300 energy dispersive XRF spectrometers and a Philips PW1404 wavelength dispersive XRF spectrometer. The conditions in which these instruments were operated are shown in Tables 5.4, 5.5 and 5.6.

Table 5.3 **Instrumental parameters for the GBC 902 flame atomic absorption spectrometer**

Element	**Cr**	**Mn**
Wavelength	357.9 / 425.4 nm	279.5 nm
Band pass	0.5 nm	0.5 nm
Lamp current	6 mA	6 mA
Flame	Air-Acetylene (reducing)	Air-acetylene (oxidising)

5.2.3 General sample preparation procedure

The samples for this study were prepared by stirring known standard concentrations or saturated solutions of Cr(III), Cr(VI), Mn(II) or Mn(VII) in 0.01M HNO_3 with a known weight of resin, usually 0.5 or 1.0 g, for 10 minutes.

The resins were then separated from the aqueous phase by filtration, dried at 40 ^{o}C and transferred to plastic sample cups for XRF analysis (*Philips*) using *Mylar* film as supporting material. Aqueous standards were also analysed directly in the XRF sample cups.

5.2.4 ***Preliminary experiments***

5.2.4.1 Optimisation of the instrumental conditions to be used during the operation of the Philips PV9500 EDXRF spectrometer

Preliminary experiments were performed using the Philips PV9500 EDXRF spectrometer. First, a study of the optimum operating conditions was completed by recording the changes in net intensity of fluorescence and net intensity to background ratio with different settings of voltage and current intensity. The radiation was measured as peak area in a window set around the Cr Kα line. Unlike the Link Analytical XR300 spectrometer, the Philips PV9500 does not provide a reading for the dead time. However, the number of counts per second was always kept below 14000 to avoid any damage to the detector.

Three specimens were studied: a powdered sample of chromium metal to give Cr^0, Cr(VI) as a solution of $K_2Cr_2O_7$ in ultra pure water adsorbed to saturation on 1.0 g of Dowex 1-X8 and Cr(III) as an aqueous solution of $CrCl_3.6H_2O$ equally saturated on 1.0 g of Dowex 50W-X8. This allowed a comparison of optimum conditions to be obtained for three different oxidation states.

5.2.4.2 Influence of the instrumental parameters on the measured Kβ/Kα ratios for chromium species

A series of standards with concentrations between 0 and 2500 μg g^{-1} was prepared, following the procedure described in section 5.2.3, for both Cr(III) on

Dowex 50W-X8 and Cr(VI) on Dowex 1-X8. Prior investigations, reported in Chapter 6, had shown that chromium species in natural waters could be determined after preconcentration on Dowex resins within this concentration range. The standards were analysed using the Philips PV9500 EDXRF spectrometer at increasing voltages (15 - 25 kV) and current intensities (100 - 300 μA). The intensity of each chromium line was measured by selecting a window around the CrKα (5.16 – 5.66 keV) and the CrKβ (5.68 – 6.13 keV) and obtaining the *peak area* by means of the EDAX XRAY 95 software. A small fraction of the scattered radiation (4.50 - 4.80 keV) was also measured following the same procedure and this was used as an internal standard to achieve normalisation of the data.

The Kβ/Kα ratio was calculated for each concentration of Cr(III) and Cr(VI), at each set of conditions, in order to determine if a change of the instrumental parameters could affect the ratio.

5.2.4.3 Determination of Kβ/Kα intensity ratios from solid pure chromium compounds

A range of solid chromium compounds in different oxidation states were analysed by EDXRF in order to obtain data on the intensity of CrKα and CrKβ lines. In this manner, the ratios between the Kβ and Kα intensities could be calculated and compared.

For this experiment, loose powder samples were simply loaded into XRF plastic sample cups fitted with Mylar film. The conditions used in this experiment are displayed in Table 5.4.

Table 5.4 **Instrumental parameters used on the Philips PV9500 EDXRF spectrometer**

Voltage	*Current*	*Vacuum*	*Filter*	*Acquisition time*
20 kV	50 μA	off	none	100 s

5.2.5 Analysis of Cr and Mn standards in solution and on Dowex resins

Several series of standards of Cr(III), Cr(VI), Mn(II) and Mn(VII) in solution and also retained on the appropriate Dowex resin were prepared following the procedure described in section 5.2.3.

The standards were analysed using the Link Analytical XR300 EDXRF spectrometer with the instrumental parameters shown in Table 5.5. Five replicate measurements of the peak area were obtained for each standard at the Kα and Kβ lines of each element and the mean intensity was plotted against concentration.

Table 5.5 **Instrumental parameters used on the Link Analytical XR300 EDXRF spectrometer**

Voltage	*Current*	*Vacuum*	*Filter*	*Acquisition time*
20 kV	80 – 120 μA	off	none	100 s

A series of these standards were also analysed using the Philips PW1404 WDXRF spectrometer utilising the conditions shown in Table 5.6. In this case, peak height measurements were used for the Kα and Kβ lines of both analytes.

Kβ/Kα ratios were calculated for each elemental species by i) using the slopes of the linear 'intensity vs. concentration' response curve and ii) calculating an average of the Kβ/Kα ratios obtained at different concentrations of the metal species retained on the resins or present in solution.

Table 5.6 **Instrumental parameters used on the Philips PW1404 WDXRF spectrometer**

Crystal	*Voltage*	*Current*	*Collimator*	*Filter*	*Detector*
LIF200	50 kV	60 mA	Fine	None	Flow + Scintillation

5.3 RESULTS AND DISCUSSION

5.3.1 Preliminary results

5.3.1.1 Optimum operating conditions for the Philips PV9500 EDXRF spectrometer

The Kα intensity results obtained from this experiment are shown in Figures 5.1 to 5.4. Figure 5.1 shows an example of the normal fluorescence response to an increase in either voltage or current intensity from the x-ray tube. As expected, an increase in the net intensity of fluorescence is observed. As the background and, therefore, the gross intensity of fluorescence increase simultaneously neither of these magnitudes are used individually for optimisation. The variation in net and gross intensity and in background, with the operating conditions for Cr(III) and Cr metal, followed the same pattern as that showed in Figure 5.1 for Cr(VI).

Consequently, the optimum operating conditions were evaluated in terms of the ratio between the net intensity and the background. This has been addressed as 'signal / background' in the figures and will be referred to as 'SBR' in the text for abbreviation. Generally, it can be seen from Figures 5.2 to 5.4 that an increase in the voltage up to 20 kV produces a greater SBR, although higher voltages do not augment the ratio; most probably because the dead time of the detector is extended.

In terms of the current intensity, the results indicate that the settings are preferably kept between 25 and 100 μA. Nearly all the plots show high SBRs at low currents (10 μA). However, because the net intensities and, especially, the backgrounds measured at this setting were very low, the errors introduced were

greater. Higher current values were therefore employed to aid instrument stability and reproducibility.

The three chromium species show similar responses to the changes in operating conditions. At this stage, it was not possible to state whether any minor dissimilarities were due to the difference in oxidation state or to the low sensitivity of the instrument when using low settings.

From calculations (similar to those displayed in Appendix A) based on the theoretical saturation capacities of the resins, 100 g of Dowex 50W-X8 would be able to retain up to 8.3 g of Cr(III) and Dowex 1-X8 would hold up to 18.2% Cr(VI). Thus, in theory, the signal obtained from Cr(VI) would be up to 2.2 times that of Cr(III). The experimental SBR values found in this investigation are in agreement with these theoretical figures: the SBRs for Cr metal were between 80 and 110, being higher than the SBRs for Cr(VI) (55-75) and these, again, higher than those found for Cr(III) (20-40). The average SBR signal for Cr(VI) is 65, i.e., 2.2 times the average SBR signal for Cr(III), which is 30.

When using the Link Analytical EDXRF spectrometer, separate optimisations of the instrumental parameters were performed every time that samples with new characteristics were to be analysed.

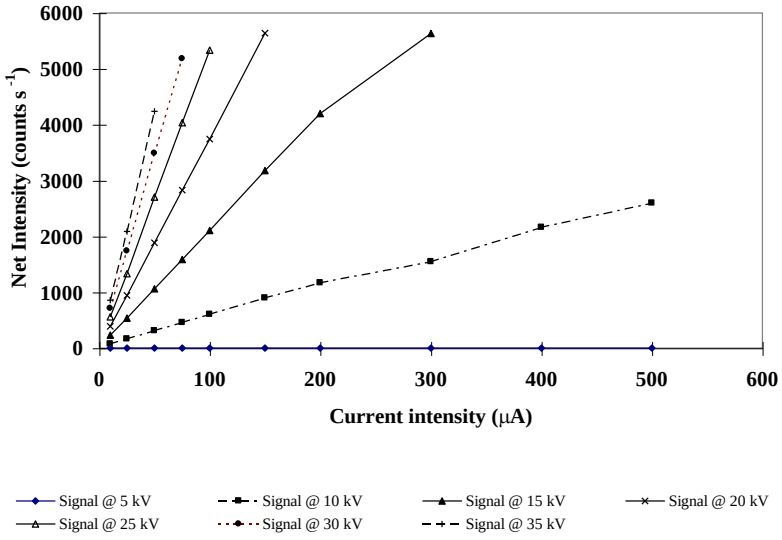

Figure 5.1 **Variation of the net intensity of fluorescence with voltage and current for Cr(VI) on Dowex 1-X8 resin**

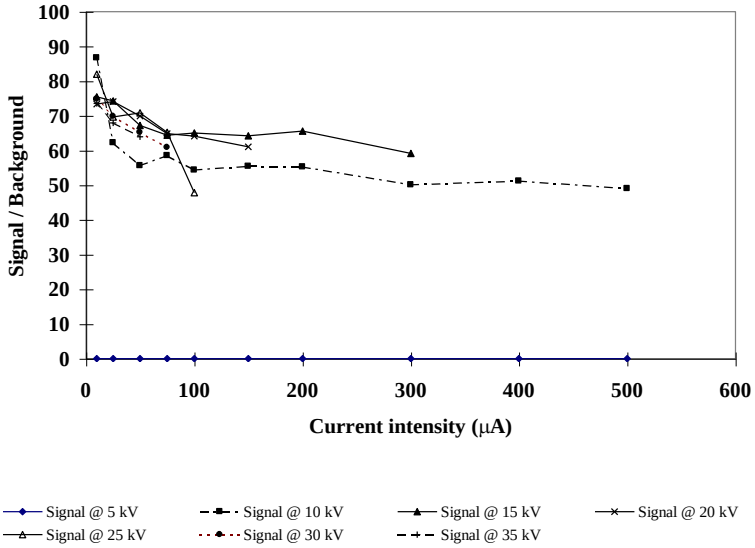

Figure 5.2 **Optimisation of the net intensity (signal) to background ratio for Cr(VI) on Dowex 1-X8 resin**

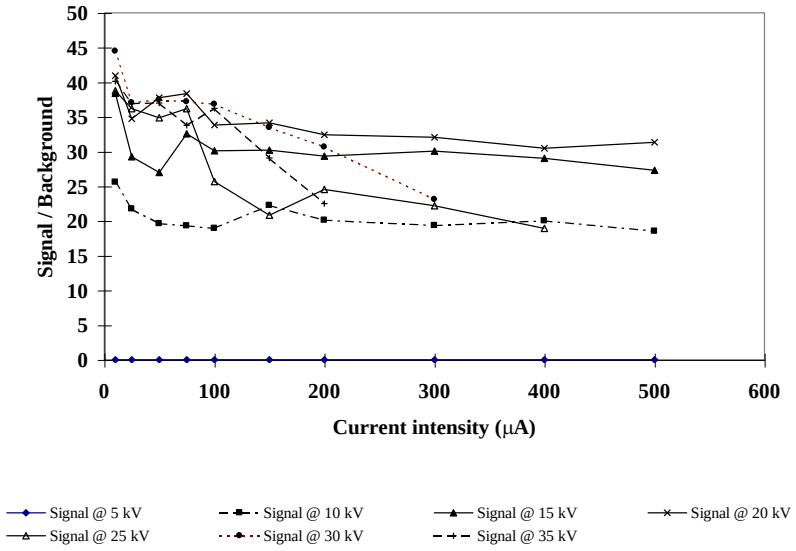

Figure 5.3 **Optimisation of the net intensity (signal) to background ratio for Cr(III) on Dowex 50W-X8 resin**

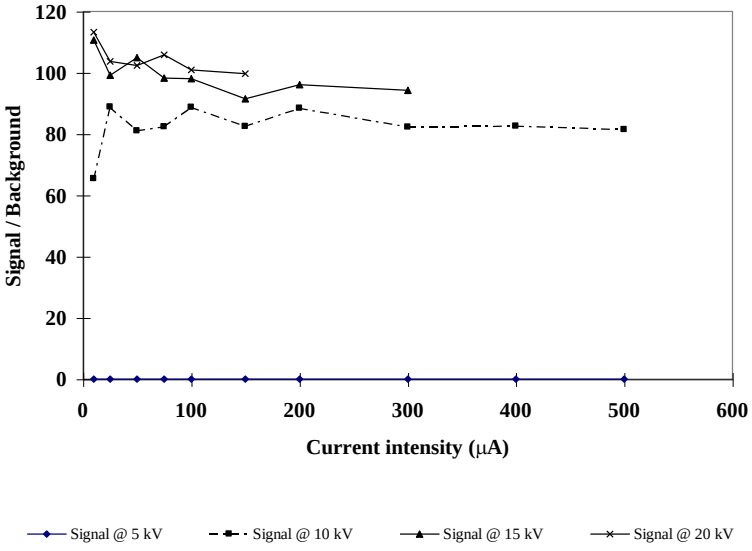

Figure 5.4 **Optimisation of the net intensity (signal) to background ratio for chromium metal**

5.3.1.2 Influence of the instrumental parameters on the measured Kβ/Kα ratios for chromium species

The Kβ/Kα ratios for standards with different concentrations of Cr(III) and Cr(VI) on Dowex resins at different operating conditions are shown in Table 5.7. The ratios in this table were calculated from net intensities that had been normalised using a small fraction of scattered radiation in the energy range 4.50 – 4.80 keV. This procedure, which is fast and simple and does not require the addition of any other reagents, was adopted because the use of scattered radiation as internal standard provided better correlations between the concentration of chromium on the resins and the intensity of fluorescence, especially for the Kβ lines. An example of this can be seen in Figure 5.5, where standards of Cr(VI) on Dowex 1-X8 were analysed at 20 kV and at different current intensities and the CrKα line, with and without internal standard correction, were plotted against concentration.

The results in Table 5.7 show no relationship between the instrumental conditions used and the intensity ratios obtained other than when the voltage and current is low. Under these latter conditions, the Kβ intensity is low and subsequently shows greater variation. Also, the ratios for standard concentrations equal or less than 1000 μg g^{-1} are inconsistent; a consequence of the Cr Kβ intensity again being too low for an accurate determination with the Philips EDXRF spectrometer. The results from the Cr concentrations between 1500 and 2500 μg g^{-1} are more uniform, as would be expected from the greater Kβ intensities. They do not however show any correlation with the operating conditions, when the Cr(III) and Cr(VI) sets are

compared. This can be seen clearly in Figures 5.6 (a) and (b), which represent the ratios obtained for the 2500 $\mu g\ g^{-1}$ standards.

From this preliminary study, there appears to be a trend in the $K\beta/K\alpha$ intensity ratios for Cr(III) and Cr(VI) on resins, with the Cr(III) ratio always being higher. However, the precision of these measurements is poor, especially in the case of Cr(III). This may be attributed to the intensity signals from this species on Dowex 50W-X8 which are always lower than those obtained for Cr(VI) on Dowex 1-X8 by approximately 60%. This point had been noted in previous experiments reported in section 5.3.1.1.

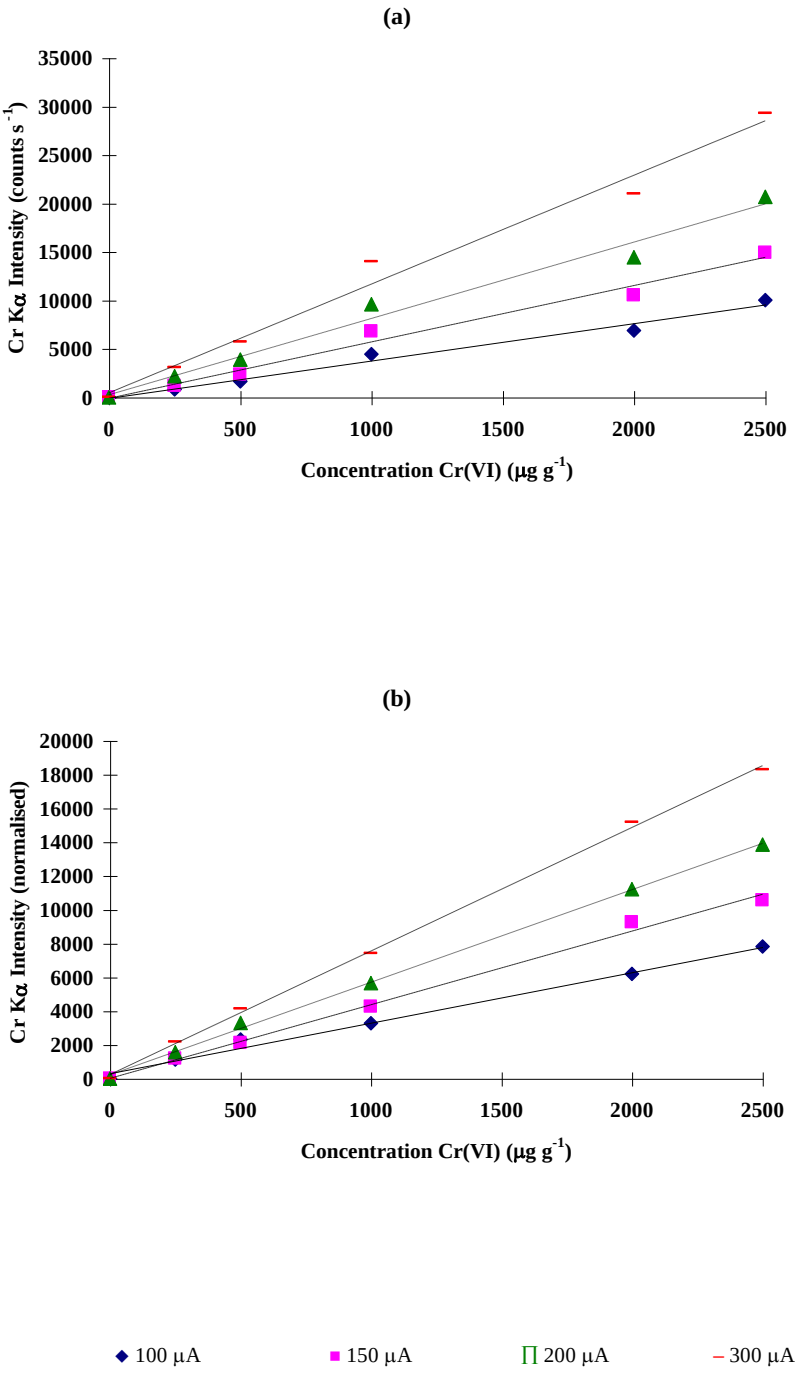

Figure 5.5 **Calibration graphs from Cr(VI) on Dowex 1-X8 standards analysed at 20 kV and different current intensities before (a) and after (b) correction of the intensity of fluorescence using scattered radiation as internal standard**

Table 5.7 **Kβ/Kα ratios for chromium standards on Dowex type resins.**

Voltage (kV)	Intensity (μA)	Concentration (μg g^{-1})											
		250		*500*		*1000*		*1500*		*2000*		*2500*	
		Cr(III)	**Cr(VI)**	**Cr(III)**	**Cr(VI)**	**Cr(III)**	**Cr(VI)**	**Cr(III)**	**Cr(VI)**	**Cr(III)**	**Cr(VI)**	**Cr(III)**	**Cr(VI)**
15	**100**	0.112	-0.170	0.320	0.096	0.234	0.143	0.198	0.134	0.216	0.140	0.144	0.113
15	**150**	0.529	0.129	0.393	0.121	0.243	0.155	0.254	0.156	0.218	0.139	0.213	0.141
15	**200**	-0.522	0.217	0.184	0.123	0.223	0.104	0.213	0.173	0.203	0.141	0.195	0.147
15	**300**	-0.301	0.084	0.192	0.089	0.198	0.067	0.137	0.134	0.160	0.127	0.122	0.129
20	**100**	0.084	0.301	0.335	0.241	0.253	0.151	0.220	0.180	0.161	0.141	0.191	0.143
20	**150**	0.211	0.195	0.110	0.122	0.272	0.090	0.202	0.177	0.201	0.141	0.174	0.137
20	**200**	-0.661	0.281	0.158	0.209	0.180	0.170	0.167	0.201	0.110	0.170	0.192	0.153
20	**300**	0.138	0.280	0.242	0.187	0.200	0.121	0.214	0.172	0.054	0.146	0.187	0.143
25	**100**	0.047	0.205	0.129	0.176	0.188	0.143	0.180	0.178	0.130	0.122	0.145	0.146
25	**150**	-0.104	0.216	0.239	0.152	0.130	0.137	0.209	0.148	0.156	0.146	0.150	0.136
25	**200**	0.252	0.241	0.193	0.157	0.217	0.129	0.213	0.165	0.153	0.138	0.190	0.151
25	**300**	-0.095	0.268	0.298	0.196	0.186	0.139	0.250	0.169	0.158	0.151	0.198	0.145
	Mean:	-0.03	0.19	0.23	0.16	0.21	0.13	0.20	0.17	0.16	0.14	0.18	0.14
	SD:	0.34	0.13	0.09	0.05	0.04	0.03	0.03	0.02	0.05	0.01	0.03	0.01
	%RSD:	-1300.0	69.0	37.8	30.3	18.2	22.7	15.9	11.9	29.6	8.4	16.0	7.7

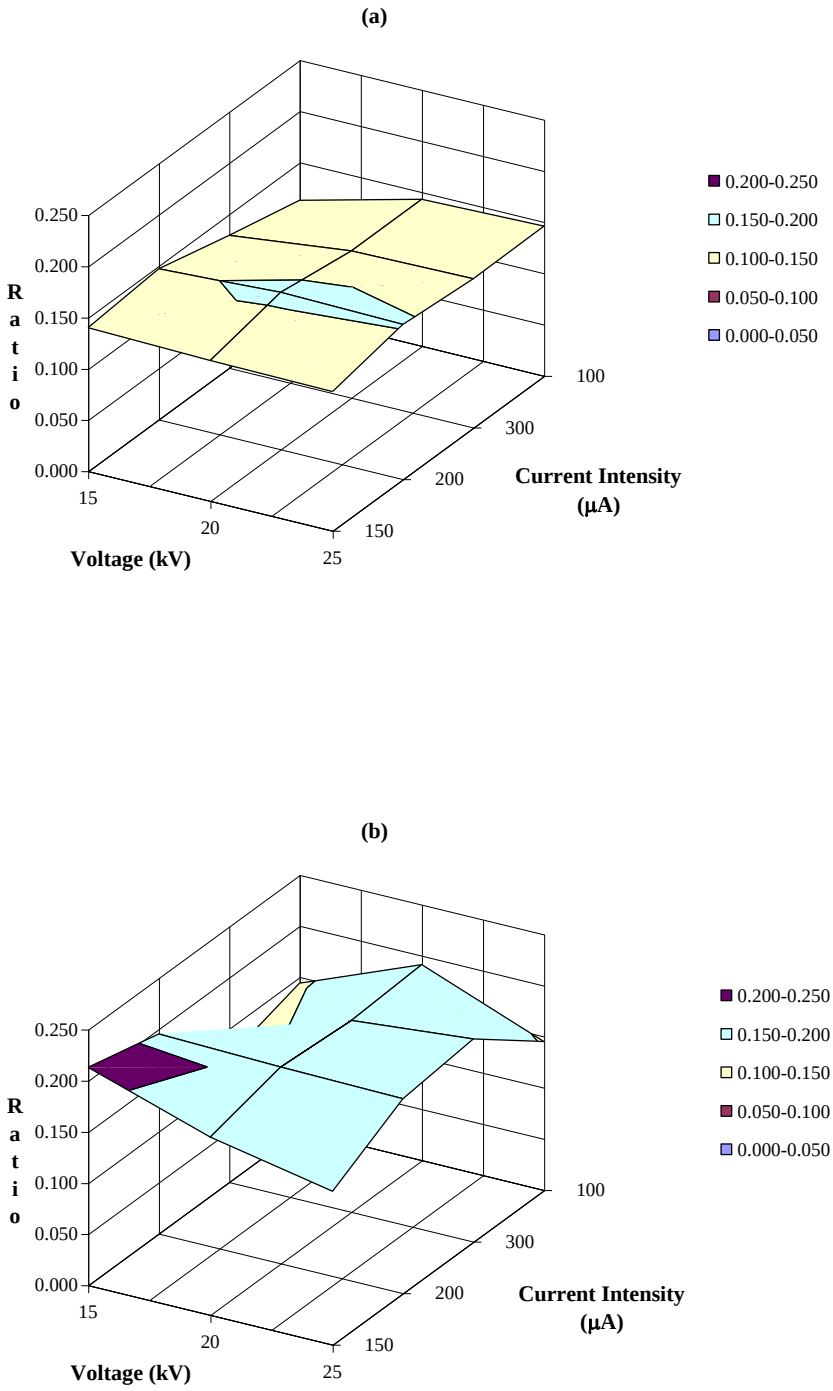

Figure 5.6 **Effect of the instrumental parameters (voltage and current intensity) on the Kβ/Kα ratios for 2500 μg g^{-1} of (a) Cr(VI) and (b) Cr(III) retained on Dowex resins**

5.3.1.3 Determination of Kβ/Kα ratios from pure solid chromium compounds

A range of solid chromium compounds were also analysed using the Philips EDXRF spectrometer and the results obtained are shown in Table 5.8. These Kβ/Kα ratios did constitute a reference point for further measurements, where the metal species have been retained on Dowex resins, which is the objective of this investigation. The values shown in the table are very close for all the solid compounds (0.17 ± 0.01) and there is no apparent relationship between any small variations in the ratios and the oxidation state of the analyte in the compound.

The intensity ratios for chromium species retained on the resins reported in the previous section were close to those displayed in Table 5.8. However, whether the chemical effect on these ratios is sufficient to guarantee that they can be used as a means of quantitative determination of metal species on resins is still uncertain and is the subject of the following investigations.

Table 5.8 **Experimentally determined Kβ/Kα ratios from pure solid chromium compounds**

Compound	*Oxidation state*	*Kα/Kβ*	*Kβ/Kα*
Cr metal	0	5.76	0.174
Cr_2O_3	+3	6.26	0.160
$CrCl_3.6H_2O$	+3	5.66	0.177
$CrK(SO_4)_2.12H_2O$	+3	5.57	0.180
CrO_3	+6	6.15	0.162
K_2CrO_4	+6	5.65	0.177
$K_2Cr_2O_7$	+6	5.79	0.173

5.3.2 Determination of Kβ/Kα intensity ratios for chromium and manganese species by EDXRF spectrometry

Table 5.9 shows the results obtained when solutions of Cr(III) and Cr(VI), with concentrations in the range 0 – 5000 mg L^{-1} were analysed using the Link Analytical EDXRF spectrometer. Each standard was measured five times and an average value was calculated from the blank subtracted gross intensities for the Kα and Kβ lines. When working at high concentrations it was possible to use the net intensities calculated by the software provided with the Link spectrometer. However, at low concentrations of Cr on the resins, the errors in measuring the peak area of the Kβ were high (up to 45%), introducing values ten times higher than when using blank-subtracted gross intensities. Therefore, the latter method was applied to all the measurements.

The determination of intensity ratios for chromium species was based upon the two methods of calculation described in section 5.2.5: i) ratios of the slopes of the separate Kα and Kβ 'intensity vs. concentration' graphs and ii) average of the Kβ/Kα ratios from each standard concentration. The two methods are in agreement. The average ratios method shows a value of 0.172 ± 0.003 for Cr(VI) and 0.163 ± 0.002 for Cr(III). The slope method shows values of 0.171 for Cr(VI) and 0.161 for Cr(III).

In order to evaluate the statistical significance of the results, the ratios obtained for Cr(III) and Cr(VI) and Mn(VII) and Mn(II) in solutions and on the resins were compared using a two-tailed t-test[88] (details can be found in Appendix C).

Table 5.9 **Kβ/Kα ratios for chromium species in solution from EDXRF determination**

	Cr(VI)		*Cr(III)*	
	Kα Intensity	***Kβ Intensity***	***Kα Intensity***	***Kβ Intensity***
Concentration range (mg L^{-1})	0 - 5000		0 - 5000	
Slope (counts s^{-1} mg^{-1} L)	6.362	1.087	6.106	0.980
Correlation coefficient	0.9997	0.9997	0.9991	0.9985
Kβ/Kα ratio of slopes	0.171		0.161	
Average ratio Kβ/Kα	0.172 ± 0.003		0.163 ± 0.002	

Table 5.10 **Kβ/Kα ratios for manganese species in solution from EDXRF determination**

	Mn(VII)		*Mn(II)*	
	Kα Intensity	***Kβ Intensity***	***Kα Intensity***	***Kβ Intensity***
Concentration range (mg L^{-1})	0 - 2500		0 - 2500	
Slope (counts s^{-1} mg^{-1} L)	23.332	4.236	20.834	3.622
Correlation coefficient	0.9972	0.9974	0.9972	0.9974
Kβ/Kα ratio of slopes	0.182		0.174	
Average ratio Kβ/Kα	0.179 ± 0.003		0.171 ± 0.003	

In this case, in a relatively free chemical environment (when compared with the solid sample), it is possible to see a difference between the two ratios and hence, species, at a 99% confidence level.

Analogous results were obtained for manganese species in solutions in the concentration range 0 – 2500 mg L^{-1} that were analysed in the same manner. The ratios for Mn(VII) and Mn(II), which can be seen in Table 5.10, are significantly different at a confidence level of 98%. The RSDs for the intensity ratios obtained for chromium and manganese species in solution were always below 2%.

The results from chromium species retained on Dowex resins are shown in Tables 5.11 and 5.12. Equivalent information about manganese species can be found in Tables 5.13 and 5.14. These figures correspond to a set of standards with concentrations ranging from 0 to 2500 μg g^{-1} (low concentration range) and a second set with concentrations between 0 and 25000 μg g^{-1} (high concentration range). The measurements obtained from the standards in the low concentration range, although better than those acquired with the Philips instrument, show very poor precision for the Kβ line at standard concentrations below 500 μg g^{-1}.

Table 5.15 shows approximate limits of detection for Kα and Kβ lines of Cr and Mn species retained on Dowex resins (500 μg g^{-1}) and analysed in the Link EDXRF spectrometer (five replicate measurements).

Table 5.11 **Kβ/Kα ratios for chromium species on Dowex resins from EDXRF determination. Low concentration range**

	Cr(VI)		*Cr(III)*	
	Kα Intensity	***Kβ Intensity***	***Kα Intensity***	***Kβ Intensity***
Concentration range (μg g^{-1})	0 - 2500		0 - 2500	
Slope (counts s^{-1} μg^{-1} g)	3.514	0.519	2.481	0.426
Correlation coefficient	0.9992	0.9953	0.9989	0.9881
Kβ/Kα ratio of slopes	0.148		0.172	
Average ratio Kβ/Kα	0.16 ± 0.01		0.16 ± 0.01	

Table 5.12 **Kβ/Kα ratios for chromium species on Dowex resins from EDXRF determination. High concentration range**

	Cr(VI)		*Cr(III)*	
	Kα Intensity	***Kβ Intensity***	***Kα Intensity***	***Kβ Intensity***
Concentration range (μg g^{-1})	0 - 25000		0 - 25000	
Slope (counts s^{-1} μg^{-1} g)	10.345	1.780	5.923	1.002
Correlation coefficient	0.9999	0.9999	0.9977	0.9982
Kβ/Kα ratio of slopes	0.172		0.169	
Average ratio Kβ/Kα	0.178 ± 0.006		0.15 ± 0.01	

Table 5.13 **Kβ/Kα ratios for manganese species on Dowex resins from EDXRF determination. Low concentration range**

	Mn(VII)		*Mn(II)*	
	Kα Intensity	***Kβ Intensity***	***Kα Intensity***	***Kβ Intensity***
Concentration range (μg g^{-1})	0 - 2500		0 - 2500	
Slope (counts s^{-1} μg^{-1} g)	17.995	2.7531	12.825	1.995
Correlation coefficient	0.9981	0.9943	0.9983	0.9958
Kβ/Kα ratio of slopes	0.163		0.156	
Average ratio Kβ/Kα	0.16 ± 0.01		0.15 ± 0.01	

Table 5.14 **Kβ/Kα ratios for manganese species on Dowex resins from EDXRF determination. High concentration range**

	Mn(VII)		*Mn(II)*	
	Kα Intensity	***Kβ Intensity***	***Kα Intensity***	***Kβ Intensity***
Concentration range (μg g^{-1})	0 - 25000		0 - 25000	
Slope (counts s^{-1} μg^{-1} g)	12.713	2.092	8.067	1.321
Correlation coefficient	0.9998	0.9996	0.9993	0.9995
Kβ/Kα ratio of slopes	0.165		0.164	
Average ratio Kβ/Kα	0.157 ± 0.009		0.167 ± 0.009	

The limits found for the Kβ lines are approximately six times higher than for the Kα lines as would be expected from both the theoretical and experimental Kβ/Kα intensity ratio. For this reason, only the ratios obtained from standards in the high concentration range (where the lowest concentration is 500 μg g^{-1}) were considered for the statistical evaluation of the ratios.

Table 5.15 **Approximate limits of detection (in μg g^{-1}) for Cr and Mn species on resins, using the Kα and Kβ lines measured by EDXRF.**

	Cr(VI)	*Cr(III)*	*Mn(VII)*	*Mn(II)*
Kα	19	47	45	33
Kβ	147	247	194	201

From these results (Table 5.12) it is possible to say that the ratios for Cr(III) and Cr(VI) are significantly different at a confidence level of 90%. However, from an equivalent set of results, displayed in Table 5.14, the ratios obtained for manganese species by EDXRF analysis would be statistically the same.

Instrument stability was of paramount importance in these measurements. It is noted that use of the internal standard correction method, previously employed did not lead to a significant improvement of the results obtained using the Link spectrometer and was, therefore, not required in the calculations. Figure 5.7 shows typical EDXRF spectra obtained using the Link Analytical spectrometer.

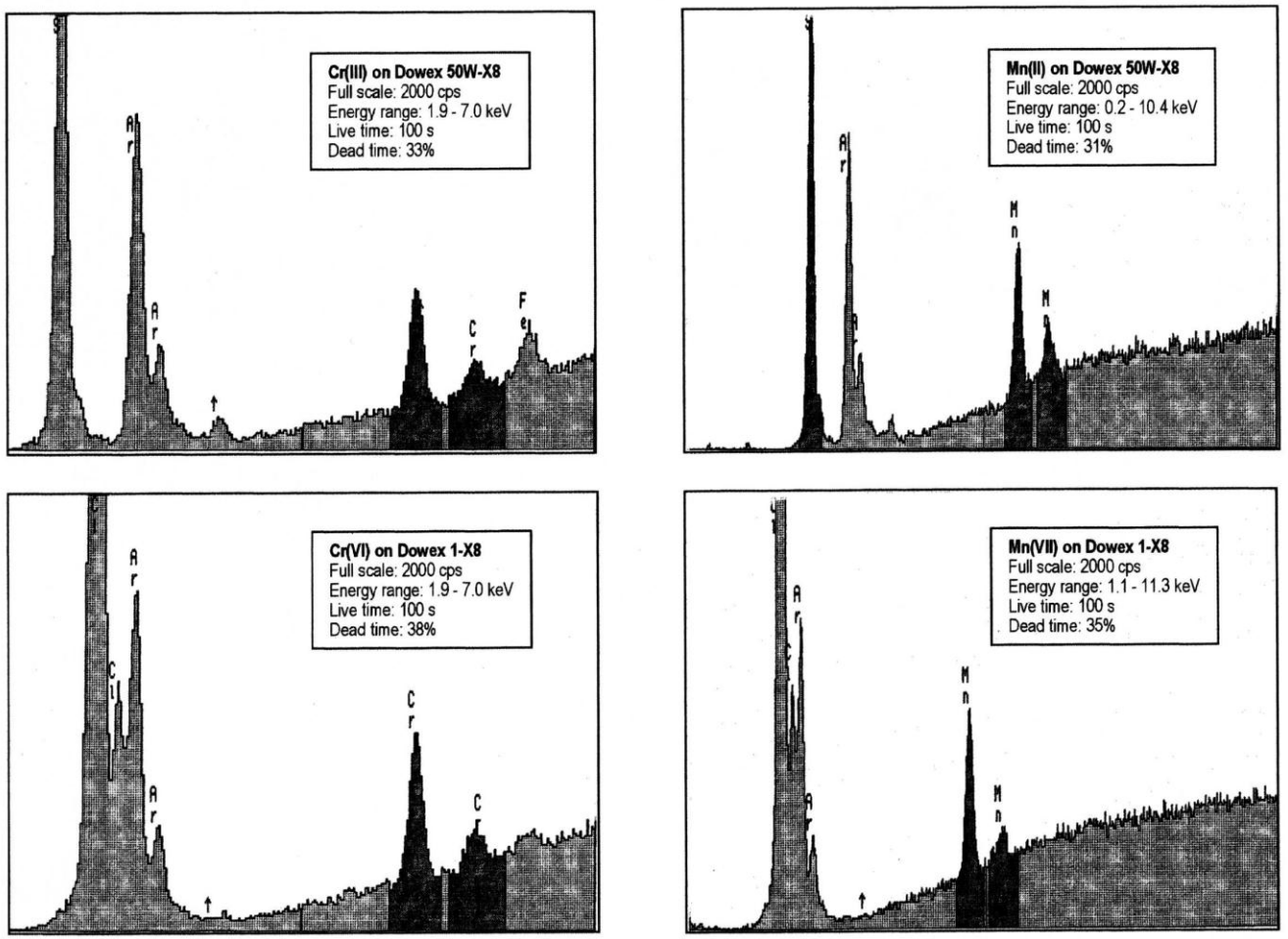

Figure 5.7 EDXRF spectra obtained from the analysis of 500 μg g^{-1} of Cr and Mn species on Dowex resins

5.3.3 Determination of Kβ/Kα intensity ratios for chromium and manganese species on resins by WDXRF spectrometry

5.3.3.1 Analysis of chromium and manganese standards with increasing concentrations

The standards of Cr and Mn retained on resins in the high concentration range were also analysed by WDXRF spectrometry, which is the preferred technique for the determination of intensity ratios by x-ray emission. The results obtained are displayed in Tables 5.17 and 5.18. In this case, for statistical counting purposes, peak height and not peak area was measured. This may account for the overall difference in ratios when these results are compared with those found by EDXRF and reported in section 5.3.2. The intensity ratios shown in Tables 5.17 and 5.18 are in agreement with the values reported in the literature[3, 81], summarised in Table 5.16.

Table 5.16 **Literature values for Kβ/Kα intensity ratios from pure solid chromium and manganese compounds**

Compound	*Oxidation state*	*Kβ/Kα*	*Ref.*	*Compound*	*Oxidation state*	*Kβ/Kα*	*Ref.*
Cr metal	0	0.133	81	*Mn metal*	0	0.132	81
Cr_2O_3	+3	0.134	81	$MnCO_3$	+2	0.134	81
$CrCl_3.6H_2O$	+3	0.134	81	$MnSO_4.4H_2O$	+2	0.133	81
$Cr(acac)_3$ [a]	+3	0.136	81	$Mn(AcO)_2.4H_2O$ [b]	+2	0.133	81
K_2CrO_4	+6	0.137	81	Mn_3O_4	+2 / +3	0.136	81
$K_2Cr_2O_7$	+6	0.140	81	MnO_2	+4	0.137	81
CrO_3	+6	0.141	81	K_2MnO_4	+6	0.135	81
$(NH_4)_2Cr_2O_7$	+6	0.139	81	$KMnO_4$	+7	0.135	81
Cr	?	0.133	3				

[a] acac = acetylacetonate

[b] AcO = acetate

To the best of the authors knowledge, there are no published ratios from EDXRF determinations but, the figures obtained in this work have consistently fallen in the 0.15 - 0.17 region and do not agree with those acquired by WDXRF. This fact indicates that the 'apparent' intensity ratios are dependent on the experimental technique.

However, in qualitative terms, some of the results observed using WDXRF are similar to those obtained using EDXRF. From the wavelength dispersive measurements, it is possible to say that the ratios for the two manganese species, Mn(II) and Mn(VII), are significantly different at the 90% level of confidence. However, no statistical difference was observed between the Cr(III) and Cr(VI) species after WDXRF determination. In either case, the separation between these ratios, with both of the techniques used, is so narrow that any general application to quantitative species analysis is unlikely to be useful.

Table 5.19 is a summary of the statistical evaluation of the results. The study was performed using a two-tailed t-test[88] at different levels of confidence. Further detail can be found in Appendix C.

A typical WDXRF spectrum of Mn species retained on Dowex resins can be seen in Figure 5.8. The scan shows how the intensity of the peaks obtained for Mn(VII) is greater than that of Mn(II). Analogous results are obtained when analysing Cr species. The results are independent of the instrumentation used (WDXRF or EDXRF).

Table 5.17 **Kβ/Kα ratios for chromium species on Dowex resins from WDXRF determination. High concentration range**

	Cr(VI)		*Cr(III)*	
	Kα Intensity	***Kβ Intensity***	***Kα Intensity***	***Kβ Intensity***
Concentration range (μg g^{-1})	0 - 25000		0 - 25000	
Slope (counts s^{-1} μg^{-1} g)	0.0024	0.0003	0.0012	0.0002
Correlation coefficient	0.9999	0.9999	0.9966	0.9965
Kβ/Kα ratio of slopes	0.132		0.133	
Average ratio Kβ/Kα	0.1320 ± 0.0005		0.133 ± 0.001	

Table 5.18 **Kβ/Kα ratios for manganese species on Dowex resins from WDXRF determination. High concentration range**

	Mn(VII)		*Mn(II)*	
	Kα Intensity	***Kβ Intensity***	***Kα Intensity***	***Kβ Intensity***
Concentration range (μg g^{-1})	0 - 25000		0 - 25000	
Slope (counts s^{-1} μg^{-1} g)	0.0035	0.0005	0.0020	0.0003
Correlation coefficient	0.9995	0.9995	0.9995	0.9994
Kβ/Kα ratio of slopes	0.144		0.147	
Average ratio Kβ/Kα	0.145 ± 0.001		0.148 ± 0.002	

Table 5.19 **Results of the significance tests performed on the Kβ/Kα ratios obtained for Cr and Mn species by EDXRF and WDXRF analysis**

		Confidence interval			
		90%	*95%*	*98%*	*99%*
		P value (two-tail)			
		0.10	*0.05*	*0.02*	*0.01*
Cr	*Solutions EDXRF analysis*	✓	✓	✓	✓
	Resins EDXRF analysis	✓	✗	✗	✗
	Resins WDXRF analysis	✗	✗	✗	✗
Mn	*Solutions EDXRF analysis*	✓	✓	✓	✗
	Resins EDXRF analysis	✗	✗	✗	✗
	Resins WDXRF analysis	✓	✗	✗	✗

✓ = Ratios are significantly different at the given level of confidence

✗ = Ratios are not significantly different at the given level of confidence

5.3.3.2 Analysis of manganese standards with fixed concentrations

The analysis of ten standards containing 25000 μg g^{-1} of Mn(II) and an equivalent set for Mn(VII) using WDXRF gave Kβ/Kα intensity ratios of 0.143 ± 0.001 for Mn(II) and 0.142 ± 0.001 for Mn(VII), where the overlap between the

ratios is evident. The RSD was 0.7%, which shows that the technique used was adequate for this determination. Instrumentation with greater resolution, however, would have allowed an investigation not only of the different intensity ratios, but also peak shifts. Recent publications[89-93] corroborate these findings and describe the difficulty of establishing systematic variations in these parameters that are only related to the oxidation state of the atom and not other factors such as other elements surrounding the atom or, in general, its environment. This is of particular note in the paper by Armstrong[93]. A reduction of the environmental (chemical/lattice) effect in solids by use of resin-based retention was an aim of this study and has been successfully attained. As a result, the effects seen by some authors in Kβ/Kα ratios may require reappraisal.

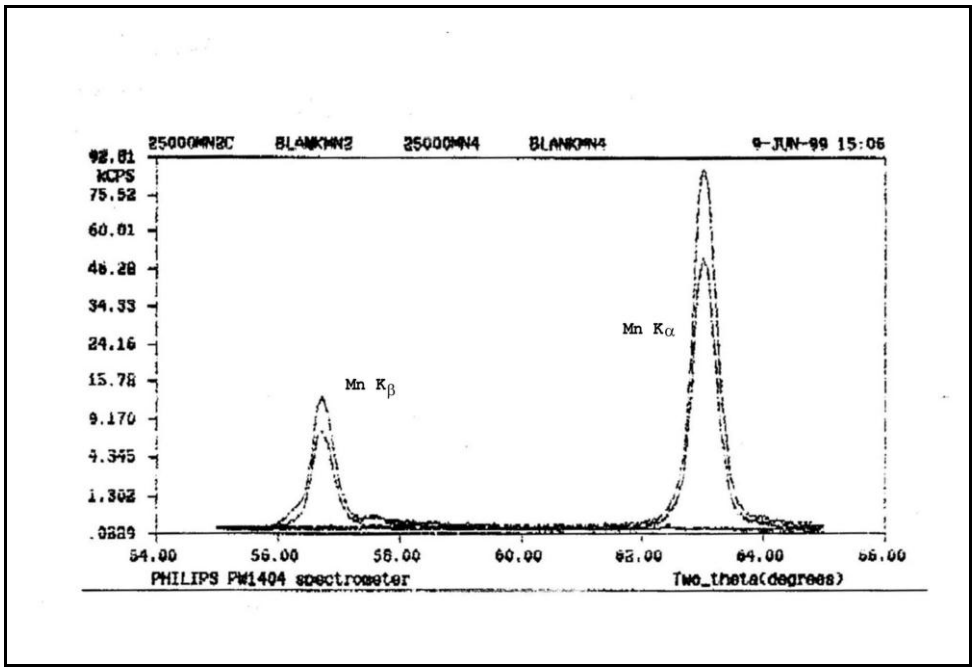

Figure 5.8 **WDXRF scan of Mn anion and cation species on the two Dowex resins (Mn concentration: 25000 μg g^{-1})**

5.4 CONCLUSIONS

The determination of Kβ/Kα intensity ratios for Cr and Mn species in solution by EDXRF spectrometry has shown that it is possible to establish a difference between the oxidation states of the analytes with, at least a 98 % level of confidence, for both elements.

When looking at intensity ratios from Cr and Mn species retained on Dowex resins determined by EDXRF, the limits of detection for the Kβ line require that the concentrations of the standards are above 500 $\mu g\ g^{-1}$ in order to obtain values with good precision. However, it is not possible to tell the oxidation state of the element from the intensity ratios measured, even at high concentrations of analyte.

The investigations have shown that, although the magnitudes of the ratios vary slightly when being determined by WDXRF in comparison to EDXRF, the wavelength dispersive technique does not accentuate the overall difference in ratios from one species to another and it does not offer an advantage over using EDXRF.

It seems clear that any chemical effects induced by oxidation states on the Kβ/Kα intensity ratio are too weak to be detected by conventional XRF spectrometry when analysing metal species retained on resins. A possibility exists and could be studied further that these effects are easier to detect when the analytes are in solution. However, even, then they are unlikely to be strong enough to become the basis of an analytical method for metal speciation.

6. *SPECIATION AND PRECONCENTRATION OF CR(III) AND CR(VI) IN WATERS BY RETENTION ON ION EXCHANGE MEDIA AND DETERMINATION BY EDXRF*

Chapter 6. Speciation and Preconcentration of Cr(III) and Cr(VI) in Waters by Retention on Ion Exchange Media and Determination by EDXRF

6.1 INTRODUCTION

X-ray fluorescence spectrometry is a well-known spectroscopic technique for major, minor and certain trace element analysis. The main advantage of this technique is its capability for direct analysis of solid and liquid samples, avoiding or at least reducing to a minimum, the sample handling. However, the energy dispersive technique possesses a number of limitations: it is generally not as sensitive as other atomic spectrometry techniques, it has a short linear range and it requires closely matching standards to overcome marked matrix effects[8].

The use of ion exchange materials as retention media for the analytes of interest offers the possibility of: extending the linear range, unifying matrix effects by fixing the same environment for both standards and samples and allowing preconcentration in order to obtain lower limits of detection. Some examples of direct analysis of trace metals on ion exchange media are seen in the literature[24, 51, 55].

This methodology can be applied to the determination of chromium, whose main oxidation states in aqueous solutions are Cr(III) and Cr(VI). The former is the most stable ion state of chromium in water, and is mainly of natural origin. The latter

exists in the environment arising from human activities[94], particularly industry, where Cr(VI) compounds have many applications (metallurgy, refractories, pigments, plating, catalysis, etc.)[95]. This results in the levels of Cr(VI) in industrial wastewaters often being high. Unfortunately, the toxicity of Cr(VI) is very high and its release to the environment as well as its generation from oxidation of Cr(III) should be controlled[94]. In the case of industrial effluents, the total amount of chromium present together with its oxidation state are two of the determining factors in the selection of the appropriate treatment for waters[96]. Information about the concentration and chemical form of chromium in natural waters will help to identify environmental and health problems.

In the last two decades, several different methods have been developed for the speciation of chromium. Many of these methods have the disadvantage that one of the species is determined as the difference between total chromium (obtained after reduction or oxidation) and the other chemical form of the element[97, 98].

The separation of chromium species prior to determination is necessary if independent results are to be obtained. In the past, coprecipitation techniques have been employed for the isolation of Cr(III) and Cr(VI) combined with thin-film XRF[99] or conventional EDXRF[54].

In this work, the preconcentration and separation of chromium species in aqueous solutions (standards and samples) has been performed by combining retention of the analytes on different ion exchange media and determination by energy dispersive XRF spectrometry. This approach should minimise the sample handling and number of chemicals used whilst the linear range is increased as a consequence of the

samples and standards being held on a light matrix. In addition, the use of a direct analytical technique (EDXRF) eliminates the need for an elution step, reducing the time and cost of the analysis and simplifying the procedure. One important consequence of the above is the ability to take samples on resins effectively on-site, thereby removing problems associated with sample stability and transportation. Furthermore, it would be possible to extend the method to portable EDXRF analysis for *in-situ* and in-field measurements by using instrumentation that is already available[100-102].

6.2 EXPERIMENTAL

6.2.1 Reagents and ion exchange media

Aristar grade concentrated nitric acid, sodium hydroxide pellets and ammonia solution and Spectrosol grade standard stock solutions (1000 mg L^{-1}) of Cr(III), Ni and V were obtained from Merck. Standard stock solution of 1000 mg L^{-1} Cr(VI) was prepared by dissolving 0.283 g of $K_2Cr_2O_7$ (Merck) in 100 ml of water. Whatman filter paper No 1 was used to separate ion exchange media and solutions. The sample cups and Mylar film were obtained from Philips Analytical X-ray. The water used was of ultra pure grade, Milli-Q, 18 MΩ cm. The ion exchange media were all obtained from Merck (Table 6.1). The Ground water and Waste Water Pollution Control Check Standard WP-15 (Spex Inc.) was obtained from Glen Spectra Reference Materials (Stanmore, Middlesex, UK). Samples of local natural waters (river and sea) were also employed.

Table 6.1 **Ion Exchange Media**

Ion Exchange Media	*Form*	*Particle Size (μm)*	*Species Retained*
Activated alumina (acidic form).	Cl^-	150 - 188	Cr(VI) / Cr(III)
Dowex 50W-X8 cation exchange resin	H^+	75 - 150	Cr(III)
Zerolite 'Decalso' (S/F) Sodium aluminosilicate	Na^+	177 - 250	Cr(III)
Dowex 1-X8 anion exchange resin	Cl^-	75 - 150	Cr(VI)

6.2.2 Instrumentation

EDXRF work was performed using a Link Analytical XR300 XRF spectrometer. Operating conditions are shown in Table 6.2.

For the determination of chromium and vanadium concentrations in solution, a GBC 902 flame atomic absorption spectrometer and a Perkin-Elmer Optima 3000 ICP-AE spectrometer were used. The instrumental parameters employed are shown in Table 6.2.

Table 6.2 **Instrumental parameters**

Link Analytical XR300 Spectrometer	
Voltage	20 kV
Current	120 μA
Vacuum	off
Filter	none
Acquisition time	100 sec

GBC 902 Flame Atomic Absorption Spectrometer		
Element	Cr	V
Wavelength	357.9 / 425.4 nm	318.5 nm
Band pass	0.5 nm	0.2 nm
Lamp current	6 mA	10 mA
Flame	Air-Acetylene (reducing)	N_2O-Acetylene

Perkin-Elmer Optima 3000 ICP-AE Spectrometer	
Element	Cr
Line	357.869 nm
RF power	1000 W
Viewing height	20 mm
Argon flow rate	
Plasma	17 L min^{-1}
Auxiliary	1 L min^{-1}
Nebuliser	1 L min^{-1}
Sample flow rate	0.9 mL min^{-1}

6.2.3 General sample preparation procedure and adsorption characteristics

The retention of Cr(III) and Cr(VI) was studied on activated alumina (acidic form), Zerolite ('Decalso' sodium aluminosilicate), Dowex 50W-X8 and Dowex 1-X8. The samples were prepared as follows: Known volumes of the standard stock solutions (1000 mg L^{-1}) were diluted to 50 mL with 0.01M HNO_3. This gives a solution of approximately pH 2 which has been widely used in the speciation of chromium[103-105]. Figure 6.1 shows that at this pH the stable oxidation states of Cr are in the forms $HCrO_4^-$ and $Cr(H_2O)_6^{3+}$ [66] allowing the separation by use of anion-cation exchangers with no further manipulation.

The samples were then mixed using a magnetic stirrer for 5 minutes with 1 g of each ion exchanger. Laboratory studies[106] have shown that the kinetics of the system are fast for Cr(III) and Cr(VI) at 20 mg L^{-1} and that both species are quantitatively retained (> 98% retention) on the Dowex ion exchangers after 2.5 minutes of stirring (Table 6.3). Each sample was then filtered through Whatman filter paper N^o 1. The adsorbing media were then air-dried and transferred into XRF sample cups fitted with *Mylar* film.

For the retention of Cr(III) on alumina a slight variation of this procedure was used. The solutions, containing the hydrated Cr^{3+} cation were treated with ammonia solution and the pH fixed at 9.5. The Cr(III) precipitates as $Cr(OH)_3$ when the pH is higher than 6. By addition of another 5 mL of ammonia solution, the precipitate redissolves as the complex $[Cr(OH)_2(NH_3)_4]^+$ [107]. When the resultant solution was mixed with 1g of alumina, the properties of the solid media changed, becoming a

cation exchanger. As a result, the complex adhered to the alumina. The procedure followed from then onwards was identical to that described above.

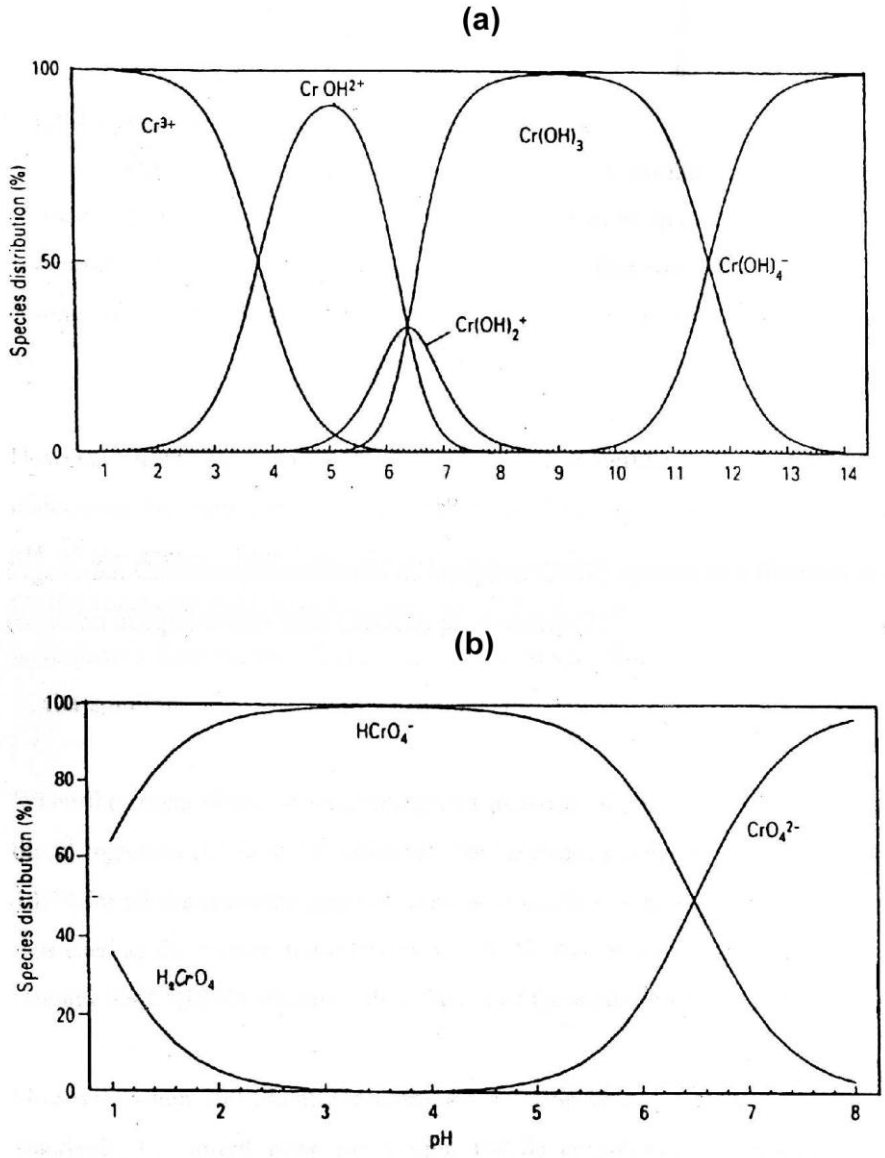

Figure 6.1. Calculated distribution of (a) inorganic Cr(III) and (b) Cr(VI) species as a function of pH[66]

The sets of samples were measured on the XRF spectrometer. Identification of the lines in the x-ray spectrum was performed and the Kα radiation of chromium (5.41 keV) was then quantified in three replicate measurements.

Atomic absorption spectrometric determination of chromium remaining in solution was performed in order to obtain recovery data. For the determination of Cr(III) in basic solutions that had been mixed with alumina, calibration standards were prepared in 10% ammonia solution. In all other cases, calibration standards were prepared by convenient dilution of Cr(III) and Cr(VI) standard stock solutions with 0.01M HNO_3. Three replicate measurements were made in all the experiments.

Table 6.3 **Retention of chromium species on Dowex resins as a function of the stirring time**

Stirring time (min)	*%Recovery Cr(VI)*	*%Recovery Cr(III)*
0	83.9	82.9
2.5	98.6	99.6
5	99.1	99.6
7.5	98.9	99.8
10	98.9	100.0
12.5	98.4	100.0
15	98.6	99.6

6.2.4 Study of the effect of the sample volume

A series of standards with the same concentration of Cr(III) or Cr(VI) (25 mg L^{-1}) and different sample volumes (25-500 mL) was prepared and each standard mixed with 0.5 g of the appropriate Dowex ion-exchanger. The samples were then filtered and air-dried, following the procedure described in section 6.2.3. The filtrates were analysed by ICP-AE spectrometry. The resins containing the Cr species were transferred into sample cups and analysed by EDXRF spectrometry.

6.2.5 Determination of the maximum retention capacity of Dowex resins

Two microcolumns were constructed by slurry loading empty *Teflon*® tubes (0.2 cm i.d. × 3 cm) with, respectively, Dowex 1-X8 and Dowex 50W-X8 (approximately 0.1 g of resin) in ultra pure water using a peristaltic pump. Both columns were ultrasonicated to eliminate voids and conditioned with 0.1M NaOH (100 mL) and 0.1M HNO_3 (100 mL) solutions.

The columns were connected on-line to an ICP-AE spectrometer as shown in Figure 6.2. The distance between the end of the columns and the plasma was kept to a minimum to reduce dead volume and dispersion effects. A solution of nickel (150 mg L^{-1}) was prepared and run through the cation exchanger (Dowex 50W-X8) at a flow of 1.67 mL min^{-1}. At the same time, a solution containing 150 mg L^{-1} of Cr(VI) was passed through the anion exchanger (Dowex 1-X8) at a rate of 1.62 mL min^{-1}. Both Ni and Cr signals were monitored simultaneously by the ICP-AES and the whole

process timed in order to determine the moment at which saturation of each resin occurred. Replicates of this experiment were performed and the average maximum capacity of the resins was then calculated from saturation curves.

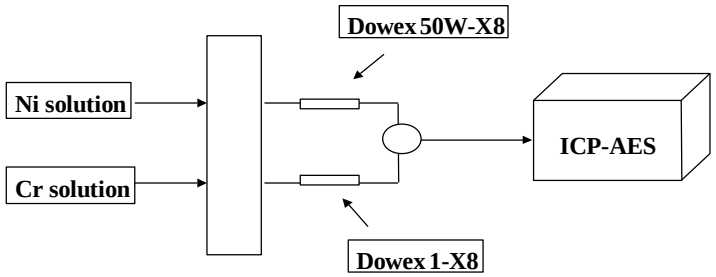

Figure 6.2. **Schematic diagram of the system used for the determination of the maximum capacity of the resins**

6.2.6 Determination of the optimum mass of resin

A series of standards with the same concentration of Cr(III) on Dowex 50W-X8 or Cr(VI) on Dowex 1-X8 (1000 μg g^{-1}) and different mass of resin (125-2000 mg) was prepared following the usual procedure. The Cr Kα line was measured in the XRF spectrometer and the optimum resin mass was selected from graphs representing net intensities vs. mass of resin.

6.2.7 Interferences study

A study of the effect of the matrix on the retention of chromium species on Dowex exchangers was performed. Standards containing 20 mg L^{-1} Cr(III) / Cr(VI) were prepared in solutions with concentrations of interfering ions (Cl^-, SO_4^{2-}, Na^+, Mg^{2+}, Ca^{2+} and K^+) ranging from 100 mg L^{-1} to those present in seawater. The solutions were mixed with 0.5 g of the appropriate exchanger and, after separation, the filtrates were analysed by FAAS and the resins by EDXRF.

6.2.8 Speciation of chromium in water samples.

For the separation of Cr species in local river and seawaters, the pH of the samples was adjusted to 2 with concentrated nitric acid and aliquots of 25 mL were transferred to volumetric flasks. Three of the aliquots were spiked with 125 μL of 1000 mg L^{-1} Cr(III) and Cr(VI). The samples were mixed with 0.5 g of each Dowex resin following the same procedure used for the standards.

The Ground Water and Waste Water Pollution Control Check Standard WP-15 was used in order to test the accuracy of the method in a complex matrix, especially since the presence of V in high concentration in this standard could constitute a serious limitation as the V Kβ line overlaps the analytical line for Cr

(Kα). The standard, whose composition is shown in Table 6.4, was diluted 100 times (to reduce the concentration of Cr(III) present to 1 mg L^{-1}) and spiked to give 1 mg L^{-1} Cr(VI). The usual sample preparation procedure (outlined in section 6.2.3) was then applied.

All solid samples were analysed by EDXRF spectrometry against a series of standards of Cr(III) or Cr(VI) prepared on the appropriate ion exchanger. A series of matrix matched aqueous standards was also prepared for the analysis of the filtrates by ICP-AE spectrometry.

The V from the WP-15 standard was partially retained on the Dowex 50W-X8 and this had to be quantified in order to apply a correction factor to the Cr Kα and obtain accurate measurements of Cr(III) on the resin. A series of V standards on Dowex 50W-X8 were prepared in the same manner as the Cr. The Kα and Kβ lines were measured and the ratio between them was calculated and used to correct the Cr Kα intensities. The retention of vanadium species on the resins was also investigated by analysing the filtrates by FAAS.

Table 6.4 **Composition of the Spex Ground Water and Waste Water Pollution Check Standard WP-15 (Matrix: 5% HNO_3).**

Element	*Concentration (mg L^{-1})*
Al	500
V	250
As, Be, Co, Cr, Cu, Fe, Mn, Ni, Pb, Zn	100
Cd, Se	25
Hg	5

6.3 RESULTS AND DISCUSSION

6.3.1 Comparison of ion exchangers

In general, the separation of the species is quantitative, with recoveries from standard solutions close to 100% (Figures 6.3 (a) and (b)), although, the retention of Cr(III) *via* the ammonia cation complex on alumina lacks repeatability and the recoveries in this case are not as good as those obtained with other exchangers. The problem of poor recoveries for Cr(VI) at higher concentrations on alumina is also noted.

Figure 6.4 indicates that the linear range extends from 0 to at least 500 mg L^{-1} for Cr(VI) on Dowex 1-X8 and for Cr(III) on Dowex 50W-X8. Each data point in this figure is the average of 5 measurements and includes the uncertainty of 1 standard deviation. For Cr(VI) on alumina the linear range goes up to 50 mg L^{-1} and for Cr(III) on alumina or Zerolite it only reaches 20 mg L^{-1}. The linearity is a direct consequence of the retention of the analyte in a known and constant media. By fixing the same environment for all the samples and standards, one of the most important problems in XRF spectrometry, the matrix effect, is reduced.

(a)

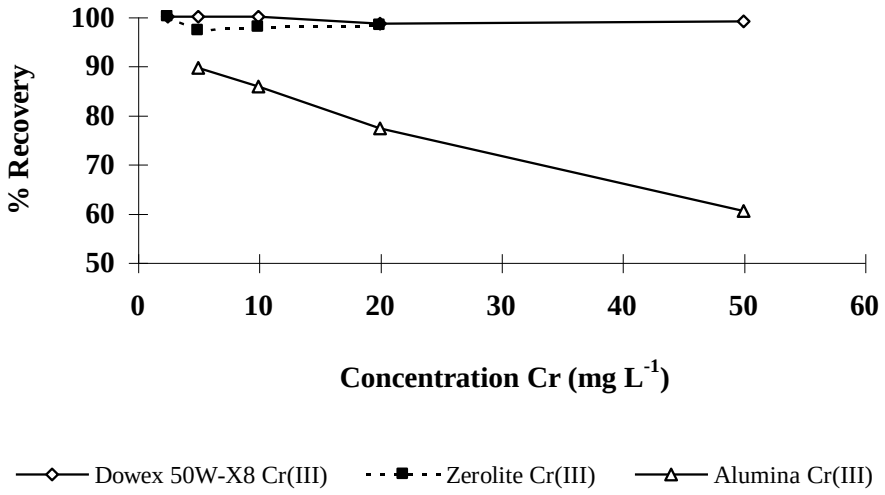

(b)

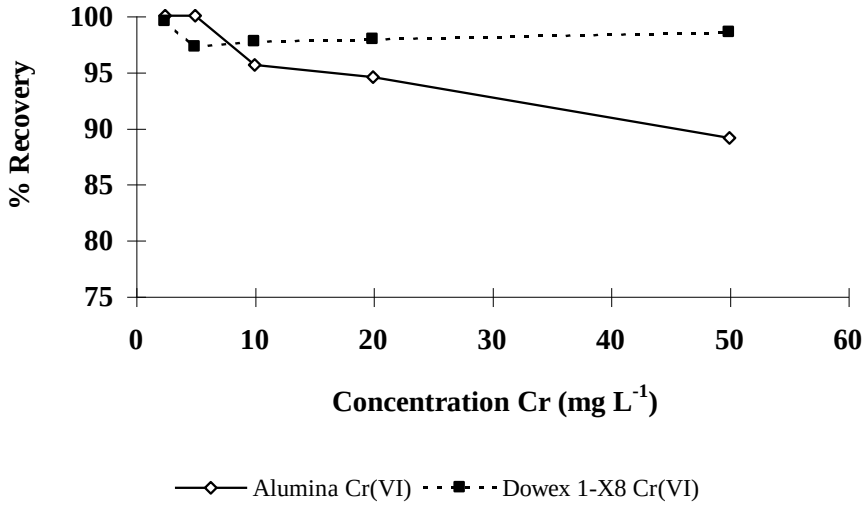

Figure 6.3. Recoveries on different ion exchangers for (a) Cr(III) and (b) Cr(VI)

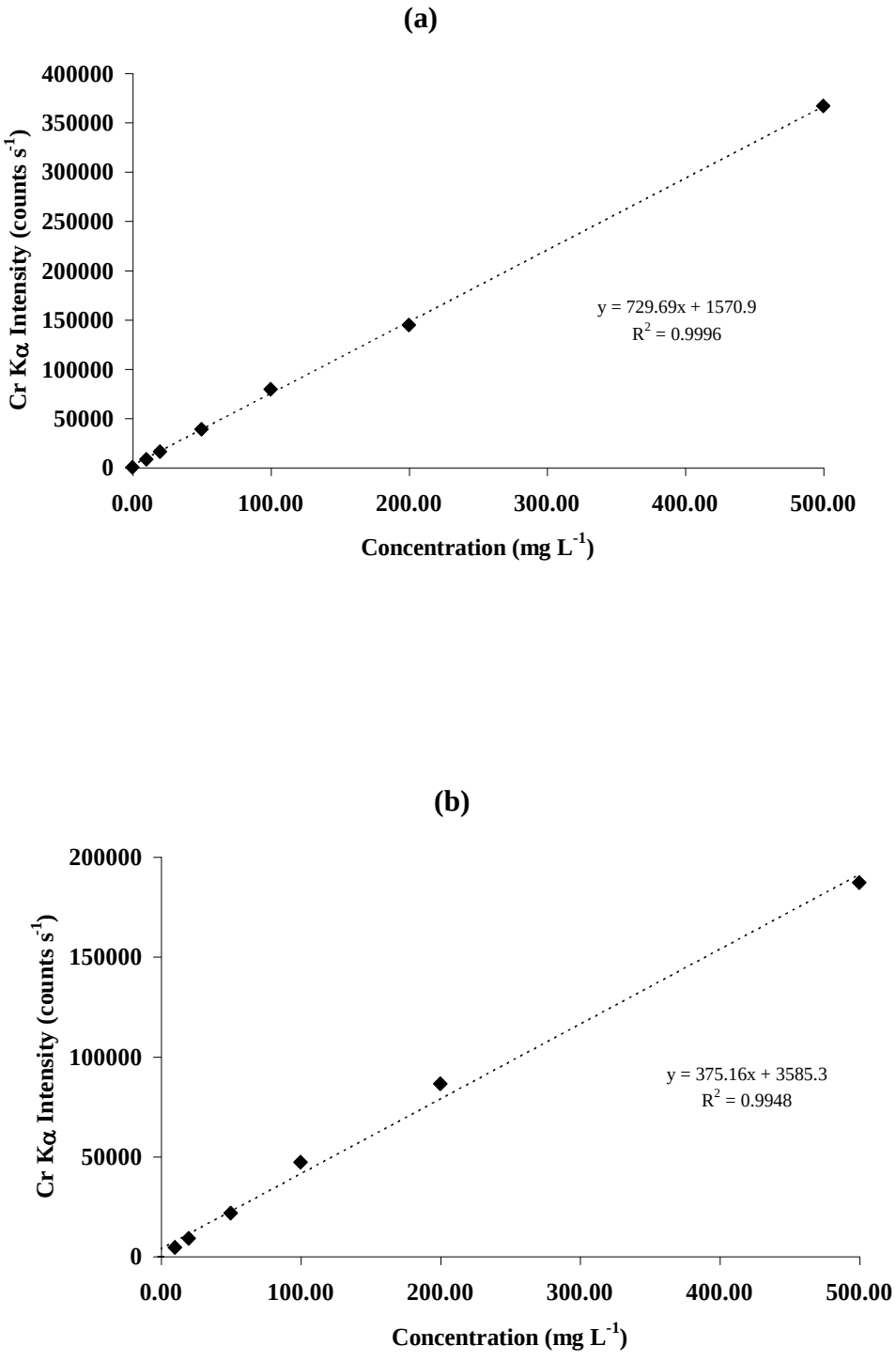

Figure 6.4. **Study of the linear range for the determination of (a) Cr(VI) on Dowex 1-X8 and (b) Cr(III) on Dowex 50W-X8 by EDXRF**

Table 6.5 shows the figures of merit obtained for the determination of Cr(III) and Cr(VI) retained on different ion exchangers. Much greater sensitivity is obtained when Dowex resins are used, together with lower limits of detection. The use of Zerolite offered a slight improvement in sensitivity over the alumina but these exchangers only produced a limit of detection 2 to 3 times higher than that of Dowex.

Table 6.5 **Figures of merit for Cr(III) and Cr(VI) (50 mL)**

	Cr(III) on Dowex 50W-X8	***Cr(III) on Alumina***	***Cr(III) on Zerolite***	***Cr(VI) on Dowex 1-X8***	***Cr(VI) on Alumina***
Background (b) / counts s^{-1}	35.79	59.56	41.98	32.44	56.85
Sensitivity (m) / counts s^{-1} mg^{-1} L	6.03	2.70	3.42	8.51	3.32
Correlation coefficient	0.9997	0.9902	0.9994	0.9965	0.9999
Lowest limit of detection/ mg L^{-1}	0.30	0.86	0.57	0.20	0.68

Note: Lowest Limits of detection calculated as: $$LLOD = \frac{3}{m} \cdot \sqrt{\frac{b}{t}}$$

t being the acquisition time on the XRF spectrometer.

An explanation for these effects and trends involves the particle size, density and mass attenuation of the matrices studied[6]. The lighter surface active matrix of the

Dowex resins results in lower backgrounds and higher intensities of fluorescence compared with the other supporting media.

Since they provide the best limits of detection and sensitivity overall for both Cr(VI) and Cr(III), the Dowex resins were selected as the retention media for the speciation of Cr in waters by XRF analysis.

6.3.2 Effect of the sample volume in the efficiency of the retention of chromium species on Dowex ion-exchange resins

In the preliminary experiments described above, preconcentration of the analytes was achieved up to a factor of 50. As shown in Figure 6.5, further tests focused on the Dowex resins demonstrated that when the sample volume increases from 25 mL to 250 mL the percentage of retention on 0.5 g of exchanger remains constant (95-100%). Increasing the volume up to 500 mL decreases the recovery by 10%. These results are in agreement with the effect of the sample volume in the kinetics of the exchange, which has been discussed in Chapter 3. Nevertheless, in the circumstances of this investigation, a preconcentration factor of 500 can be used without any detriment to the retention properties of the resins.

The results shown in Figure 6.5 were obtained by determining the concentration of Cr species left in the filtrates by ICP-AES. These results were confirmed by the determination of chromium species retained on Dowex resins by EDXRF.

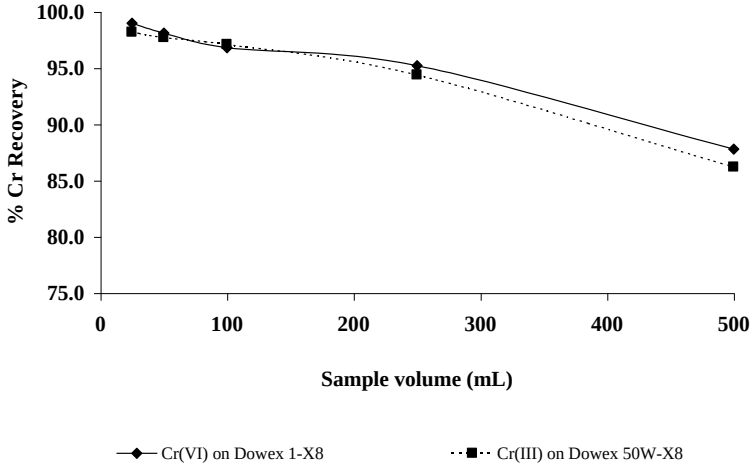

Figure 6.5. Effect of the sample volume on the retention of Cr species on Dowex resins

6.3.3 Maximum retention capacity of Dowex resins

The working capacity of the Dowex exchangers can be determined directly from Figures 6.6 (a) and (b). These results confirm those previously observed in the preliminary experiments: increasing concentrations of analyte have no major effect in the retention capacity of the resins. When the maximum retention capacity is exceeded, saturation occurs rapidly. For this investigation, the maximum retention capacity has been stated as the capacity at which the resin is 50% saturated, i.e., 3.2 mEq g^{-1} for Dowex 50W-X8 and 1.1 mEq g^{-1} for Dowex 1-X8. Therefore, the working concentrations in this study are well below the maximum capacity of the resins (2-4% saturation).

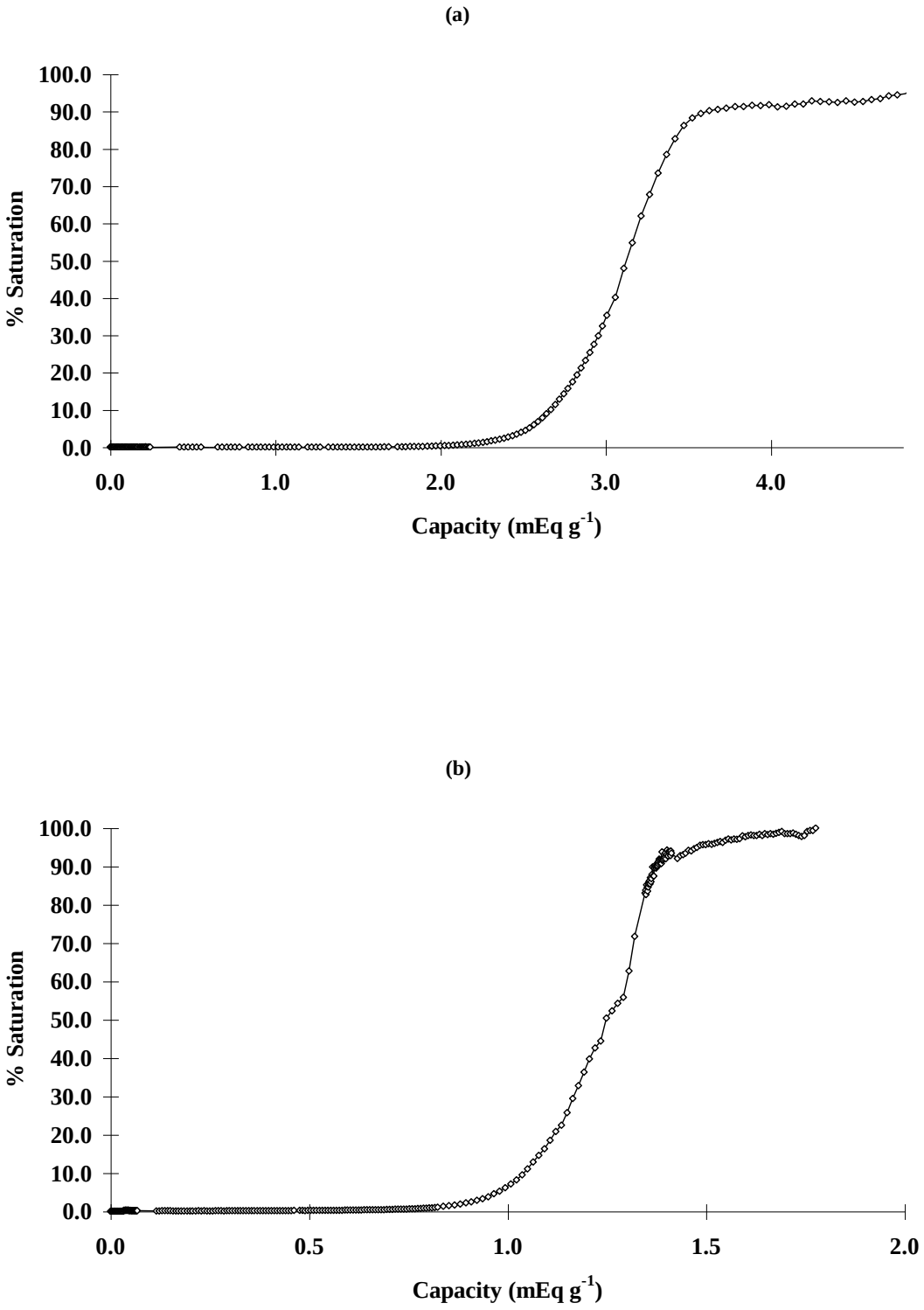

Figure 6.6. **Determination of the maximum capacity for resins (a) Dowex 50W-X8 and (b) Dowex 1-X8**

6.3.4 Optimum mass of resin

The results shown in Figure 6.7 indicate that in order to obtain a response in net intensity of fluorescence that is proportional to the concentration of Cr in the sample, a minimum of 500 mg of resin is required. Using less than 500 mg, not only the concentration of analyte, but also other factors such as specimen thickness and physical distribution in the sample cup influence the intensity of fluorescence and contribute to poor precision. With greater than 500 mg there is no improvement of the sensitivity and a dilution effect occurs as the preconcentration factor decreases. These observations are applicable to both Cr(III) on Dowex 50W-X8 and Cr(VI) on Dowex 1-X8 and are in agreement with the results reported in Chapter 3 for Cr(III) retained on Dowex 50W-X8 of various particle sizes. Consequently, a mass of resin of 500 mg was used in the remaining experiments.

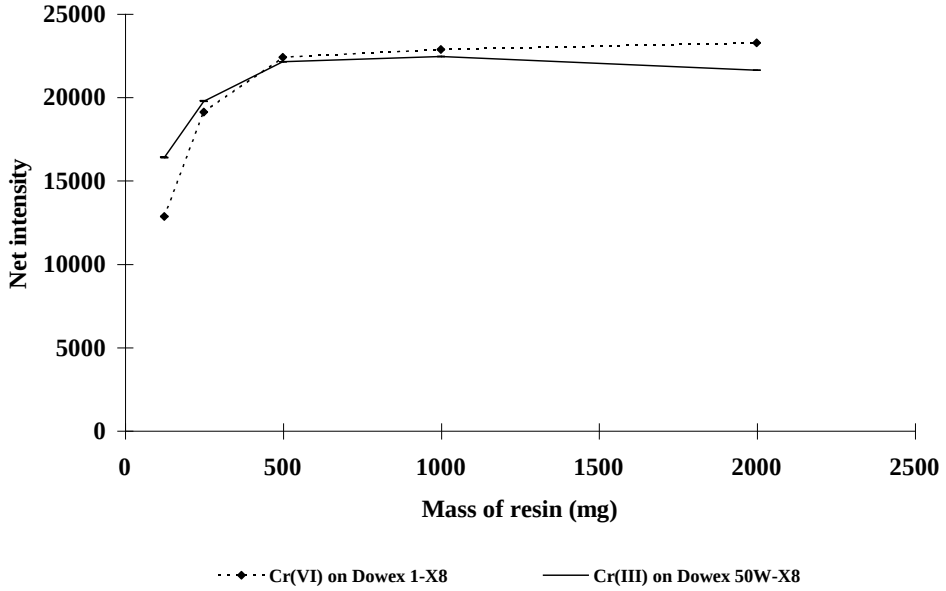

Figure 6.7. Determination of the optimum mass of resin

6.3.5 Speciation of chromium in waters

In order to test the method in the presence of a complex matrix and the influence of interfering ions, the speciation of chromium in the Ground Water Waste Water Pollution Control Check Standard (diluted and spiked with Cr(VI)) and in spiked natural waters was undertaken. The actual levels of Cr in unpolluted natural waters are too low for EDXRF determination, even considering the preconcentration factor. The results obtained are shown in Table 6.6.

Table 6.6 **Recovery of chromium added to water samples**

Sample	***Cr(VI) on Dowex 1-X8***		***Cr(III) on Dowex 50W-X8***	
	Recovery (%)	***RSD (%)***	***Recovery (%)***	***RSD (%)***
Spex WP-15 Standard [1]	101 ± 4	4	103 ± 2	2
Natural River Water [2]	87 ± 6	7	84 ± 1	1
Natural Sea Water [2]	59 ± 3	5	30 ± 3	10

[1] Sample diluted 1:100 and spiked with 1 mg L^{-1} Cr(VI), n = 5.

[2] Sample spiked with 5 mg L^{-1} Cr(III) and Cr(VI), n = 3.

Quantitative recoveries were obtained for Cr species in the *Spex* WP-15 standard. Other metals present in this sample were also retained by the cation exchanger, but do not impair the retention of Cr(III). The overlap of V Kβ with the analytical line, Cr Kα, was satisfactorily corrected using the ratio of intensity between the vanadium lines. The recovery of vanadium on Dowex 50W-X8 (30%) was in total agreement with the results of the pH studies described in Chapter 4.

The recoveries for spiked natural waters were lower, especially in the case of seawater. This was expected as the salinity of sea water is typically 35 parts per thousand with both the predominating cations, Na^{+}, Mg^{2+}, Ca^{2+} and K^{+}, present in concentrations of 11000, 1300, 420 and 400 mg L^{-1} respectively and the predominating anions, Cl^{-} and SO_4^{2-}, in concentrations of 19800 and 2800 mg L^{-1} respectively[108] competing with the Cr species for the active sites. The extreme conditions of competition for these sites on the exchanger are obviously not favourable to the analytes when interfering ions are present in such high concentration. The study serves to set the limits of the procedure in this sample and resin case and is corroborated by the results of the interferences study summarised in Table 6.7. The ions Cl^{-} and Na^{+}, present in solution in higher concentrations, are the greatest obstacles to the retention of chromium. Figure 6.8 shows how the recovery of Cr species diminishes as the concentration of these ions increases.

This problem is inherent to the determination of trace elements in seawaters. In less drastic conditions the method has proved to cope with the presence of other ions and could therefore be applied to the speciation of chromium in aqueous samples with low salinity.

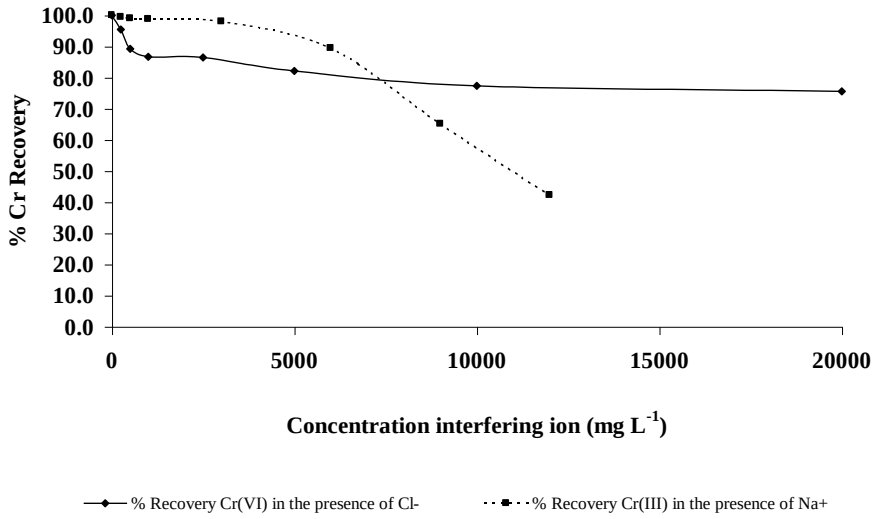

Figure 6.8. **Effect of interfering ions Cl^- and Na^+ on the retention of Cr species on Dowex exchangers (Concentration of Cr: 20 mg L^{-1})**

Table 6.7 **Results of the interferences study**

Interfering Ion	*Maximum Concentration (mg L^{-1}) before Recovery < 90%*
Chloride	500
Sulphate	> 3000
Sodium	6000
Magnesium	> 1400
Calcium	> 500
Potassium	> 500

6.3.6 Limits of detection

Although the lowest limits of detection (LLOD) are easily calculated from the calibration curves (LLOD = 3/m $(b/t)^{1/2}$, where m is the sensitivity, b the counting rate for the background and t the counting time which, in this case, is 100 s), a more realistic approach is often preferred in order to know the limitations of the method. For this reason, working limits of detection (LOD) for the analytes were determined using the operating conditions for the EDXRF spectrometer described in Table 6.2 for the analysis of pure elemental standards of 250 μg g^{-1} Cr(VI) on Dowex 1-X8 and Cr(III) on Dowex 50W-X8, respectively. Each standard was analysed seven times, the net intensity of fluorescence recorded and the LOD calculated as three times the standard deviation of the net signal. The values obtained can be seen in Table 6.8.

Table 6.8 **Results of the determination of the working limits of detection**

	Cr(VI) on Dowex 1-X8	***Cr(III) on Dowex 50W-X8***
LOD (3σ) in μg g^{-1}	17	19
LOD (3σ) in μg	8	10
LOD (3σ) in mg L^{-1} (1)	0.3	0.4
LOD (3σ) in mg L^{-1} (2)	0.03	0.04

(1) Preconcentration factor of 50 times

(2) Preconcentration factor of 500 times.

These working limits of detection are very close in value to the calculated lowest limits of detection for chromium species on Dowex resins shown in Table 6.5. This coincidence will only occur when a physically and chemically homogeneous matrix and analyte are present. For the preconcentration factor used (50 times), limits of detection of 0.3 and 0.4 mg L^{-1} are obtained for Cr(VI) and Cr(III) respectively. If a preconcentration factor of 500 is employed, the limits of detection are reduced to 30 μg L^{-1} for Cr(VI) and 40 μg L^{-1} for Cr(III).

6.4 CONCLUSIONS

Sequential separation and preconcentration of Cr(III) and Cr(VI) can be achieved by trapping the analytes on Dowex 50W-X8 and Dowex 1-X8, respectively. These resins provide the best performance when compared with other ion-exchangers, such as alumina, in terms of retention properties and sample support media for the determination of chromium by EDXRF. Linear ranges obtained by other workers[54] have been improved by a factor of 10 while other figures of merit remain comparable. Preconcentration factors up to 500 are possible, giving rise to limits of detection of 30 μg L^{-1} for Cr(VI) and 40 μg L^{-1} for Cr(III). These limits are substantially lower than those usually associated with EDXRF. Although the presence of high concentrations of competing ions in a matrix such as sea water can reduce the retention of analytes on the resins, quantitative recoveries can be achieved in the speciation of chromium in waste waters using the method proposed. This application could be extended to other

aqueous solutions with low to medium salinity with the advantages of being a simple, fast and inexpensive procedure.

7. CONCLUSIONS AND SUGGESTIONS FOR FURTHER WORK

Chapter 7. Conclusions and Suggestions for Further Work

7.1 CONCLUSIONS

The characteristics of the commercially available ion-exchange and chelation resins (Dowex 50W-X8, Dowex 1-X8 and Chelex-100) and their influence on the application of these solid retention media as substrates for EDXRF analysis have been investigated. The effect of parameters such as pH, distribution of active sites and collected ions in the exchangers, maximum retention capacity, sample volume and the relationship between intensity of fluorescence and mass of resin has been investigated separately for each exchanger. Other important parameters such as the effect of the particle size, interelement phenomena and the effect of the retention method used (batch or column) have also been studied by using specific analyte-resin systems.

Methodologies for three different applications of the resins to EDXRF determinations have been developed and their analytical possibilities explored. These applications include the multi-elemental determination of trace metals in sewage sludge, the separation and preconcentration of chromium species in waters and the determination of $K\beta/K\alpha$ intensity ratios for metal species and its evaluation as a potential tool for direct analysis.

Images of resin beads, obtained by scanning electron microscopy, have shown morphological differences between the Dowex resins and Chelex-100. The x-ray microanalysis and mapping of sectioned and whole resins has demonstrated a

homogeneous distribution of functional groups and retained ions. This indicates that the ion-exchange or chelation process occurs throughout the entire resin bead.

Batch and column systems for solid retention media used in XRF analysis have been compared. The batch process has shown the best characteristics for the analysis, in terms of linearity, accuracy and precision. This method is also faster and simpler than the use of mini-columns. The efficiency of the retention, however, has been shown to be dependent on the pH and ionic strength of the solution, on the concentration of competing ions and on the volume of the sample.

Different particle size ranges of Dowex 50W-X8 (38 – 840 μm) have been used in the determination of Cr(III) by EDXRF and the results compared. Contrary to those results previously published and often quoted, the particle size has been shown to have no effect on the relationship between intensity of fluorescence and concentration or between intensity of fluorescence and mass of resin. It is noted that, a reduced number of active sites has been observed in the cation exchanger of larger particle size (300 – 840 μm) compared with those of smaller size ranges. Thus, it has been recommended to work with a particle size less than 150 μm, in order to overcome possible capacity effects

The maximum retention capacity has been determined as 3.2, 1.1 and 0.67 mEq g^{-1} for Dowex 50W-X8, Dowex 1-X8 and Chelex-100 respectively. The optimum mass of resin has been found to be 0.5 g, for all the resins tested. However, a larger mass of resin (1.0 g) has been recommended for Chelex-100, in order to compensate for the lower exchange capacity.

The information above has been applied to the development of methods for the multi-elemental determination of metals in sewage sludge. The results obtained from loading the metals onto Dowex 50W-X8 at pH 2 and Chelex-100 at pH 4 have been compared and found to be in agreement with the characteristics of the resins. Chelex-100 allows quantitative recoveries for Cu and Zn in these 'complex' solutions. With Dowex 50W-X8, the recoveries are poorer, but it is possible to determine a wider range of elements. Inter-element suppression and enhancement effects, which can result in serious limitations of accuracy for certain solid samples, are not observed when ion-exchange / chelation media are used in the measurement of multielemental specimens by EDXRF. This may be attributed to the unique retention characteristics of the media; a result of the homogeneous low density (open framework) distribution of active sites present. The limits of detection were 10 – 21 μg when Dowex 50W-X8 was used and 8 – 49 μg when the retention medium was Chelex-100. Although high concentrations of competitive interferent elements such as Fe have been shown to reduce the applicability of the method, this is a simple and cost-effective option for the analysis of trace metals in a complex matrix, such as sewage sludge.

The determination of Kβ/Kα intensity ratios for Cr and Mn species and its application as a means to perform direct elemental speciation has also been studied. The analysis of solutions of the metal species by EDXRF spectrometry has shown that a difference between the oxidation states of the analytes exists at a 98 % level of confidence. This difference has not been found when looking at intensity ratios from Cr and Mn species retained on Dowex resins determined by EDXRF or WDXRF, even when high concentrations of the analyte were used. Thus, it has been concluded that the chemical effects originating from oxidation states on the Kβ/Kα intensity

ratio cannot be detected by conventional XRF spectrometry when analysing metal species retained on resins. It also may call into question those results previously published where the measurement of species in solids are dependent upon the chemical/lattice environment.

Finally, the presentation of analytes on solid retention media and EDXRF determination have been combined and applied to the speciation and preconcentration of Cr(III) and Cr(VI) in waters. Dowex 50W-X8 and Dowex 1-X8 have been compared with other adsorbers, such as alumina, and have shown optimum properties for the determination of chromium by EDXRF. Preconcentration factors, although limited by the effect of the sample volume, can reach 500. This leads to limits of detection of 30 $\mu g\ L^{-1}$ for Cr(VI) and 40 $\mu g\ L^{-1}$ for Cr(III). These are considerably lower than those usually associated with conventional EDXRF. The retention of analytes on the resins can be hampered by high concentrations of competing ions. This is the case during the analysis of sea water. However, using this method, which is simple, fast and inexpensive, quantitative recoveries have been achieved in the speciation of chromium in waste waters.

On the whole, the resins studied have demonstrated their potential to overcome the main limitations of XRF analysis, whether instrumental or matrix-related. A ‘model’ has been proposed, based on the formation of thin layers within the resin beads, which helps to explain why the observed characteristics of the resins give rise to the advantages of improved homogeneity, long linear ranges and reduction in both particle size effects and inter-element phenomena in trace analyte determination by EDXRF. With the deeper understanding of specific solid retention systems derived from the information obtained in this work, it is possible to suggest other routes of

investigation that would help to expand the applicability of these media to the problem of sample presentation in XRF spectrometry.

7.2 FURTHER WORK

Further studies on the 'internal' structure of ion-exchange and chelating resins would be advantageous. Preliminary results from surface area and pore structure measurements by gas adsorption have shown to be promising although inconclusive. An extended investigation may enable the suitability of the resins to be predicted for specific determinations, based on characteristics such as surface area and pore size distribution. This would include a kinetic study, associated with the exchange process, which has been shown to limit retention under particular conditions.

The analysis of Cr species in waters using retention on Dowex resins and EDXRF determination has the potential to be used *in situ*. The applicability of the method to environmental and industrial problems, in the field, could be tested using portable EDXRF instrumentation.

The method described could also have other applications of industrial interest, such as the determination of Cr species in plastics such as high-density polyethylene. The presence of Cr, a contaminant from the catalyst used in the production, is undesirable due to the toxicity of the metal, especially in its Cr(VI) form. Preliminary experiments recently performed have shown that it is possible to dissolve the plastics

using toluene at elevated temperatures and that this solvent does not cause changes to the species.

More work on the determination of metals in sewage sludge and other 'complex' bio-environmental samples could be performed in order to extend the applicability of the method. Studies on pre-complexation, aimed at reducing the effect of high concentrations of competing ions, such as Fe, are important. Also, the determination of the target element Mn, retained on Chelex-100, could be achieved by using a high pH an the full methodology for its efficient retention should be explored.

The use of other ion-exchange, reversed phase and chelation media for speciation of elements of high environmental and toxicological interest (e.g., As, Se, Sn, Hg, etc.) using EDXRF determination is still widely open to experimentation. Resins with different functional groups and specific size ranges could be used in admixture, allowing retention of various target analyte species in solution to be performed at the same time. Simple nylon sieve separation could then be employed prior to measurement by EDXRF as necessary.

The use of resins has shown that a much reduced inter-element effect is observed for certain analytes retained in the concentration range generally encountered. The boundaries of this desirable effect have yet to be ascertained. The measurement of such boundaries, if present, would allow the limitations of the technique to be known, together with a greater understanding of the inter-element effect itself.

The chemical effects induced by oxidation states on the $K\beta/K\alpha$ intensity ratio when analysing metal species retained on resins have shown to be too weak to be

detected by conventional XRF spectrometry. However, these effects have been observed when the analytes are in solution. It would be interesting to compare these results with others obtained from the analysis of these samples by extended x-ray absorption fine structure spectroscopy (EXAFS). The effects found might be magnified and it may be possible to gain further information on the characteristics of the bond between the analytes and the functional groups of the resins.

APPENDICES

APPENDIX A

A.1 SYMBOLS AND TERMINOLOGY

I_o	Initial fluorescent radiation	μ_r	Mass absorption coefficient of the resin
I	Emerging fluorescent radiation	μ_i	Mass absorption coefficient of element / group *i*
ρ_r	Density of resin	w_i	Weight fraction of element / group *i*
x	Fluorescent beam path length	C_r	Capacity of resin
ψ	Radiation take-off angle	n	Ion charge
d	Depth of penetration	W_i	Relative molar mass
d_c	Critical depth of penetration		

A.2 CALCULATION FOR THE DETERMINATION OF THE CRITICAL PENETRATION DEPTH OF CHELEX-100 SATURATED WITH MANGANESE

The critical penetration depth (d_c) for a given sample is considered as the distance at which 99% of the fluorescent radiation is absorbed by the matter or matrix.

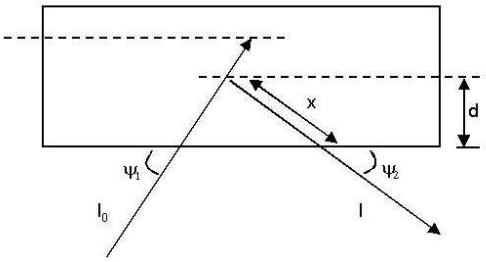

Figure A-1

This distance can be calculated from equation A-1 (equation 1-6 in Chapter 1):

$$I = I_o \cdot e^{-\mu_r \cdot \rho_r \cdot x} \qquad \text{(A-1)}$$

Figure A-1 shows how the fluorescent beam path length (x) can be expressed in terms of the penetration depth (d):

$$x = \frac{d}{\sin \psi} \qquad \text{(A-2)}$$

Substituting A-2 in A-1:

$$I = I_o \cdot e^{-\frac{\mu_r \cdot \rho_r \cdot d}{\sin \psi}} \qquad \text{(A-3)}$$

which can also be written as:

$$d = -\frac{Ln\frac{I}{I_o} \cdot \sin \psi}{\mu_r \cdot \rho_r} \qquad \text{(A-4)}$$

In order to solve equation A-4, it is necessary to obtain the mass absorption coefficient of the sample. This can be found from:

$$\mu_r = \Sigma \mu_i \cdot w_i \qquad \text{(A-5)}$$

The approximate weight fractions of the components of the samples can be calculated from the capacity of the resin:

$$w_i(\%) = \frac{C_r \cdot W_i}{n} \cdot 100 \qquad \text{(A-6)}$$

Considering Chelex-100 saturated with Mn, it is possible to calculate the weight fraction for Mn and for the functional group [$CH_2N(CH_2COO^-)_2$]. The weight fraction for the rest of the polymer (simplified as C_8H_8) can be calculated by difference:

Table A-1

Element / Group	**C_r (Eq g^{-1})**	**W_i (g mol^{-1})**	**n**	**w_i (%)**
Mn	0.002	54.9	2	*5.49*
$CH_2N(CH_2COO^-)_2$	0.002	144.4	2	*14.44*
C_8H_8	-	-	-	*80.07*

From these values it is possible to obtain the weight fraction of each component of the sample. These values can be multiplied by the mass absorption coefficient of each element at the Mn Kα line[109].

Table A-2

Sample component	Mn	C	H	N	O
w_i (%)	5.4	80	6.8	1.4	6.4
μ_i	78.6	10.9	0.54	17.8	27.2
$w_i \cdot \mu_i$	4.24	8.72	0.04	0.25	1.74
$\mu_r = \Sigma \mu_i \cdot w_i$	*14.99*				

Thus, equation A-4 can be solved for μ_r = 14.99 $cm^2\ g^{-1}$, ρ_r = 1.2 g cm^{-3} and ψ = 45°, and considering that, when 99% of the radiation is absorbed by the sample, I = 1, I_o = 100 and d = d_c. Therefore, the critical penetration depth of Chelex-100 loaded to saturation with Mn will be:

$$d_c = -\frac{Ln\frac{1}{100} \times \sin 45^o}{14.99 \times 1.2} = \frac{3.256}{14.99 \times 1.2} = 0.1810\ cm$$

d_c = 1810 μm

APPENDIX B

B.1 SYMBOLS AND TERMINOLOGY

V_b	Volume of bead	r_b^Y	Film thickness of bead (occupied)
m_b	Mass of bead	r_b^Z	Radius of bead (unoccupied)
ρ_b	Density of bead	c_s	Concentration of solution
r_b	Radius of bead	Vs	Volume of solution
d_b	Diameter of bead	n	Ion charge
N	Number of beads	W	Relative molar mass
m_r	Mass of resin	N_A	Avogadro's number
C_r	Capacity of resin	D	Density of sites per unit of volume
X_b	Total number of active sites per bead	V_D	Volume occupied by one active site
Y_b	Number of occupied active sites per bead	x	Distance between active sites
Z_b	Number of unoccupied active sites per bead		

B.2 CALCULATION FOR THE DETERMINATION OF THE NUMBER OF OCCUPIED ACTIVE SITES PER RESIN BEAD

Considering that the shape of the resin bead has been shown to be spherical, the volume of each bead will be given by the equation:

$$V_b = \frac{4}{3} \cdot \pi \cdot r_b^3 \qquad \text{(B-1)}$$

which for $r_b = \frac{d_b}{2}$

can also be written as:

$$V_b = \frac{\pi \cdot d_b^3}{6} \qquad \text{(B-2)}$$

The mass of the resin bead can be expressed as:

$$m_b = V_b \cdot \rho_b \qquad \text{(B-3)}$$

Combining equations B-2 and B-3 the mass of resin bead will be:

$$m_b = \frac{\pi \cdot d_b^3}{6} \cdot \rho_b \qquad \text{(B-4)}$$

Therefore, the total number of beads in a resin batch of mass m_r, will be:

$$N = \frac{m_r}{m_b} = \frac{6}{\pi} \cdot \frac{m_r}{\rho_b \cdot d_b^3} \quad \text{(B-5)}$$

The total number of active sites per bead can be defined as:

$$X_b = C_r \cdot m_b = \frac{\pi}{6} \cdot C_r \cdot d_b^3 \cdot \rho_b \quad \text{(B-6)}$$

whereas, the number of occupied active sites per bead, considering 100% efficiency of retention of the analyte, can be expressed as:

$$Y_b = \frac{c_s \cdot V_s \cdot n}{N \cdot W} \quad \text{(B-7)}$$

and substituting B-5 in equation B-7:

$$Y_b = \frac{c_s \cdot V_s \cdot n \cdot m_b}{W \cdot m_r} = \frac{\pi}{6} \cdot \frac{c_s \cdot V_s \cdot n \cdot \rho_b \cdot d_b^3}{W \cdot m_r} \quad \text{(B-8)}$$

B.3 CALCULATION FOR THE DETERMINATION OF THE THICKNESS OF THE LAYER OF OCCUPIED ACTIVE SITES IN A RESIN BEAD

If Z_b is the number of unoccupied active sites per bead so that:

$$X_b = Y_b + Z_b \quad \text{(B-9)}$$

and

$$r_b = r_b^Y + r_b^Z \quad \text{(B-10)}$$

Z_b should be proportional to the volume of the bead with unoccupied sites, in the same way that X_b is proportional to the total volume of the bead. Therefore:

$$Z_b = X_b \cdot \frac{\frac{4}{3} \cdot \pi \cdot r_b^{Z\,3}}{\frac{4}{3} \cdot \pi \cdot r_b^3}$$

and simplifying,

$$Z_b = X_b \cdot \frac{r_b^{Z^3}}{r_b^3} \qquad \text{(B-11)}$$

Substituting B-11 in B-9:

$$Y_b = X_b - X_b \cdot \frac{r_b^{Z^3}}{r_b^3}$$

This equation can be rearranged to:

$$\frac{Y_b}{X_b} = 1 - \frac{r_b^{Z^3}}{r_b^3}$$

which gives:

$$r_b^Z = r_b \cdot \left(1 - \frac{Y_b}{X_b}\right)^{\frac{1}{3}} \qquad \text{(B-12)}$$

Therefore, substituting B-10 in equation B-12 and rewriting:

$$r_b^Y = r_b \cdot \left[1 - \left(1 - \frac{Y_b}{X_b}\right)^{\frac{1}{3}}\right] \qquad \text{(B-13)}$$

And finally, substituting the values of X_b and Y_b from equations (B-6) and (B-8) and simplifying:

$$r_b^Y = r_b \cdot \left[1 - \left(1 - \frac{c_s \cdot V_s \cdot n}{C_r \cdot m_r \cdot W}\right)^{\frac{1}{3}}\right] \qquad \text{(B-14)}$$

This equation provides the film thickness of the bead where the active sites have been occupied by metal ions.

B.4 CALCULATION FOR THE DETERMINATION OF THE DISTANCE BETWEEN ACTIVE SITES IN A RESIN BEAD

The distance between active sites within a resin bead, x, can be calculated by first obtaining the density of sites per unit volume as:

$$D = \rho_b \cdot C_r \cdot N_A \qquad \text{(B-15)}$$

where N_A is *Avogadro's Number* of sites (6.023×10^{23}) .

The 'free' volume occupied by each site will then be

$$V_D = \frac{1}{D} = \frac{\pi \cdot x^3}{6} \qquad \text{(B-16)}$$

Substituting B-15 in B-16 and rearranging the equation:

$$x = \left(\frac{6}{\pi} \cdot \frac{1}{\rho_b \cdot C_r \cdot N_A} \right)^{\frac{1}{3}} \qquad \text{(B-17)}$$

B.5 SOLVED EXAMPLE: COPPER ON DOWEX 50W-X8 (100-200 MESH)

It has been considered that 25 cm^3 of Cu solution of concentration 20 μg cm^{-3} were retained on 0.5 g of Dowex 50W-X8. For a mesh size between 100 and 200, the average particle size is 112 μm. The capacity of the resin has been taken as that at 50% saturation (3.2 mEq g^{-1}) from Figure 6.6 (a). Thus, the following values:

ρ_b	= 1.2 g cm^{-3}	c_s	= 0.00002 g cm^{-3}
d_b	= 0.0112 cm	Vs	= 25 cm^3
m_r	= 0.5 g	n	= 2
C_r	= 0.0032 Eq g^{-1}	W	= 63.5 g mol^{-1}

can be transferred to equation B-6 in order to obtain the total number of active sites per bead (X_b), measured in equivalents (Eq):

$$X_b = \frac{\pi}{6} \times 0.0032 \times 1.2 \times 0.0112^3 = 2.82 \times 10^{-9}\ Eq\ per\ bead$$

and to equation B-8 in order to calculate the number of occupied active sites per bead (Y_b), also in equivalents:

$$Y_b = \frac{\pi}{6} \times \frac{0.00002 \times 25 \times 2 \times 1.2 \times 0.0112^3}{63.5 \times 0.5} = 2.78 \times 10^{-11}\ Eq\ per\ bead$$

Thus, 1000 μg g^{-1} of Cu on Dowex 50W-X8 occupy only 1% of the active sites available on the resin.

More importantly, the thickness of the layer of occupied active sites can be calculated by using equation B-14:

$$r_b^Y = 0.0056 \times \left[1 - (1 - \frac{0.00002 \times 25 \times 2}{0.0032 \times 0.5 \times 63.5})^{\frac{1}{3}} \right] = 1.84 \times 10^{-5} cm = 0.184 \mu m$$

This is less than 0.2% of the diameter of an average resin bead. In this case, 184 nm may be considered a 'thin film'.

Similarly, the theoretical distance between active sites in a resin bead can be calculated by substituting in equation B-17:

$$x = \left(\frac{6}{\pi} \times \frac{1}{1.2 \times 0.0032 \times 6.023 \times 10^{23}} \right)^{\frac{1}{3}} = 9.38 \times 10^{-8} cm = 9.38 \mathring{A}$$

This figure is in agreement with theoretical data that sets ionic radii of atoms between 0.07 and 2.94 $\mathring{A}$ [70].

APPENDIX C

STATISTICAL ANALYSIS OF Kβ/Kα INTENSITY RATIOS FOR CHROMIUM AND MANGANESE SPECIES, USING A TWO-TAILED T-TEST[88]

TABLE C-1 ***Raw data and results of the t-test on Kβ/Kα ratios from sets of 1000-5000 μgmL^{-1} CrIII and CrVI standards in solution. EDXRF determination.***

Raw data	*CrVI*	*CrIII*
	0.176433019	0.166411363
	0.168295663	0.163335579
	0.171634958	0.163761633
	0.170264734	0.160414748
	0.171412372	0.161273588

	Variable 1	*Variable 2*
Mean (x_i)	0.171608149	0.163039382
SD (s_i)	0.003003987	0.002344481
s_i^2	9.02394E-06	5.49659E-06
Determinations (n_i)	5	5

	t-test	
Confidence interval (%)	**95**	**99**
P value (two-tail)	0.05	0.01
Hypothesized mean	0	0
s^2	0.0000072603	7.26026E-06
s	0.0026944878	0.002694488
Degrees of freedom	8	8
t critical	**2.31**	**3.36**
t	5.028194907	5.028194907
/ t /	**5.028194907**	**5.028194907**

Hypothesis REJECTED. There is only 5% probability of the difference in ratios arising by chance.

Hypothesis REJECTED. There is 99% probability of the difference in ratios being statistically significant.

Where $s^2 = \{(n_1 - 1)\, s_1^2 + (n_2 - 1)\, s_2^2\} / (n_1 + n_2 - 2)$

and $t = (x_1 - x_2) / s\, (1/n_1 + 1/n_2)^{1/2}$

TABLE C-2 ***Raw data and results of the t-test on Kβ/Kα ratios from sets of 1000-2500 µgmL^{-1} MnII and MnVII standards in solution. EDXRF determination.***

Raw data	***MnVII***	***MnII***
	0.175879397	0.171581328
	0.176897517	0.166422601
	0.180174915	0.173489137
	0.181571155	0.174049033

	Variable 1	***Variable 2***
Mean (x_i)	0.178630746	0.171385525
SD (s_i)	0.002683559	0.003473155
s_i^2	7.20149E-06	1.20628E-05
Determinations (n_i)	4	4

		t-test
Confidence interval (%)	**95**	**98**
P value (two-tail)	0.05	0.02
Hypothesized mean	0	0
s^2	0.0000096321	9.63215E-06
s	0.0031035701	0.00310357
Degrees of freedom	6	6
t critical	**2.45**	**3.14**
t	3.301452771	3.301452771
/ t /	**3.301452771**	**3.301452771**

Hypothesis REJECTED. There is only 5% probability of the difference in ratios arising by chance.

Hypothesis REJECTED. There is 98% probability of the difference in ratios being statistically significant.

Where $s^2 = \{(n_1 - 1)\, s_1^2 + (n_2 - 1)\, s_2^2\} / (n_1 + n_2 - 2)$

and $t = (x_1 - x_2) / s\, (1/n_1 + 1/n_2)^{1/2}$

TABLE C-3 ***Raw data and results of the t-test on Kβ/Kα ratios from sets of 500-25000 μgmL^{-1} CrIII and CrVI standards on Dowex resins. EDXRF determination.***

Raw data	***CrVI***	***CrIII***
	0.184420023	0.138689648
	0.176822761	0.157465386
	0.172861628	0.166928672

	Variable 1	***Variable 2***
Mean (x_i)	0.178034804	0.154361235
SD (s_i)	0.005873747	0.01437315
s_i^2	3.45009E-05	0.000206587
Determinations (n_i)	3	3

		t-test
Confidence interval (%)	**95**	**90**
P value (two-tail)	0.05	0.1
Hypothesized mean	0	0
s^2	0.0001205442	0.000120544
s	0.0109792610	0.010979261
Degrees of freedom	4	4
t critical	**2.78**	**2.13**
t	2.640804473	2.640804473
/ t /	**2.640804473**	**2.640804473**

Hypothesis RETAINED. No evidence of ratios being significantly different at a confidence level of 95%.

Hypothesis REJECTED. There is 90% probability of the difference in ratios being statistically significant.

Where $s^2 = \{(n_1 - 1)\, s_1^2 + (n_2 - 1)\, s_2^2\} / (n_1 + n_2 - 2)$

and $t = (x_1 - x_2) / s\, (1/n_1 + 1/n_2)^{1/2}$

TABLE C-4 ***Raw data and results of the t-test on Kβ/Kα ratios from sets of 500-25000 μgmL^{-1} MnII and MnVII standards on Dowex resins. EDXRF determination.***

Raw data	***MnVII***	***MnII***
	0.146456524	0.176426788
	0.159820311	0.159599139
	0.163576654	0.164143799

	Variable 1	***Variable 2***
Mean (x_i)	0.15661783	0.166723242
SD (s_i)	0.008998146	0.00870532
s_i^2	8.09666E-05	7.57826E-05
Determinations (n_i)	3	3

		t-test
Confidence interval (%)	**95**	**90**
P value (two-tail)	0.05	0.1
Hypothesized mean	0	0
s^2	0.0000783746	7.83746E-05
s	0.0088529436	0.008852944
Degrees of freedom	4	4
t critical	**2.78**	**2.13**
t	-1.39801543	-1.39801543
/ t /	**1.39801543**	**1.39801543**

Hypothesis RETAINED. No evidence of ratios being significantly different at a confidence level of 95%.

Hypothesis RETAINED. No evidence of ratios being significantly different at a confidence level of 90%.

Where $s^2 = \{(n_1 - 1)\, s_1^2 + (n_2 - 1)\, s_2^2\} / (n_1 + n_2 - 2)$

and $t = (x_1 - x_2) / s\, (1/n_1 + 1/n_2)^{1/2}$

TABLE C-5 ***Raw data and results of the t-test on Kβ/Kα ratios from sets of 500-25000 μgmL^{-1} CrIII and CrVI standards on Dowex resins. WDXRF determination.***

Raw data	***CrVI***	***CrIII***
	0.132257800	0.131564400
	0.131198207	0.134919082
	0.132282514	0.133569057
	0.132283662	0.133121413

	Variable 1	***Variable 2***
Mean (x_i)	0.132005546	0.133293488
SD (s_i)	0.000538358	0.001382974
s_i^2	2.8983E-07	1.91262E-06
Determinations (n_i)	4	4

		t-test
Confidence interval (%)	**95**	**90**
P value (two-tail)	0.05	0.1
Hypothesized mean	0	0
s^2	0.0000011012	1.10122E-06
s	0.0010493917	0.001049392
Degrees of freedom	6	6
t critical	**2.45**	**1.94**
t	-1.735696239	-1.735696239
/ t /	**1.735696239**	**1.735696239**

Hypothesis RETAINED. No evidence of ratios being significantly different at a confidence level of 95%.

Hypothesis RETAINED. No evidence of ratios being significantly different at a confidence level of 90%.

Where $s^2 = \{(n_1 - 1)\, s_1^2 + (n_2 - 1)\, s_2^2\} / (n_1 + n_2 - 2)$

and $t = (x_1 - x_2) / s\, (1/n_1 + 1/n_2)^{1/2}$

TABLE C-6 ***Raw data and results of the t-test on Kβ/Kα ratios from sets of 500-25000 µgmL^{-1} MnII and MnVII standards on Dowex resins. WDXRF determination.***

Raw data	***MnVII***	***MnII***
	0.143781654	0.151524359
	0.146228368	0.146097231
	0.144632908	0.147545964
	0.144455736	0.146583605

	Variable 1	***Variable 2***
Mean (x_i)	0.144774667	0.14793779
SD (s_i)	0.0010362	0.002465663
s_i^2	1.07371E-06	6.07949E-06
Determinations (n_i)	4	4

		t-test
Confidence interval (%)	**95**	**90**
P value (two-tail)	0.05	0.1
Hypothesized mean	0	0
s^2	0.0000035766	3.5766E-06
s	0.0018911907	0.001891191
Degrees of freedom	6	6
t critical	**2.45**	**1.94**
t	-2.365352032	-2.365352032
/ t /	**2.365352032**	**2.365352032**

Hypothesis RETAINED. No evidence of ratios being significantly different at a confidence level of 95%.

Hypothesis REJECTED. There is 90% probability of the difference in ratios being statistically significant.

Where $s^2 = \{(n_1 - 1)\, s_1^2 + (n_2 - 1)\, s_2^2\} / (n_1 + n_2 - 2)$

and $t = (x_1 - x_2) / s\, (1/n_1 + 1/n_2)^{1/2}$

TABLE C-7 ***Raw data and results of the t-test on Kβ/Kα ratios from sets of ten 25000 μgg^{-1} MnII and MnVII standards on Dowex resins. WDXRF determination.***

Raw data	***MnVII***	***MnII***
	0.144933060	0.141737799
	0.144129975	0.143877481
	0.141976785	0.143574771
	0.142886312	0.142868144
	0.144598020	0.141846185
	0.142957806	0.140742091
	0.142544218	0.141868683
	0.142154089	0.142966819
	0.143606007	0.141198903
	0.143285669	0.142305161

	Variable 1	***Variable 2***
Mean (x_i)	0.143307194	0.142298604
SD (s_i)	0.001003183	0.001012614
s_i^2	1.00638E-06	1.02539E-06
Determinations (n_i)	10	10

		t-test
Confidence interval (%)	**95**	**90**
P value (two-tail)	0.05	0.1
Hypothesized mean	0	0
s^2	0.0000010159	1.01588E-06
s	0.0010079092	0.001007909
Degrees of freedom	18	18
t critical	**2.45**	**1.94**
t	2.237579336	2.237579336
/ t /	**2.237579336**	**2.237579336**

Hypothesis RETAINED. No evidence of ratios being significantly different at a confidence level of 95%.

Hypothesis REJECTED. There is 90% probability of the difference in ratios being statistically significant.

Where $s^2 = \{(n_1 - 1)\, s_1^2 + (n_2 - 1)\, s_2^2\} / (n_1 + n_2 - 2)$

and $t = (x_1 - x_2) / s\, (1/n_1 + 1/n_2)^{1/2}$

REFERENCES

REFERENCES

1.- Roentgen, W.C., *Ann. Phys. Chem*., 1898, 64, 1.

2.- Jenkins, R., *An Introduction to X-ray Spectrometry*, John Wiley & Sons, New York, USA, 1986.

3.- Tertian, R. and Claisse, F., *Principles of Quantitative X-ray Fluorescence Analysis*, Heyden, London, UK, 1982.

4.- Jenkins, R., Gould, R.W. and Gedcke, D., *Quantitative X-ray Spectrometry*, Marcel Dekker Inc., New York, USA, 1981.

5.- *Link Analytical XR300 XRF User Manual*, Link Analytical Ltd., High Wycombe, Bucks., UK, 1989.

6.- Bermúdez-Polonio, J., *Teoría y Práctica de la Espectroscopia de Rayos X*, Ed. Alhambra S.A., Madrid, España, 1967.

7.- Blanco, M., Cerdá, V. and Sanz-Medel, A., *Espectroscopia Atómica Analítica*, Ed. Bellaterra, Barcelona, España, 1990.

8.- Williams, K.L., *Introduction to X-ray Spectrometry*, Allen & Unwin, London, UK, 1987.

9.- Russ, J.C., *Fundamentals of Energy Dispersive X-ray Analysis*, Butterworths, London, UK, 1984.

10.- Gunn, E.L., *Adv. X-ray Anal*., 1960, **4**, 382.

11.- Bernstein, F., *Adv. X-ray Anal*., 1962, **6**, 436.

12.- Allen, A.L. and Rose, V.C., *Adv. X-ray Anal.*, 1972, **15**, 534.

13.- Huberman, H., Warner, G. and Widman, F., *Norelco Rep.*, 1973, **20**, 10.

14.- Grubb, W.T. and Zemany, P.D., *Nature,* 1955, **176**, 221.

15.- Lochmüller, C.H., Galbraith, J.W. and Walter, R.L., *Anal. Chem.*, 1974, **46**, 440.

16.- Van Grieken, R.E., Bresseleers, C.M. and Vanderborght, B.M., *Anal. Chem.*, 1977, **49**, 1326.

17.- Luke, C.L., *Anal. Chem.*, 1964, **36**, 318.

18.- Kashuba, A.T. and Hines, C.R., *Anal. Chem.*, 1971, **43**, 1758.

19.- Leyden, D.E., Channell, R.E. and Blount, C.W., *Anal. Chem.*, 1972, **44**, 607.

20.- Blount, C.W., Leyden, D.E., Thomas, T.L. and Guill, S.M., *Anal. Chem.*, 1973, **45**, 1045.

21.- Blount, C.W., Morgan, W.R. and Leyden, D.E., *Anal. Chim. Acta,* 1971, **53**, 463.

22.- Leyden, D.E., *Adv. X-ray Anal.*, 1973, **17**, 293.

23.- Agarwal, M., Bennet, R.B., Stump, I.G. and D'Auria, J.M., *Anal. Chem.*, 1975, **47**, 924.

24.- Leyden, D.E., Patterson, T.A. and Alberts, J.J., *Anal. Chem.*, 1975, **47**, 733.

25.- Campbell, W.J., Spano, E.F. and Green, T.E., *Anal. Chem.*, 1966, **38**, 987.

26.- Hubbard, G.L. and Green, T.E., *Anal. Chem.*, 1966, **38**, 428.

27.- Spano, E.F. and Green, T.E., *Anal. Chem.*, 1966, **38**, 1341.

28.- Radcliffe, D., *Anal. Lett.*, 1970, **3**, 573.

29.- Walton, R.D., *Dev. Appl. Spectrosc.*, 1971, **9**, 287.

30.- Robert, A. and Valles, R., *Radiochem. Radioanal. Letters*, 1973, **15**, 279.

31.- Law, S.L. and Campbell, W.J., *Adv. X-ray Anal.*, 1973, **17**, 279.

32.- Leyden, D.E. and Luttrell, G.H., *Anal. Chem.*, 1975, **47**, 1612.

33.- Leyden, D.E. in *X-ray Fluorescence Analysis of Environment Samples*, Ann Arbor Science Publishers, Ann Arbor, MI, USA, 1977.

34.- Leyden, D.E., Luttrell, G.H., Nonidez, W.K. and Werho, D.B., *Anal. Chem.*, 1976, **48**, 67.

35.- Robberecht, H.J. and Van Grieken, R.E., *Anal. Chem.*, 1980, **52**, 449.

36.- Vanderborght, B.M. and Van Grieken, R.E., *Anal. Chem.*, 1977, **49**, 311.

37.- Vanderborght, B., Verbeeck, J. and Van Grieken, R., *Bull. Soc. Chim. Belg.*, 1977, **86**, 23.

38.- Lengar, Z., Hudnik, V. and Gomiscek, S., *Vestn. Slov. Kem. Drus.*, 1981, **28**, 379.

39.- Smits, J. and Van Grieken, R., *Int. J. Environ. Anal. Chem.*, 1981, **9**, 81.

40.- Haas, H.F., Krivan, V. and Ortner, H.M. , *Anal. Chim. Acta*, 1983, **149**, 77.

41.- Ping, L., Matsumoto, K. and Fuwa, K, *Anal. Chem.*, 1983, **55**, 1819.

42.- Haas, H.F. and Krivan, V., *Fresenius Z. Anal. Chem.,* 1985, **322**, 261.

43.- Honjo, T. and Benya, T., *Fresenius Z. Anal. Chem.,* 1989, **334**, 558.

44.- Cesareo, R. and Gigante, G.E., *Water, Air, Soil Pollut.*, 1978, **9**, 99.

45.- Roelandts, I., *Anal. Chem.*, 1981, **53**, 676.

46.- Kingston, H. and Pella, P.A., *Anal. Chem.*, 1981, **53**, 223.

47.- Smits, J., Nelissen, J. and Van Grieken, R., *Anal. Chim. Acta,* 1979, **111**, 215.

48.- Van Grieken, R., *Anal. Chim. Acta,* 1982, **143**, 3.

49.- Bumbalova, A., Pikulikova, A., Komova, M. and Muchova, A., *J. Radioanal. Nucl. Chem. Lett.*, 1992, **164**, 357.

50.- McComb, M.E. and Gesser, H.D., *Anal. Chim. Acta,* 1997, **341**, 229.

51.- Masi, A.N. and Olsina, R.A., *X-ray Spectrom.,* 1996, **25**, 221.

52.- Ducosfonfrede, S., Clanet, F. and Malingre, G., *Analusis*, 1995, **23**, 125.

53.- Peräniemi, S., Vepsalainen, J., Mustalahti, H. and Ahlgrén, M., *Fresenius J. Anal. Chem.,* 1992, **344**, 118.

54.- Peräniemi, S. and Ahlgrén, M., *Anal. Chim. Acta*, 1995, **315**, 365.

55.- Russell, P.A. and James, R., *J. Anal. At. Spectrom.,* 1997, **12**, 25.

56.- *Philips PV9500 Operation Manual*, Philips Analytical X-Ray, Cambridge, UK, 1979.

57.- *Link Analytical XR300 XRF Operation and Reference Manual*, Link Analytical Ltd., High Wycombe, Bucks., UK, 1989.

58.- Barnard, T.W., Crockett, M.I., Ivaldi, J.C., Lundberg, P.L., Yates, D.A., Levine, P.A. and Saver, D.J., *Anal. Chem.*, 1993, **65**, 1231.

59.- Barnard, T.W., Crockett, M.I., Ivaldi, J.C. and Lundberg, P.L., *Anal. Chem*., 1993, **65**, 1225.

60.- *Chelex-100 User Manual*, Bio-Rad Laboratories, Hemel Hempstead, Herts, UK, 1998.

61.- *Dowex Ion Exchange Resins Data Sheet*, Merck, Poole, Dorset, UK.

62.- *Dowex Ion Exchange Resins Information Sheet*, Sigma-Aldrich Chemical Co. Ltd., Poole, Dorset, UK.

63.- Valcárcel, M. and Gómez, A., *Técnicas Analíticas de Separación*, Ed. Reverté, Barcelona, España, 1990.

64.- Fleger, S.L., Heckman, J.W.Jr., Klomparens, K.L., *Scanning and Transmission Electron Microscopy. An Introduction*, W.H. Freeman & Co., New York, USA, 1993.

65.- Chescoe, D. and Goodhew, P.J., *The Operation of Transmission and Scanning Electron Microscopes*, Oxford University Press, Oxford, UK, 1990.

66.- Sperling, M. in *Encyclopaedia of Analytical Science*, Vol.2, Academic Press, London, UK, 1995.

67.- Van Niekerk, J.N., De Wet, J.F. and Wybenga, F.T., *Anal. Chem*., 1961, **33**, 213.

68.- Span, J. and Ribaric, M., *J. Chem. Phys.*, 1964, **41**, 2347.

69.- *Findlay's Practical Physical Chemistry*, Longman Group Ltd., London, 1973.

70.- Babor, J.A. and Ibarz Aznárez, J., *Química General Moderna*, Ed. Marín, Barcelona, España, 1972.

71.- Burriel Martí, F., Lucena Conde, F., Arribas Jimeno, S. and Hernández Méndez, J., *Química Analítica Cualitativa*, Ed. Paraninfo, Madrid, España, 1989.

72.- Atkins, P.W., *Physical Chemistry*, Oxford University Press, Oxford, UK, 1994.

73.- Jones, J.B. and Urch, D.S., *Analyst*, 1983, **108**, 1477.

74.- Luck, S. and Urch, D.S., *Physica Scripta*, 1990, **41**, 970.

75.- Alkadier, M.A. and Urch, D.S., *J. Chem. Soc. Dalton Trans*., 1984, 263.

76.- Horn, R. and Urch, D.S., *Spectrochim. Acta B*, 1987, **42**, 1177.

77.- Martins, E. and Urch, D.S., *Anal. Chim. Acta*, 1994, **286**, 411.

78.- Carrol, M. and Rutherford, M., *American Mineralogist*, 1988, **73**, 845.

79.- Smith, S., Taylor, D.A., Hillier, I.H., Vincent, M.A., Guest, M.F., MacDowell, A.A., Vonniessen, W. and Urch, D.S., *J. Chem. Soc. Faraday Trans. II*, 1988, **84**, 209.

80.- Taylor, D.A., Hillier, I.H., Vincent, M., Guest, M.F., MacDowell, A.A., Vonniessen, W. and Urch, D.S., *Chem. Phys. Lett.*, 1985, **121**, 482.

81.- Tamaki, Y., *X-ray Spectrom.*, 1995, **24**, 23.

82.- Urch, D.S., *Mineralogical Magazine*, 1989, **53**, 153.

83.- Urch, D.S., *Arabian J. Sci. Eng.*, 1988, **13**, 211.

84.- Pickering, I.J., Brown, Jr., G.E. and Tokunaga, T.K., *Env. Sci. Technol.*, 1995, **29**, 2456.

85.- Bertsch, P.M., Hunter, D.B., Sutton, S.R., Bajt, S. and Rivers, M.L., *Env. Sci. Technol.*, 1994, **28**, 980.

86.- Lamoureux, M.M., Hutton, J.C., Styris, D.L. and Gordon, R.L., *Appl. Spectrosc.*, 1995, **49**, 808.

87.- Arber, J.M., Urch, D.S. and West, N.G., *Analyst*, 1988, **113**, 779.

88.- Miller, J.C. and Miller, J.N., *Statistics for Analytical Chemistry*, Ellis Horwood Ltd., Chichester, UK, 1993.

89.- Rebohle, L., Lehnert, U. and Zschornack, G., *X-ray Spectrom.*, 1996, **25**, 295.

90.- Kucukonder, A., Sahin, Y., Buyukkasap, E. and Kopya, A., *J. Physics B – Atomic, Molecular and Optical Physics*, 1993, **26**, 101.

91.- Raghavaiah, C.V., Rao, N.V., Murty, G.S.K., Rao, M.V.S.C. and Reddy, S.B., *X-ray Spectrom.*, 1992, **21**, 239.

92.- Kucukonder, A., Buyukkasap, E., Yilmaz, R. and Sahin, Y., *Acta Physica Polonica A*, 1999, **95**, 243.

93.- Armstrong, J.T., *Anal. Chem.*, 1999, **71**, 2714.

94.- Cary, E.E., in *Biological and Environmental Aspects of Chromium*, Elsevier, Amsterdam, Netherlands, 1982.

95.- Nriagu, J.O., in *Chromium in the Natural and Human Environments*, Wiley, New York, USA, 1988.

96.- Beszedits, S., in *Chromium in the Natural and Human Environments*, Wiley, New York, USA, 1988.

97.- Isshiki, K., Sohrin, Y., Karatani, H. and Nakayama, E., *Anal. Chim. Acta*, 1989, **224**, 55.

98.- Pasullean, B., Davidson, C.M. and Littlejohn, D., *J. Anal. At. Spectrom.*, 1995, **10**, 24.

99.- Pik, A.J., Eckert, J.M. and Williams, K.L., *Anal. Chim. Acta*, 1981, **124**, 351.

100.- Potts, P.J., Webb, P.C., Williams Thorpe, O. and Kilworth, R., *Analyst*, 1995, **120**, 1273.

101.- Argyraki, A., Ramsey, M.H. and Potts, P.J., *Analyst*, 1997, **122**, 743.

102.- Potts, P.J., Williams Thorpe, O. and Webb, P.C., *Geostandards Newsletter*, 1997, **21**, 29.

103.- Beere, H.G. and Jones, P., *Anal. Chim. Acta*, 1994, **293**, 237.

104.- Sperling, M., Xu, S. and Welz, B., *Anal. Chem*., 1992, **64**, 3101.

105.- Cox, A.G., Cook, I.G. and McLeod, C.W., *Analyst*, 1985, **110**, 331.

106.- Menéndez-Alonso, E., Hill, S.J., Foulkes, M.E. and Crighton, J.S., *J. Anal. At. Spectrom.*, 1999, **14**, 187.

107.- Cotton, F.A. and Wilkinson, G., *Advanced Inorganic Chemistry*, Wiley, New York, USA, 1980.

108.- *The Determination of Trace Metals in Natural Waters*, IUPAC, Blackwell Scientific, Oxford, UK, 1988.

109.- Leroux, J. and Thinh, T.P., *Revised Tables of X-ray Mass Attenuation Coefficients*, Corporation Scientifique Claisse Inc., Quebec, Canada, 1977.

RELATED ACTIVITIES

LECTURES AND MEETINGS ATTENDED

i. **8th Biennial National Atomic Spectroscopy Symposium**, University of East Anglia, Norwich, UK, July 1996.

ii. **Research and Development Topics in Analytical Chemistry**, Nottingham Trent University, Nottingham, UK, July 1996.

iii. ***Calibrations 'off the peg'* – one day seminar on XRF,** MRI, Sheffield Hallam University, South Yorkshire, UK, March 1997.

iv. **Atomic Spectroscopy Updates Meeting, *'Towards 2000: Challenges for Atomic Spectrometry',*** University of Edinburgh, UK, March 1997.

v. **20th Durham Conference on X-Ray Analysis**, University of Durham, UK, September 1997.

vi. **Atomic Spectroscopy Updates Meeting, *'The Relevance of Chemometrics in Atomic Spectroscopy'***, University of Nottingham, UK, March 1998.

vii. **9th Biennial National Atomic Spectroscopy Symposium**, University of Bath, UK, July 1998.

viii. ***'Challenges in Analytical Atomic Spectrometry'* – half day meeting,** University of Plymouth, UK, September 1998.

ix. **RSC Analytical Science Network – Young Scientists Meeting,** University of Plymouth, UK, November 1999.

x. **Various RSC and Invited Lectures,** University of Plymouth, UK, 1995-1999.

xi. **Weekly Departmental Research Seminars,** University of Plymouth, UK, 1995-1999.

OTHER TRAINING AND ACTIVITIES PERFORMED

i. Attending the ***Teaching Skills for Graduate Teaching Assistants,*** course and receiving the teaching certificate. University of Plymouth, UK, 1997.

ii. Attending the ***Users of the software Perkin-Elmer ICP 'WinLab'*** training course, Perkin-Elmer, UK, 1997.

iii. Demonstrating to undergraduates and post-graduates during practical classes.

iv. Assisting 3rd year undergraduate project students.

v. Performing research and consultancy for external firms.

vi. Preparing lecture notes for the MSc short course held annually at the University of Plymouth.

PRESENTATIONS AND PUBLICATIONS

ORAL

- **20th Durham Conference on X-Ray Analysis**, University of Durham, UK, September 1997. '*The Direct Determination on Resins of Chemical Species from Bio-Environmental Matrices by EDXRF',* E. Menéndez-Alonso, S.J. Hill, M.E. Foulkes and J.S. Crighton.
- **20th Durham Conference on X-Ray Analysis**, University of Durham, UK, September 1997. '*Speciation Studies using α/β Ratios',* M.E. Foulkes , E. Menéndez-Alonso, S.J. Hill and J.S. Crighton.
- **9th Biennial National Atomic Spectroscopy Symposium**, University of Bath, UK, July 1998. *'Direct Determination of Trace Metals in Bio-Environmental Samples by Retention with Resins and EDXRF Detection'*, E. Menéndez-Alonso, S.J. Hill, M.E. Foulkes and J.S. Crighton.
- **10th Biennial National Atomic Spectroscopy Symposium**, University of Sheffield and Sheffield Hallam University, Sheffield, UK, July 2000. *'The Use of Physico-Chemical Characterisation Studies for Solid Retention Media to Optimise the Determination of Trace Metals by EDXRF'*, M.E. Foulkes, E. Menéndez-Alonso, S.J. Hill and J.S. Crighton.

POSTER

- **8th Biennial National Atomic Spectroscopy Symposium**, University of East Anglia, Norwich, UK, July 1996. *'The Separation and Direct Determination of*

Trace Chemical Species in Highly Complex Mixtures from Industrial Sources', E. Menéndez-Alonso, S.J. Hill, M.E. Foulkes and J.S. Crighton.

- **Research and Development Topics in Analytical Chemistry**, Nottingham Trent University, Nottingham, UK, July 1996. '*The Retention and Direct Determination of Inorganic Chemical Species on Resins / Media at Major to Trace Levels in Highly Complex Matrices',* E. Menéndez-Alonso, S.J. Hill and M.E. Foulkes.

PAPER

- '***Speciation and Preconcentration of Cr(III) and Cr(VI) in Waters by Retention on Ion Exchange Media and Determination by EDXRF'***, E. Menéndez-Alonso, S.J. Hill, M.E. Foulkes and J.S. Crighton. *J. Anal. At. Spectrom*., 1999, **14**, 187.
- '***The Use of Physico-Chemical Characterisation Studies for Solid Retention Media to Optimise the Determination of Trace Metals by EDXRF'***, E. Menéndez-Alonso, S.J. Hill, M.E. Foulkes and J.S. Crighton. *J. Anal. At. Spectrom*. Submitted.